

From the Institute of Veterinary Pathology
Department of General Pathology and Pathological Anatomy
Chair: Prof. Dr. W. Hermanns
and the
Institute of Molecular Animal Breeding and Biotechnology
Head: Prof. Dr. E. Wolf
Ludwig-Maximilian-University Munich

Under the supervision of Prof. Dr. R. Wanke and Prof. Dr. E. Wolf

**Clinical and pathological characterization of a novel transgenic
animal model of diabetes mellitus expressing a dominant negative
glucose-dependent insulinotropic polypeptide receptor (GIPR^{dn})**

Inaugural – Dissertation
to achieve the doctor title of veterinary medicine
at the Faculty of Veterinary Medicine of the
Ludwig-Maximilian-University, Munich

by Nadja Herbach
from Berlin

Munich 2002

Gedruckt mit der Genehmigung der Tierärztlichen Fakultät der Ludwig-Maximilians-
Universität
München

Dekan:	Univ.-Prof. Dr. R. Stolla
1. Referent:	Univ.-Prof. Dr. R. Wanke
2. Referent:	Univ.-Prof. Dr. E. Wolf
1. Korreferent:	Univ.-Prof. Dr. W. Kraft
2. Korreferent:	Univ.-Prof. Dr. J. Braun
3. Korreferent:	Priv.Doz. Dr. R. G. Erben

Tag der Promotion: 19. Juli 2002

Table of content

1. Introduction	7
2. Literature review	8
2.1 Diabetes mellitus	8
2.1.1 Definition and description of diabetes mellitus	8
2.1.2 Diagnosis of diabetes mellitus	9
2.1.3 Classification of diabetes mellitus	10
2.1.4 Screening for diabetes mellitus	12
2.1.5 Screening for diabetes-associated organ lesions	13
2.1.6 Diabetic animal models	14
2.1.6.1 Animal models of type 1 diabetes	14
2.1.6.2 Animal models of type 2 diabetes	17
2.2 Diabetic nephropathy	19
2.2.1 Diabetic glomerulosclerosis	20
2.2.2 Tubular changes	21
2.2.3 Interstitial changes	21
2.2.4 Pathophysiology of proteinuria	22
2.2.5 Development of proteinuria	23
2.2.6 Animal models of diabetic kidney disease	23
2.3 Pancreas development	24
2.3.1 Patterning and early pancreas development	24
2.3.2 Morphogenesis and differentiation	26
2.3.3 Transcription factors linked to pancreas development	27
2.3.4 Postnatal pancreatic B-cell growth	32
2.3.5 Incretin hormones and pancreas development	38
2.4 The enteroinsular axis	40
2.4.1 Definition	40
2.4.2 Components of the enteroinsular axis	41

2.4.2.1 Neural components	41
2.4.2.2 Hormonal components (Incretin candidates)	41
2.4.3 Glucagon-like peptide-1 (GLP-1)	41
2.4.4 Glucose-dependent insulintropic polypeptide (GIP)	43
2.4.5 GIP receptor	43
2.4.5.1 GIP receptor structure	43
2.4.5.2 GIP receptor signal transduction	44
2.4.5.3 GIP receptor mediated functions	46
2.4.6 Neural mediation of the incretin effect	47
2.4.7 Quantification of the incretin effect	47
2.4.8 Pathophysiology of the enteroinsular axis in diabetes	48
2.5 Generation of GIPR^{dn} transgenic animals	49
2.5.1 Targeted mutation of the human GIP receptor	49
2.5.2 <i>In vitro</i> analysis of the mutated GIP receptor	50
2.5.3 Generation of mutant mice	51
3. Research design and methods	52
3.1 Transgenic animals	52
3.2 Urine glucose	56
3.3 Blood/serum glucose and serum insulin values	57
3.4 Glycated hemoglobin (HbA _{1c})	57
3.5 Oral glucose tolerance test (OGTT)	58
3.6 Subcutaneous glucose tolerance test (SCGTT)	58
3.7 Daily food and water intake, urine volume	59
3.8 Serum parameters	59
3.9 Body and organ weights	59
3.10 Pancreas preparation and morphometric analysis	60
3.11 Immunohistochemistry of pancreatic tissue	61
3.12 Urine protein analysis	62
3.12.1 Sodium dodecyl sulfate (SDS) polyacrylamide gel electrophoresis (PAGE)	63
3.12.2 Western blot analysis	65
3.13 Immunohistochemistry of the kidneys	66

3.14 Kidney preparation and morphometric analysis	67
3.15 Histological techniques	69
3.16 Twelve-month survival	70
3.17 Data presentation and statistical analysis	70
4. Results	71
4.1 Urine glucose	71
4.2 Blood/serum glucose and serum insulin levels	72
4.3 Glycated hemoglobin (HbA _{1c}) levels	78
4.4 Oral glucose tolerance test (OGTT)	80
4.5 Subcutaneous glucose tolerance test (SCGTT)	83
4.6 Daily food and water intake, urine volume	85
4.7 Serum parameters	90
4.8 Body weight	91
4.9 Organ weights	96
4.10 Descriptive histological and immunohistochemical findings of the pancreas	99
4.11 Quantitative-stereological findings of the pancreas	101
4.11.1 Total islet volume	101
4.11.2 Volume density of islets in the pancreas	102
4.11.3 Total B-cell volume	102
4.11.4 Volume density of B-cells in the islets	103
4.11.5 Total volume of endocrine non-B-cells	104
4.11.6 Volume density of non-B-cells in islets	105
4.11.7 Total volume of isolated B-cells	107
4.11.8 Volume density of isolated B-cells in the pancreas	108
4.12 Urine protein analysis	109
4.13 Macroscopical, histological and immunohistochemical findings of the kidneys	111
4.14 Quantitative-stereological findings of the kidneys	116
4.14.1 Kidney volume	116
4.14.2 Mean glomerular volume	117
4.15 Twelve-month survival	119

5. Discussion	125
6. Perspective	136
7. Summary	137
8. References	140
9. Attachment	156
9.1 Silver stain for SDS-PAGE gels	156
9.2 Drying of SDS-PAGE gels	156
9.3 Staining procedures for plastic embedded sections	157
9.3.1 H&E	157
9.3.2 Periodic acid-Schiff stain (PAS)	158
9.3.3 Periodic acid silver methenamine PAS stain	158
9.4 Staining procedures for paraffin embedded sections	159
9.4.1 H&E	159
9.4.2 PAS stain	159
9.4.3 Gomori's silver stain (modified)	160
9.4.4 Best's carmine	161
9.5 Fat red stain	162
Acknowledgement	165
Curriculum vitae	167

1. Introduction

The connection of the gastrointestinal tract and the endocrine pancreas was shown in the 1960s when insulin became measurable in plasma. Comparison of oral and intravenous glucose tolerance tests revealed a much higher insulin secretory response of the endocrine pancreas after oral or intrajejunal glucose administration than after intravenous glucose injection (McIntyre *et al.* 1964). The enteroinsular axis was found to be in charge of approximately 50% of the insulin release after oral glucose (Unger & Eisentraut 1969). One of the major incretin hormones responsible for the greater insulin secretory response after oral vs. intravenous glucose administration is GIP (glucose-dependent insulinotropic polypeptide or gastric inhibitory polypeptide). Immunoneutralization of GIP reduced the insulin secretory response by up to 72% and was therefore thought to be of major importance in regulating postprandial glycemia.

Disturbances in the enteroinsular axis have been described in diabetic patients and animal models of diabetes. Especially the insulin response to GIP administration was regularly found to be diminished in diabetes mellitus.

In the present study, transgenic mice expressing a dominant negative GIP receptor (GIPR^{dn}) under the control of the rat insulin gene promoter were investigated; non-transgenic littermates served as controls. Since the GIP-/GIPR-axis is regarded to be of importance in the pathogenesis of diabetes mellitus, a precise clinical survey was performed in GIPR^{dn} transgenic mice, in order to characterize the metabolic state in comparison to their non-transgenic counterparts.

GIP was recently found to be a mitogenic factor for B-cells via pleiotropic signaling pathways and could therefore be of importance for the development of the endocrine pancreas. In this study, the effects of transgene expression on postnatal pancreatic islet and B-cell development were determined, using quantitative stereological methods. In addition, functional and morphological renal changes resulting from chronic disturbance of the metabolic state were investigated.

2. Literature review

2.1 Diabetes mellitus

2.1.1 Definition and description of diabetes mellitus

Diabetes mellitus comprises a heterogeneous group of metabolic diseases, which is characterized by hyperglycemia resulting from defects in insulin secretion, insulin action or both. Chronic hyperglycemia leads to long-term damage, dysfunction and failure of various organs, especially the eyes, kidneys, nerves and the cardiovascular system (The expert committee on the diagnosis and classification of diabetes mellitus 1997).

At least three different factors are involved into the *pathogenesis* of diabetes mellitus (Table 2.1).

Table 2.1 Pathogenetic factors of diabetes mellitus (Lehmann & Spinas 2000)

1. Genetic predisposition, e.g. mutation in the glucokinase gene, in different transcription factors, mutations in the insulin receptor
2. Insulin resistance (muscle, liver, adipose tissue)
3. Defective insulin secretion of the pancreatic B-cell

Signs of diabetes mellitus include hyperglycemia, polyuria, polydipsia, weight loss, hyperphagia and sometimes blurred vision. Impairment of growth and susceptibility to certain infections may also accompany chronic hyperglycemia. Acute and life-threatening consequences of diabetes are hyperglycemia with ketoacidosis or the nonketotic hyperosmolar syndrome.

Long-term complications of diabetes include retinopathy with potential loss of vision, nephropathy leading to renal failure (see 2.2), peripheral neuropathy with risk of foot ulcers, amputation and Charcot joints, and autonomic neuropathy causing gastrointestinal, genitourinary, cardiovascular symptoms and sexual dysfunction. Glycation of tissue proteins and other macromolecules and excess production of polyol com-

pounds from glucose are among the *mechanisms* thought to produce tissue damage from chronic hyperglycemia. Patients with diabetes have an increased incidence of atherosclerotic cardiovascular, peripheral vascular and cerebrovascular disease. Hypertension, abnormalities of lipoprotein metabolism, and periodontal disease are often found in diabetic patients (The expert committee on the diagnosis and classification of diabetes mellitus 1997).

2.1.2 Diagnosis of diabetes mellitus

There are different methods for diagnosing diabetes mellitus in humans (Mayfield 1998):

1. Casual plasma glucose levels (at any time of the day) ≥ 200 mg/dl and clinical symptoms of diabetes mellitus
2. Fasting plasma glucose (FPG) (no caloric intake for at least 8 h) ≥ 126 mg/dl
3. Plasma glucose two hours after an oral glucose load (75 g anhydrous glucose dissolved in water) ≥ 200 mg/dl

According to the American Diabetes Association (ADA), the measurement of fasting plasma glucose (FPG) levels is sufficient for the diagnosis of diabetes mellitus (The expert committee on the diagnosis and classification of diabetes mellitus 1997). The World Health Organization (WHO) rather suggests performing an oral glucose tolerance test (OGTT), using 75 g glucose per person. Only if an OGTT cannot be performed, FPG levels should be used for diagnosis, according to the WHO (Alberti & Zimmet 1998). FPG and OGTT do not identify the same persons; especially patients with impaired fasting glucose (IFG) can be actually diagnosed as diabetics in an OGTT (Mannucci *et al.* 1999). Epidemiological studies have shown that unlike FPG, impaired glucose tolerance (IGT) is a predictor for the risk of developing cardiovascular disease (Tominaga *et al.* 1999).

The expert committee on the diagnosis and classification of diabetes mellitus (1997) recognizes an intermediate group of subjects whose glucose levels, although not meeting criteria for diabetes, are nevertheless too high to be considered normal. Di-

agnostic criteria for non-diabetic subjects, the intermediate group and criteria for diagnosing diabetes mellitus are listed in Table 2.2.

Table 2.2 Diagnostic criteria for diagnosing diabetes mellitus: fasting plasma glucose values and two-hour post-load plasma glucose (PG) values after oral glucose challenge (The expert committee on the diagnosis and classification of diabetes mellitus 1997)

Diagnosis	Criteria
Non-diabetic	FPG < 110 mg/dl 2-hour post-load PG values < 140 mg/dl
Impaired fasting glucose (IFG)	FPG \geq 110 and < 126 mg/dl
Impaired glucose tolerance (IGT)	2-hour post-load PG values \geq 140 mg/dl and < 200 mg/dl
Diabetes mellitus	FPG \geq 126 mg/dl 2-hour post-load PG values \geq 200 mg/dl

Since hyperglycemia can be transitory e.g., due to infections, cardiovascular episodes, trauma and other stress factors, the diagnosis should be confirmed on a different day, by one of the three methods (see above).

2.1.3 Classification of diabetes mellitus

The etiology is the main criteria for the new classification of human diabetes mellitus, according to the ADA and WHO (Lehmann & Spinas 2000). Therefore, terms like insulin-dependent diabetes mellitus (IDDM) and non-insulin-dependent diabetes mellitus (NIDDM) are no longer used. The same is true for the terms juvenile and adult diabetes, because 50% of type 1 diabetic patients are diagnosed when they are over 20 years of age and the incidence is equal for every decade after the 20th year of one's life. According to the ADA and WHO, four main types of diabetes mellitus can be distinguished (Table 2.3) (Lehmann & Spinas 2000).

Table 2.3 Etiologic classification of diabetes mellitus according to the ADA and WHO 1998 (Lehmann & Spinas 2000)

Type 1 Diabetes mellitus

B-cell destruction, usually leading to absolute insulin deficiency

- Immune mediated
- Idiopathic (rare, no indices for autoimmune disease)

Type 2 diabetes mellitus

Ranges from predominantly insulin resistance with relative insulin deficiency to a predominantly insulin secretory defect with insulin resistance

Specific types of diabetes

- Genetic defects of B-cell function, maturity onset diabetes of the young (MODY):
 - MODY 1: Defective HNF (hepatocyte nuclear factor) -4 α , chromosome 20
 - MODY 2: defective glucokinase, chromosome 7
 - MODY 3: defective HNF-1 α , chromosome 12
 - MODY 4: defect of the insulin promoter factor-1 (IPF-1)
 - MODY 5: defective HNF-1 β , mitochondrial diabetes and others
- Genetic defects in insulin action (type A insulin resistance, Leprechaunism, Rabson-Mendenhall-Syndrome: defective insulin receptor, lipotrophic diabetes and others)
- Diseases of the exocrine pancreas (pancreatitis, trauma/pancreatectomy, cystic fibrosis, neoplasia, hemochromatosis, fibrocalculous pancreatopathy and others)
- Endocrine disorders (acromegaly, Cushing's syndrome, Conn's syndrome, pheochromocytoma, hyperthyroidism and others)
- Chemically induced (steroids, pentamidine, diazoxide, thiazides, nicotinic acid and others)
- Infections (congenital rubella, measles, Coxsackie viruses, cytomegaly virus)
- Rare forms of immunogenic diabetes (Stiff-Man Syndrome, anti-insulin receptor antibodies and others)
- Other genetic syndromes, associated with diabetes mellitus (Down syndrome, Klinefelter's syndrome, Turner's syndrome, myotonic dystrophy and others)

Gestational diabetes mellitus

Women who develop type 1 diabetes mellitus during pregnancy and women with undiagnosed asymptomatic type 2 diabetes mellitus that is discovered during pregnancy are classified with gestational diabetes mellitus. Most women with gestational diabetes mellitus develop a relative insulin deficiency during the second half of the pregnancy, leading to hyperglycemia. After delivery, hyperglycemia resolves in most women but places them with increased risk of developing type 2 diabetes mellitus later in life (Mayfield 1998).

2.1.4 Screening for diabetes mellitus

For screening and diagnosis of diabetes mellitus, FPG and 2-hour post-load PG values after oral glucose challenge are most suitable (see chapter 2.1.2). Due to non-reproducible values in healthy subjects and a high range of variation, despite identical blood glucose values, glycosylated hemoglobin (HbA_{1c}) is unsuitable for the screening for diabetes mellitus (Kilpatrick *et al.* 1998; Simon *et al.* 1999). However, HbA_{1c} levels above 6.2% have shown to correlate with the likelihood of having or developing macro- or microvascular disease; measuring this parameter has therefore been recommended for monitoring the treatment of diabetes mellitus and glycemia (The expert committee on the diagnosis and classification of diabetes mellitus 1997).

Screening for type 1 diabetes mellitus

According to the depth of the prevalence and incidence of type 1 diabetes, a general screening for type 1 diabetes seems to be unsuitable (prevalence of type 1 diabetes mellitus in the total German population 0.3%; incidence of type 1 diabetes in Germany 12/100,000 (Ziegler & Scherbaum 1998)). The determination of auto-antibodies in healthy subjects, especially of relatives of type 1 diabetics, is not being advised in other than clinical surveys because to date, there are no effective intervention strategies for the prevention of type 1 diabetes (Mayfield 1998).

Screening for type 2 diabetes mellitus

Determination of FPG should be performed from 45 years of age onwards and is recommended to be repeated in three-year intervals if normal. Screening for diabetes in

younger subjects is advisable if one or more of the following criteria are true (Mayfield 1998):

- Obesity (body mass index = body weight (kg) / height (m)² ≥ 27 kg/m²).
- First-degree relative with diabetes mellitus
- Member of high risk-ethnic group (black, Asians, Hispanic, Native American and others)
- History of gestational diabetes mellitus or delivering a baby weighing more than 4 kg
- Hypertension (≥ 140/90 mm Hg)
- HDL-cholesterol < 0.9 mmol/l and/or triglyceride level ≥ 2.8 mmol/l
- History of IGT or IFG on prior testing (FPG ≥ 110 and < 200 mg/dl)

2.1.5 Screening for diabetes-associated organ lesions

Screening for diabetes-associated organ lesions in type 1 diabetic patients should be first carried out five years after diagnosis. In contrast to type 1 diabetes, onset of type 2 diabetes is not acute and cannot be clearly defined. Since 30-50% of type 2 diabetics, even in western countries are not diagnosed and taking into account that 50% of newly diagnosed diabetics already exhibit secondary organ lesions, a regular screening for type 2 diabetes is recommended. In case of diagnosis, cardiovascular risk factors and secondary organ lesions should be surveyed according to the criteria in Table 2.4 (The Diabetes Control and Complications Trial Research Group 1993).

Table 2.4 Screening for secondary organ lesions in type 1 and 2 diabetes mellitus (The Diabetes Control and Complications Trial Research Group 1993)

Retinopathy	yearly ophthalmologic examination
Nephropathy	determination of urinary albumin excretion (night urine < 20 µg/min, 24-hour urine < 30 mg/24h, albumin : creatinine ratio < 2.5 (male) / < 3.5 (female))
Peripheral neuropathy	yearly examination for the presence of peripheral

	sensorimotor neuropathy, testing of nerve conduction in at least two peripheral nerves and autonomic nerve testing
Cardiovascular risk factors	measurement of blood pressure and detection of plasma lipids (in contrast to type 2 diabetics, in type 1 diabetic patients, disturbances in plasma lipid content and hypertension only occur in coincidence with bad diabetes control and overt diabetic nephropathy, respectively)

2.1.6 Diabetic animal models

Animal models have been used intensively in order to clarify the etiology and pathogenesis of diabetes mellitus, as well as to try to prevent its development and progression. Some of these animal models are presented below in order to give a brief overview of the most commonly used models.

2.1.6.1 Animal models of type 1 diabetes

The Bio Breeding (BB) rat

The spontaneously diabetic rat syndrome was recognized in 1974 at the Bio Breeding Laboratories, Canada. The inheritance pattern of susceptibility is that of an autosomal recessive gene, however, only 50% of the susceptible animals develop diabetes (Janle-Swain 1985). Diabetes onset is mainly between 60 and 120 days of age; an abrupt onset with glucosuria, hyperglycemia, ketonuria, hypoinsulinemia and death from ketoacidosis within one or two weeks is typically found in younger animals, whereas in older animals, diabetes development is slower and less dramatic. Besides classic diabetic symptoms, rapid weight loss is a good predictor of diabetes development (Buschard 1996). A variety of hormonal and metabolic abnormalities have also been found in this strain. Glucagon and somatostatin are elevated in diabetic animals; growth hormone secretion is initially normal but decreases with metabolic decompensation. Elevation in free fatty acids and branched chain amino acid levels are proportional to the severity of diabetes. There is an increased hepatic glu-

coneogenesis and decreased glucose utilization comparable to human type 1 diabetes (Janle-Swain 1985). The disease mechanisms have been intensively investigated. As in human type 1 diabetes, insulinitis is seen prior to clinical diabetes and in some BB rats, which do not develop diabetes mellitus. The infiltrate consists of CD4- and CD8-positive lymphocytes and NK cells. Macrophages are believed to be the first cells invading the islets. The BB rat shows lymphocytopenia, which can be recognized before clinical onset of diabetes. NK cells have been suggested to be responsible for the destruction of B-cells, due to their capability of lysing islet cells *in vitro*. However, it now seems proven that the small number of CD4 cells is ultimately responsible. The BB rat displays islet cell antibodies, which can be detected up to two weeks before onset of diabetes. Furthermore, antibodies against lymphocytes as well as against smooth muscles and gastric parietal cell antigens have been found (Buschard 1996).

The nonobese diabetic mouse (NOD mouse)

The NOD mouse strain was established in 1974 in Osaka, Japan. In this strain, up to 80-90% of females develop diabetes between 80 and 200 days of age. The incidence in male mice is between 10-50%, but there is a substantial variation in different colonies. Gonadal sex hormones are important modulators of diabetes development in NOD mice: castrated males show higher incidence and oophorectomized females a lower incidence of diabetes. The appearance of diabetes is followed by classic symptoms, such as hyperglycemia, hypoinsulinemia, glucosuria, ketonuria, polydipsia and polyuria. In contrast to BB rats, NOD mice can survive up to several months after onset of diabetes. NOD mice display islet cell and islet cell surface antibodies with a peak after the age of six months and an incidence of up to 80%. Insulin autoantibodies are present in up to 80% of the mice after three months. Up to 95% of the mice show insulinitis, which may already be seen at 5-6 weeks of age. The earliest changes are periinsulinitis followed by invasion of the islet capsule. In its final form, insulinitis in NOD mice is typically present in one part of the islet, which is heavily infiltrated, whereas the other part is completely normal. The mononuclear infiltrate looks more like a leukemia infiltrate than an inflammatory process; its shape can be crescent. B- and T-cells, as well as NK cells and activated lymphocytes are seen in insulinitis, the

first infiltrating cells being monocytes. The odd looking insulinitis could be a major disadvantage in this otherwise convenient model (Buschard 1996).

Virus-induced diabetes

Environmental factors are thought to play a pathogenetic role in the development of diabetes mellitus and in this context, virus is a likely candidate. For experimental models, encephalomyocarditis (EMC virus) is the most widely used. The result of the virus infection is dependent on the virus strain (diabetogenic, non-diabetogenic) and is also highly dependent on the mouse strain used (Buschard 1996). Encephalomyocarditis virus is a picornavirus possessing many of the biologic and pathogenetic properties of the group B Coxsackie viruses. Infection of genetically susceptible strains of mice leads to the development of lesions of the islets of Langerhans, accompanied by diabetes mellitus. The occurrence of diabetes in this model is affected by complex interrelated genetic, immunologic and environmental influences. After subcutaneous inoculation, encephalomyocarditis virus multiplies in the islets of Langerhans and causes lesions of the B-cells. During early stages of infection, B-cells degranulate and the insulin content of the pancreas decreases markedly with hyperglycemia appearing concomitantly. A mononuclear cell infiltrate appears transiently (until the second week of infection) around the islet with the persistence of the infection. During convalescence (two to three weeks after inoculation), three patterns of metabolic disease can be observed. Some animals display profound hyperglycemia and ketoacidosis. These mice lose weight and die several months after inoculation. Histologically, islets are shrunken, distorted and lack detectable amounts of insulin. In other animals, hyperglycemia is less marked for an extended period of time. After several months, animals can recover, apparently due to the regeneration of insular tissue. Finally, a number of animals exhibit normal fasting blood glucose concentrations and disturbed oral glucose tolerance (Craighead 1981).

Four other human viruses are known to cause lesions of pancreatic islets in experimental animals. Venezuelan encephalitis virus damages islets of hamsters and non-human primates, resulting in carbohydrate intolerance. Further, rubella virus infection, reovirus and cytomegalovirus cause damage of pancreatic islets and B-cells (Craighead 1981).

Streptozotocin induced diabetes

The streptozotocin diabetic rat is a well-described and widely used model for the study of type 1 diabetes. Streptozotocin is a by-product of the bacterium *Streptomyces achromogenes* with extensive antimetabolic properties (Weil *et al.* 1976). It causes necrosis of B-cells of the pancreas and diabetes in the mouse, rat, guinea pig, and dog. Streptozotocin is administered intravenously or intraperitoneally in single doses (Janle-Swain 1985). Rats develop hypoinsulinemia, hyperglycemia, and increased gluconeogenesis, lipo- and glycogenolysis. Drawbacks of this chemical include nephro- and hepatotoxicity. In rats treated with streptozotocin, cystic changes occur in both liver and kidney. Furthermore, up to 30% of the animals rendered diabetic using streptozotocin develop renal tumors within six or seven months (Steffes & Mauer 1984).

The mentioned models of type 1 diabetes have all proven useful in diabetes research, however, none of them is ideal. The BB rat develops lymphopenia and a low percentage of CD4 cells; the NOD mouse has odd insulinitis and female dominance, the virus model is difficult to handle and it does not simulate fully the picture of type 1 diabetes in man (Buschard 1996), and streptozotocin causes the development of renal tumors (Steffes & Mauer 1984).

2.1.6.2 Animal models of type 2 diabetes

Cohen diabetic rat

The strain was developed by genetic selection of albino rats from the Hebrew University strain for their propensity to develop overt diabetes and diabetes-related complications when fed a diet rich in sucrose or other refined sugars and poor in copper content (Velasquez *et al.* 1990). Hyperglycemia, glucosuria and hyperinsulinemia, insulin resistance, and a decrease in the number and sensitivity of insulin receptors are characteristic findings in diabetic Cohen rats. When Cohen rats are fed a starch or stock diet, no overt diabetes develops (Velasquez *et al.* 1990).

Obese spontaneously hypertensive rat (SHR)

The obese spontaneously hypertensive rat (SHR) strain was developed by mating a female SHR of the Kyoto-Wistar strain with a normotensive Sprague-Dawley male. After several generations of selective inbreeding, the obese SHR exhibited obesity, hypertension, and hyperlipidemia. In addition, some animals develop hyperglycemia and glucosuria associated with giant hyperplasia of pancreatic islets. Hypertension occurs early and precedes the development of kidney disease (Velasquez *et al.* 1990).

Obese mouse (ob/ob)

The obese mouse was discovered as a spontaneous autosomal recessive mutation at the Jackson Laboratory, Bar Harbor, Maine, USA, where the mutant originally presented with massive obesity and marked hyperglycemia. The mutation in the ob gene leading to leptin deficiency was transferred later and maintained in different inbred strains. Depending on the inbred background, the ob/ob mouse may present with different obesity-diabetic syndromes. Thus, the ob mutant maintained on the C57BL/6J mouse strain (C57BL/6J ob/ob) develops massive obesity, mild glucose intolerance, transient hyperglycemia, and severe hyperinsulinemia associated with hyperplasia of pancreatic islets. In contrast, the C57BL/KsJ ob/ob mouse develops severe diabetes marked by initial transient hyperinsulinemia, followed by rapidly developing insulinopenia due to pancreatic B-cell atrophy, leading to the early death of the animal (Janssen *et al.* 1999).

Diabetes mouse (db/db)

The diabetes mouse is another strain derived from the autosomal recessive mutation discovered at the Jackson Laboratory in Bar Harbor, Maine, USA. This mutation occurred spontaneously in mice of the C57BL/KsJ strain. On this background, the diabetes mouse (C57BL/KsJ db/db) consistently develops a severe diabetic syndrome similar to that in C57BL/KsJ ob/ob mouse, characterized by early onset (4-6 weeks of age) of hyperphagia, obesity, hyperglycemia, hyperinsulinemia, weight loss, down-regulation of insulin receptors and early death. Diabetes is more severe in this strain

compared to other obese mutants. The db gene has also been transferred to the C57BL/6J strain; the C57BL/6J db/db mouse develops obesity with mild hyperglycemia, and hyperinsulinemia (Velasquez *et al.* 1990).

Kuo Kondo (KK) mouse

The KK mouse is one of a series of genetically diabetic strains, established by Kondo and coworkers (Kondo *et al.* 1957; Nakamura & Yamada 1967). The mode of inheritance is not fully understood but assumed to be polygenic. This strain is characterized by slowly developing obesity, mild hyperglycemia with hyperinsulinemia, and an increase in size and number of pancreatic islets. Metabolic abnormalities are maximal at 4-9 months and normalize at one year. Because of polygenic inheritance, there is a lack of an appropriate control mouse with which to make comparisons (Janssen *et al.* 1999). From mating of KK females and yellow KK^{ay} males at the Takeda Chemical Corporation, Osaka, Japan, the KK^{ay} mouse was established. It differs from the KK mouse, because it carries yellow obese and diabetic genes, whereas the KK mouse carries only the diabetic gene. KK^{ay} mice are obese and have early onset and prolonged hyperinsulinemia and hyperglycemia (Janle-Swain 1985; Velasquez *et al.* 1990).

2.2 Diabetic nephropathy

Diabetic kidney disease is known for a long time, but it was only after insulin therapy, that renal complications became an important problem in diabetic patients. Longer life expectancy is probably the reason since the increased life span would give a longer time for the various structural changes to develop (Heptinstall 1991). Kimmelstiel and Wilson first described glomerular lesions characteristic for diabetes (Kimmelstiel & Wilson 1936). The knowledge of the structure of kidney lesions has extended ever since. Today, diabetic kidney disease is the single commonest cause of end-stage renal failure worldwide (Thomas & Viberti 2000).

2.2.1 Diabetic glomerulosclerosis

The first morphological change of the human diabetic kidney after onset of diabetes is an increase in glomerular size and therefore, a rise in filtration area, resulting in an increase in glomerular filtration rate (Romen 1980). Approximately two years after onset of diabetes, glomerular basement membranes begin to thicken and the expansion of capillary walls and the mesangium leads to the development of the so-called diffuse form of glomerulosclerosis. Nodular glomerulosclerosis may develop in more advanced kidney damage. Another group of lesions that comprises diabetic glomerulosclerosis are the exudative lesions (Ritz & Usadel 1999).

The *nodular lesion* is the type of change originally described by Kimmelstiel and Wilson in 1936. It typically consists of a rounded, homogeneous, eosinophilic, PAS positive area situated in the central part of a lobule, usually toward the periphery. Several lobules within a given glomerulus can be affected, and the nodules are usually of varying size. The nodules are often acellular, but elongated cells may appear concentrically arranged near the periphery. Around the periphery of the nodule, the capillaries are usually patent with the capillary walls appearing thickened. Glomerular capillaries may be dilated as to be microaneurysmal, and lipophages are sometimes seen, apparently in capillary lumens. The glomerular tuft often retains size, which is in contrast to the shrinkage that accompanies the purely ischemic glomerulus. In late stages, exudative lesions (see below) appear more frequently and glomeruli are reduced in size (Heptinstall 1991). It has been postulated that nodules result from repair processes of microaneurysmal glomerular capillaries, breakage and lysis of the mesangium, as well as organization of mesangial destruction (Ritz & Usadel 1999).

The *diffuse lesion* consists of an increase in eosinophilic, PAS-positive material in the mesangium. The process also includes thickening of the capillary walls, which is often wide spread within a glomerulus and may affect all glomeruli. In later stages, as thickening progresses, capillary lumens become reduced. The capsule of Bowman becomes thickened in more advanced lesions and both afferent and efferent arterioles are hyalinized. Unlike the nodular lesion, the diffuse lesion is not specific for diabetes and can occur in other conditions, such as glomerulonephritis (Heptinstall 1991).

Another type of lesion seen in diabetic patients is the *exudative lesion*, which includes fibrinoid caps and capsular drops, as well as arteriolar hyalin changes. The

fibrinoid cap appears as an eosinophilic, smooth, homogenous crescentic structure lying in the concavity of a capillary, usually at the periphery of a lobule. It has general appearance of fibrin, is sometimes foamy, and contains lipid. The lesion is most commonly in diabetic kidneys with severe vascular disease but not specific for diabetic glomerulosclerosis. *Capsular drops* appear as small, rounded, eosinophilic masses on the inside of Bowman's capsule between the basement membrane and the parietal epithelial cells (Heptinstall 1991). This lesion was first described in Kimmelstiel and Wilson's (1936) original paper, but only later it was regarded as diagnostic aid for diabetic glomerulosclerosis. The *arteriolar hyalin change* is a lesion of both afferent and efferent arterioles, the walls of which are thick, homogenous or slightly fibrillar and vacuolated, and strongly eosinophilic and PAS positive. The normally occurring structures disappear and no muscle coat can be seen in an arteriole with well-developed hyalin change. The PAS positive arteriolar lesion is continuous with the diffuse lesion in the lobules through a PAS positive thickening in the capillary stalk (Heptinstall 1991; Olsen 1969). Arteriolar hyaline change of the afferent arterioles may also be seen in patients with essential hypertension, whereas the hyalin change of the efferent arterioles is considered diabetes specific (Ritz & Usadel 1999).

2.2.2 Tubular changes

The proximal convoluted segment of the tubules often appears finely vacuolated, with lipid being demonstrable in frozen sections. In more advanced lesions there is tubular loss, with atrophic tubules showing thickened basement membranes. Glycogen containing tubular epithelia (Armanni-Ebstein change), once considered characteristic for diabetes, are seen only very occasional now, being sited in the pars recta of the proximal tubule (Heptinstall 1991).

2.2.3 Interstitial changes

The interstitial tissue is frequently fibrotic and may contain inflammatory cells. Lymphocytes and plasma cells may be so plentiful that the reaction is indistinguishable from that seen in chronic infections. Interstitial infiltrates become more numerous with the increasing duration of diabetes and with the degree of arteriosclerosis (Heptinstall 1991).

These morphological changes of the human diabetic kidney are the underlying cause of functional abnormalities, such as proteinuria, with urinary albumin excretion being the most powerful predictor of progression of renal injury (Wang *et al.* 2000). Proteinuria is no longer simply considered a marker for renal dysfunction – protein is nephrotoxic and a causative agent for renal damage (Marshall & Williams 1998).

2.2.4 Pathophysiology of proteinuria

Due to filtration and re-absorption mechanisms of the healthy kidney, only very small amounts of protein are found in urine (Marshall & Williams 1998). The glomerular filtration system stops albumin (67 kDa) and larger proteins from passing into primary urine. Smaller serum proteins are filtrated but reabsorbed by the tubular system. Therefore, the localization of kidney damage can be estimated from the type of protein(s) present in urine. Large proteins prove a glomerulopathy, if postrenal serum or blood contamination can be excluded. Podocyte damage causes a *selective glomerular* proteinuria (60-150 kDa: transferrin, albumin, dimeric albumin), damage of glomerular basement membranes and mesangium cause an *unselective glomerular* proteinuria (60-350 kDa, dimeric albumin) (Bergstein 1999; Oser & Boesken 1993; Stierle *et al.* 1990). Both types of proteinuria can be observed in diabetic kidney disease. Small proteins reflect tubular or interstitial injury resulting in insufficient re-absorption of microproteins. Depending on the grade of alteration, an incomplete *microproteinuria* (40-70 kDa) or a complete microproteinuria (10-70 kDa) can occur (Marshall & Williams 1998). *Tubular proteinuria* can be observed in patients with chronic interstitial nephritis, rejected kidney transplantate and others. Many nephropathies damage both, glomeruli and tubules and therefore, mixed types of glomerular and tubular proteinuria can be found (Marshall & Williams 1998). Since urinary proteins can already be altered before proteinuria can be detected with routinely used diagnostic methods, the urine profile determined using the SDS-PAGE (sodium dodecyl sulfate-polyacrylamide gel electrophoresis) is an excellent diagnostic aid for early detection of nephropathy. Especially in individuals with systemic diseases, such as diabetes mellitus, and in follow up studies (diagnosed acute kidney diseases, transplantation), this method is recommended for early diagnosis of secondary kidney damage. An important advantage is that the SDS-PAGE makes it possible to distinguish between renal and postrenal cause of blood appearance in urine.

Postrenal blood contamination of urine shows a characteristic protein profile in a SDS-PAGE, containing a specific microprotein (~30 kDa) and hemoglobin but the urine usually does not consist of proteins larger than 400 kDa or microproteins as observed in tubular proteinuria (Oser & Boesken 1993).

2.2.5 Development of proteinuria

The onset of clinically overt diabetic kidney disease in humans is defined as persistent proteinuria. Diabetic patients that develop proteinuria pass through the different stages in sequence, from normoalbuminuria to microalbuminuria and finally proteinuria (Parving *et al.* 1996). Very low rates of albumin excretion, i.e. microalbuminuria, are potent predictors of renal and cardiovascular risk in diabetic patients. The degree of albuminuria has turned out to be the most powerful predictor of progression of renal injury (Wang *et al.* 2000). This finding is in coincidence with the current opinion that exposure of tubular epithelial cells to protein is a crucial step in perpetuating progression through activation of tubular epithelial cells and the start of interstitial fibrosis (Klahr 1999; Odoni & Ritz 1999; Wang *et al.* 2000). The overall prevalence of microalbuminuria and macroalbuminuria is about 30-35% in both types of diabetes mellitus. The annual rise in urinary albumin excretion is about 20% in both type 1 and 2 diabetic patients (Parving *et al.* 1996).

2.2.6 Animal models of diabetic kidney disease

Since Kimmelstiel and Wilson (1936) described diabetic glomerulosclerosis, numerous studies have been conducted to investigate the disease. The validity of the findings in human diabetics is limited, since studies were always carried out after prolonged duration of the disease. Hence introduction of experimental models of diabetes constituted great progress since very early stages of the disease could then be studied (Wehner & Petri 1983). Rodents, particularly rats and mice are used as experimental models of diabetic kidney disease. Major advantages of these rodent models are the low cost of acquiring and maintaining and the fact that large numbers can be studied in a reasonable amount of time. However, there are several disadvantages of rodent models. The renal lesions do not completely parallel the renal lesions in human diabetes, which might be due to short life span and lack of adequate time for the complete syndrome to develop or due to a difference in the pathological proc-

ess in the rodent kidney. The lesions in the diabetic rat kidney only resemble the lesions of early human diabetes to a certain extent and do not tend to progress. Further, because of the small size of the animals, repeated sampling of renal tissue is not always possible on the same animal. In models where diabetes is induced, studying of the consequences of the metabolic state is being carried out without confounding hereditary factors, which could influence the development of diabetic nephropathy (Janle-Swain 1985). As mentioned above, streptozotocin given in sufficient amounts to induce diabetes mellitus causes renal tumor development within 6-7 months in up to 30% of the animals (Steffes & Mauer 1984). The dog is considered a useful model for the study of diabetic nephropathy. Due to its large size, long life span, tractable nature, and ease of blood sampling, long-term studies with repeated blood and biopsy sampling is possible. The diabetic dog kidney more closely resembles the lesions in human diabetes. Similar lesions, reminiscent of the nodular form of human glomerulosclerosis and exudative lesions have been observed in spontaneously diabetic dogs (Bloodworth *et al.* 1969; Janle-Swain 1985). In contrast, another workgroup did not observe lesions identical to human diabetic glomerulosclerosis in spontaneous diabetic dogs or cats (Gepts & Toussaint 1967). A disadvantage of canine models of diabetes is the high cost of acquiring and maintaining large animals. The same is true for nonhuman primate models of diabetes. Furthermore, specialized facilities are required for maintaining primates and a long period is necessary for the renal lesions to develop (Janle-Swain 1985). Despite a number of similarities between human diabetic kidney and lesions produced in experimental animals, there is profound difference to the morphology of characteristic human lesions (Olsen 1969). The above listed disadvantages of currently used animal models for studying diabetic kidney disease explain the need for an animal model that develops kidney lesions which closely match the changes in the human diabetic kidney.

2.3 Development of the endocrine pancreas

2.3.1 Patterning and early pancreas development

In mammals, the pancreas develops as two outpocketings – the dorsal and the ventral bud – from the primitive foregut (Pictet *et al.* 1972). The two buds consist of endodermal cells surrounded by mesenchyme, giving rise to both the endocrine and

exocrine division of the pancreas. The dorsal pancreatic bud forms at about 9.5 days (20-25 somites) post conception in the mouse, the ventral bud appears at around day 10 post conception (30 somites) (Pictet *et al.* 1972). As the buds grow, they rapidly form new protrusions leading to a highly branched structure. Acini and ducts become clearly visible by about E14.5 in the mouse. Various terminally differentiated products are found throughout the pancreatic development. Endocrine cells can be detected in the forming pancreas from the earliest stages, being largely individual and associated with ducts. Islet formation of endocrine cells is first observed by the end of gestation (E18.5d) in the mouse (Herrera *et al.* 1991). Pancreas organogenesis involves a sequential cascade of inductive events in association with the activation of specific transcription factors (St-Onge *et al.* 1999). Early events that define and pattern the region of the endoderm, which will give rise to the pancreas are still unknown. However, a pre-patterning of the endoderm seems to occur that will define and specify the area of the embryonic foregut from which the pancreatic buds will form (St-Onge *et al.* 1999). Spatial expression of members of the hedgehog family of signaling molecules in the endoderm strongly suggests such a patterning of the foregut. Both Sonic hedgehog (Shh) and Indian hedgehog (Ihh) are expressed along the entire endodermic gut, apart from the region that will give rise to the future pancreas. The region devoid of hedgehog expression also coincides to the region where homeodomain transcription factor PDX-1 (pancreatic and duodenal homeobox gene-1) will first be expressed (Ahlgren *et al.* 1996; Offield *et al.* 1996). This part of the gut becomes committed to a pancreatic fate at the ~10 somite stage (E8.5), a few somite before this PDX-1 expressing region of the duodenal epithelium will begin to evaginate, thus forming the dorsal and ventral pancreatic buds. Notochord derived factors, such as activin- β and fibroblast growth factor (FGF) 2 have been implicated in the initial repression of Shh and Ihh expression in the presumptive dorsal pancreatic endoderm (Edlund 1999). Since the ventral pancreatic bud is never in contact with the notochord, the exclusion of Shh and Ihh gene expression must be achieved by a distinct, notochord-independent mechanism. Several transcription factors (TF), including homeodomain and basic helix-loop-helix families of TFs, have recently been implicated in the development of neural structures, and have also been found to be important for islet cell development and function (Ahlgren *et al.* 1997; Naya *et al.* 1997; Sander *et al.* 1997; Sosa-Pineda *et al.* 1997; St-Onge *et al.* 1997). Hlxb9 (encoding the transcription factor Hb) is transiently expressed in the region that gives rise to the dorsal

and ventral pancreatic anlage. Hb9 expression becomes restricted to the insulin producing B-cells later in development. In the dorsal bud, Hb9 expression precedes the expression of PDX-1, whereas in the ventral anlagen, Hb9 and PDX-1 are expressed concurrently (Edlund 1999). In mice lacking Hlx9 function, dorsal pancreatic development is blocked, whereas the ventral pancreas develops and contains both endocrine and exocrine cells; however, the relative proportions and spatial organization of the various endocrine cells is perturbed (Harrison *et al.* 1999; Li *et al.* 1999). Immunohistochemistry has demonstrated expression of PDX-1 in most cells of the early ventral and dorsal pancreatic buds (Guz *et al.* 1995). Later in the development, PDX-1 expression becomes restricted to insulin producing B-cells. Endocrine cells can be found even in the earliest buds, which are characterized by immunoreactivity for glucagon, peptide tyrosine tyrosine (PYY), and insulin (Larsson 1998). Since all early-appearing endocrine cells of the mouse and rat pancreas express PYY, the peptide was thought to constitute a marker for early differentiating endocrine cells. PYY could be expected to exert some functional role during pancreatic development. Thus, the earliest endocrine cells (E9.5) to appear are multihormonal and express PYY and glucagon; some are even triple positive for PYY, glucagon and insulin. Cells expressing somatostatin and pancreatic polypeptide (PP) appear rather late in the developing mouse pancreas. Bud cells expressing hormonal markers are negative for PDX-1 (Larsson 1998). This suggests that PDX-1 is not needed for early expression of pancreatic insulin, glucagon or PPY. In mice lacking the PDX-1 gene (Jonsson *et al.* 1994), which fail to grow and form a pancreas, multihormonal cells (insulin, glucagon) can be detected in the early pancreatic buds (Ahlgren *et al.* 1996). In contrast, Offield *et al.* (1996) did not observe insulin positive cells using immunohistochemical analysis, which is in coincidence with the proposed role for PDX-1 in the derivation of mature B-cells (further details are presented below) (Guz *et al.* 1995).

2.3.2 Morphogenesis and differentiation

From E10 onwards, the pancreatic epithelium proliferates and invades the surrounding mesenchyme. Epitheliomesenchymal interaction(s) then stimulate the proliferation, branching and differentiation of the epithelium into endocrine and exocrine cells. The importance of mesenchymal factors for pancreatic development was already demonstrated in 1962 (Edlund 1998), however, the nature of these factors is cur-

rently largely unknown. The mesenchyme is critically required for exocrine differentiation, but impairs endocrine development (Miralles *et al.* 1998). The branching of the pancreatic epithelium is an important aspect of pancreas morphogenesis. The factors responsible are presently unknown, but there is evidence, that FGF signaling is critically involved in controlling branching morphogenesis in the mouse (Edlund 1999). Islet morphogenesis is a complex process that involves differentiation, proliferation, and migration of pancreatic endocrine cells, culminating in the formation of properly organized, three dimensional, sphere-like structures. At about E14.5, developing endocrine cells aggregate in interstitial clusters, adjacent to the ductal epithelia. At this time of organogenesis, endocrine cell clusters do not exhibit the typical architecture of mature islets and do not contain all four islet cell types. In the remaining four days of gestation, the endocrine cells detach from the exocrine matrix, increase in number, and reorganize to form mature islets. Morphologically distinct islets are first detected with the proper distribution of endocrine cell types at E17.5 (Herrera *et al.* 1991; Picotet *et al.* 1972). Although the molecular mechanisms that control islet formation are unknown, it has been demonstrated recently that members of the cadherin family of cell adhesion molecules (CAMs) and neural CAM (N-CAM) are expressed in the pancreas and also appear to have functional roles in the aggregation and organization of the principal endocrine cell types (Dahl *et al.* 1996; Larsson 1998). Mature pancreatic islets constitute 1-2% of total mass of the adult pancreas and are composed of the principal endocrine cell types: B-cells (~80%), A-cells, D-cells and PP-cells. In murine islets, the B-cells are localized in the core of the islet, surrounded by a mantle of A-, D- and PP-cells. The integrity of islet structure has been suggested to be essential for normal islet function of regulating glucose homeostasis (Pipeleers *et al.* 1982).

2.3.3 Transcription factors linked to pancreas development

As mentioned above, several transcription factors are linked to pancreas development. In the following chapter, some of the most important transcription factors are discussed.

PDX-1 (pancreatic and duodenal homeobox gene-1)

PDX-1 expression is initiated before hormone expression at the 10-12 somite stage, and is restricted to the dorsal and ventral walls of the primitive gut endoderm. The pattern of PDX-1 expression and its ability to stimulate insulin gene transcription suggests that PDX-1 functions both in regionalization of the primitive gut endoderm and the maturation of the pancreatic B-cells (Ahlgren *et al.* 1996; Ohlsson *et al.* 1993). Homozygosity for mutations in the PDX-1 gene in mice and humans results in complete agenesis of the pancreas (Jonsson *et al.* 1994; Offield *et al.* 1996). PDX-1 does not seem to be required for the evagination and initial bud formation, but rather appears to specify the early pancreatic epithelium, permitting its proliferation, branching and subsequent differentiation (Ahlgren *et al.* 1996; Offield *et al.* 1996). Since early hormone producing cells appear in PDX-1 deficient embryos, additional transcription factors must exist, acting upstream of PDX-1. However, the subsequent morphogenesis of the pancreatic epithelium and progression of differentiation of the endocrine cells are arrested in PDX-1 deficient embryos. Since the mesenchyme that normally promotes pancreatic morphogenesis develops normal in these knockout mice, PDX-1 might act cell-autonomously, and the lack of pancreas is due to a defect in pancreatic epithelium (Edlund 1998).

Recent studies provide further insights into PDX-1 function in differentiated B-cells. Heterozygous mice, carrying a targeted mutation of the PDX-1 gene (knockout) develop diabetes with aging (Ahlgren *et al.* 1998; Dutta *et al.* 1998). Analysis of these PDX-1 +/- mice revealed that PDX-1 is required for maintaining the hormone producing phenotype of the B-cell by positively regulating insulin and islet amyloid polypeptide expression and by repression of glucagon expression. This transcription factor is also essential for expression of glucose transporter type 2 (GLUT2) in B-cells. The GLUT2 expression seems to be regulated by PDX-1 in a dose dependent manner, suggesting that lowered PDX-1 activity may contribute to the development of type 2 diabetes by causing impaired expression of both GLUT2 and insulin (Ahlgren *et al.* 1998). Interestingly, heterozygosity for mutations in the human PDX-1 gene causes MODY 4, a form of diabetes that results from defects in insulin secretion, suggesting the PDX-1 function being conserved from mice to humans (Edlund 1998).

ISL1 (islet 1)

During ontogeny, the expression of the LIM homeodomain protein islet 1 (ISL1) is initiated soon after the islet cells leave the cell cycle, and in adult pancreas, ISL1 is expressed in all classes of islet cells. ISL1 is also expressed in mesenchymal cells surrounding the dorsal, but not the ventral, evagination of the gut endoderm. In mice lacking ISL1 function, the dorsal pancreatic mesenchyme does not form, and there is an associated failure of exocrine cell differentiation in the dorsal but not the ventral pancreas. In addition, there is a complete loss of differentiated islet cells. Thus, ISL1 is necessary for the development of the dorsal exocrine pancreas and ISL1 function is required for the generation of all endocrine islet cells (Ahlgren *et al.* 1997; Edlund 1998).

PAX6 (paired box factor 6)

Paired box factor 6 (PAX6) is a member of the *pax* gene family and, along with ISL1, is expressed in all endocrine cells both during development and in the adult pancreas. In mice lacking the PAX6 gene, the numbers of differentiated endocrine cell types are markedly reduced and there is a significant reduction in hormone production (Sander *et al.* 1997; St-Onge *et al.* 1997). PAX6 expression cannot be detected in E9.5 ISL1 deficient mice, indicating that ISL1 may act upstream of PAX6 during pancreatic endocrine differentiation (Edlund 1998).

PAX4 (paired box factor 4)

PAX4 expression is evident in both pancreatic buds as early as E9.5 and becomes restricted to the developing B-cells later in ontogeny (Sosa-Pineda *et al.* 1997). Inactivation of PAX4 by homologous recombination results in the absence of mature insulin and somatostatin producing cells in the pancreas of homozygous mutant mice. Glucagon producing A-cells are present in considerably higher numbers (Sosa-Pineda *et al.* 1997). Thus, PAX4 is possibly responsible for the B-cell fate and, in the absence of PAX4, the default fate would be to become a glucagon positive A-cell. Therefore, PAX6 might directly or indirectly be involved in repressing glucagon expression (Edlund 1998).

Nkx2.2

Nkx2.2 belongs to the Nk2 homeobox family of transcription factors and is expressed from at least E8.75 in the dorsal and ventral pancreatic epithelium. Later in development, Nkx2.2 is expressed in B-, A- and PP-cells, but not in somatostatin producing cells. Mice homozygous for a null mutation of the Nkx2.2 gene lack insulin producing B-cells and have fewer A- and PP-cells. Further, a large population of islet cells does not produce any of the four hormones, but express some B-cell markers such as PDX-1 and IAPP, while lacking other definitive B-cell markers including Nkx6.1 and GLUT2. Therefore, Nkx2.2 seems to be required for the final differentiation of pancreatic B-cells, and in the absence of this member of the Nk2 homeobox family, B-cells are trapped in an incompletely differentiated state (Sussel *et al.* 1998).

Nkx6.1

Nkx6.1 is another member of the Nk2 homeobox family of transcription factors, which is initially (E9.0-9.5) expressed predominantly in the dorsal pancreatic epithelium in a subset of PDX-1 positive cells. Later in development, Nkx6.1 becomes restricted to differentiated B-cells (Jensen *et al.* 1996) and preliminary analysis of Nkx6.1 knock-out mice showed that they have drastically reduced numbers of B-cells, while the number of other islet cells remained normal (Edlund 1998).

NeuroD/BETA2

NeuroD/BETA2 is a cell-type restricted basic helix-loop-helix (bHLH) transcription factor that is expressed in all pancreatic endocrine cells (Edlund 1998; Naya *et al.* 1997). Together with its ubiquitous counterpart, the E2A gene product E12, NeuroD/BETA2 binds to the E-boxes of the insulin regulatory region. In NeuroD/BETA2-deficient mice, endocrine cells still appear, but at markedly reduced numbers: B-cells are reduced by ~75%, A-cells by 40%, and D-cells by 20%, and the remaining endocrine cells fail to form mature islets (Naya *et al.* 1997). Mice carrying the targeted disruption of the BETA2 gene develop severe early onset diabetes and die perinatally. BETA2 is present in the earliest islet precursors within or adjacent to ductal epithelia in both +/- and -/- mice. NeuroD is thought to be the earliest marker of differentiating endocrine cells and is co-expressed with PAX6, glucagon and insulin (Jensen *et al.* 2000 a). Disruption in pancreatic islet morphogenesis occurs after E14.5 in BETA2 deficient mice. From E17.5 onwards, BETA2 expressing cells are localized exclu-

sively to islets in +/- mice. The observed increase in the number of apoptotic cells in -/- mouse pancreata suggests that BETA2 is required for endocrine islet cell survival (Naya *et al.* 1997).

Ngn3 (Neurogenin3)

Neurogenin3 (Ngn3) is another member of the bHLH family of transcription factors, which is supposed to act upstream of NeuroD in a bHLH cascade. Neurogenin3 is expressed in a subset of the proto-differentiated PDX-1 positive epithelial cells. A few Ngn3 positive cells co-express early endocrine markers, such as ISL1 and PAX6, whereas no co-expression with glucagon or insulin could be observed. Ki-67, a proliferation marker is readily detected in Ngn3 positive cells, but not in NeuroD/BETA2 positive cells. A molecular pathway has been suggested, where Ngn3 positive precursor cells become committed to endocrine differentiation, marked by activation of NeuroD and subsequently ISL1, PAX6 and the hormones, whereas Ngn3 expression is extinguished (Jensen *et al.* 2000 a). Ngn3 expression increases between E9.5 and E15.5, but then decreases until day E17.5, such that very few Ngn3 positive cells are detectable in neonatal pancreas. In contrast to the findings of Jensen *et al.* (2000), Apelqvist *et al.* (1999) did not observe co-expression of Ngn3 and ISL1 or PDX-1, which led to the conclusion that Ngn3 positive cells and post-mitotic endocrine cells represent distinct populations. Therefore, Ngn3 positive cells were suggested to be endocrine precursor cells that may correspond to the primary (endocrine) fate in a lateral specification model (i.e. generation of scattered differentiated cells from an initial homogenous field of cells, as in neuronal differentiation) (Apelqvist *et al.* 1999). Overexpression of Ngn3 in transgenic mice results in an accelerated differentiation of pancreatic endocrine cells, paralleled by a depletion of the pool of pancreatic precursor cells, similar to mice genetically altered in different steps of the Notch signaling pathway (Apelqvist *et al.* 1999; Edlund 1999). Collectively, these data suggest that Ngn3 acts as a pro-endocrine gene during pancreatic development, a function analogous to that of Ngn genes in neurogenesis (Apelqvist *et al.* 1999).

Notch-signaling/HES

Mammalian homologues of the *Drosophila* hairy and enhancer-of-split factors (HES proteins) are negatively acting bHLH proteins that antagonize members of the Neurogenin and NeuroD family (Edlund 1999; Jensen *et al.* 2000 a). HES1 mutant ani-

mals display pancreatic hypoplasia due to accelerated differentiation of endocrine cells that results in a depletion of epithelial precursors (Jensen *et al.* 2000 b). HES1 is a known downstream component of the Notch-signaling system, which is thought to generate endocrine precursor cells by lateral specification. Notch-1, -2, and -3 are expressed during pancreas development. Notch-1 is expressed in epithelium at E12 in the developing mouse pancreas. At E15.5, Notch-1 mRNA is located in the forming exocrine tissue, at E17.5, localization of both Notch-1 and -2 in exocrine tissue and absence from endocrine tissue is evident. Notch-1 is also absent from most endocrine cells at E13.5, although a few PAX6 positive cells are still located in the Notch-1 positive domain. The decline in Notch expression is marked by increased expression of insulin and amylase. The presence of Notch-1 and -2 and their ligands Jagged1 (also known as Serrate1) and Dll1 (Delta-like gene1) in the pancreatic epithelium suggested that the Notch pathway could provide an inhibitory signal and thereby prevent premature differentiation of Ngn3 positive precursor cells (Apelqvist *et al.* 1999; Jensen *et al.* 2000 a). Notch signaling is thought to be critical for the decision between endocrine and progenitor/exocrine fates in the developing pancreas (Apelqvist *et al.* 1999). Notch signaling appears to control the choice between endocrine and exocrine fates, so that lack of Notch-pathway signaling, resulting in high Ngn3 levels for example in mice deficient for Dll1 or Notch-3, promotes the endocrine fate. In contrast, cells with active Notch-signaling adopt the exocrine fate and/or remain as undifferentiated progenitor cells, allowing the subsequent proliferation, morphogenesis and differentiation of the pancreatic epithelial cells (Edlund 1999).

2.3.4 Postnatal pancreatic B-cell growth

Until 15 years ago, the concept was that one was born with all pancreatic B-cells one ever had and therefore, insulin resistance would lead to diabetes without change in B-cell mass (Bonner-Weir 2000 c). Now the concept that diabetes only results where there is inadequate functional mass of B-cells has gained general acceptance. B-cells actually do compensate for increased demand, resulting from obesity, insulin resistance or pregnancy. The new concept is that the B-cell mass is dynamic and increases and decreases both in function and mass to maintain glycemic level within a very narrow physiological range. The changes in mass can be both in number (hyperplasia) and size (hypertrophy). When the B-cell mass cannot increase adequately,

diabetes ensues. The general acceptance of dynamic rather than static B-cell mass is based on clear evidence of changes in B-cell mass in both normal rodents and transgenic or knockout mice. Varying replication rates of B-cells have been observed *in vivo* and *in vitro*, and the presence of neogenesis of islets postnatally and in adults, and physiological loss of B-cells indicating turnover of B-cells has led to the new concept (Bonner-Weir 2000 c).

Changes in the B-cell mass in normal rodents

Replication is the major mechanism for adding new B-cells to the pancreas from shortly after birth onwards. In rats, a linear increase in the B-cell mass from weaning until 3-4 months of age was observed (Finegood *et al.* 1995). Morphometric data obtained from male C57/B6/129 mice ranging from four weeks to six months of age show that the B-cell mass expands at least 10-fold and is linearly correlated with body weight (Bonner-Weir 2000 a). In a longitudinal study, the addition of new cells slowly distended B-cell mass in the male Lewis rat, but from 15 months onwards, hypertrophy of the B-cell was the main mechanism of B-cell mass growth. Besides this age-related expansion in B-cell mass, pregnancy induces a stimulation of B-cell proliferation through placental lactogen and cell volumes distend as a functional adaptation. Post partum, the B-cell mass involutes by reduction of the B-cell volume, reduction of cell proliferation and an increase in B-cell apoptosis (Scaglia *et al.* 1995).

B-cell renewal by replication and neogenesis

As in the embryo, two mechanisms contribute to B-cell renewal in the adult: *neogenesis* or differentiation from ductal precursor cells and *proliferation* of differentiated B-cells. Islet neogenesis appears frequently in the first few days after birth, and a second wave of neogenesis occurs at about weaning (Bonner-Weir 2000 b; Scaglia *et al.* 1995). B-cell replication is significantly higher during late gestation and the neonatal period than following weaning. After weaning throughout adult life, both neogenesis and a low level of replication is maintained, which can be stimulated for example by chronic glucose infusion, treatment with exendin-4, a long lasting GLP-1 (glucagon-like peptide-1) agonist, and by pancreatectomy (Bonner-Weir *et al.* 1993; Bonner-Weir *et al.* 1989; Xu *et al.* 1999). Chronic glucose infusion leads to both increased replication and hypertrophy of B-cells, treatment with exendin-4 stimulates both replication and neogenesis, resulting in a 40% expansion of the B-cell mass in

rodents. After pancreatectomy, both proliferation and neof ormation of islet and exocrine tissue is observed (Bonner-Weir 2000 c). Similarly, new lobes of pancreas continue to form in 6-month-old mice (retired breeders), as evidenced by high bromodeoxyuridine (BrdU) incorporation in some pancreatic lobes (Bonner-Weir 2000 b). The signaling responsible for stimulating neogenesis is unknown. *In vivo* as well as in the pancreatic cell line AR42J, GLP-1 and exendin-4 cause endocrine differentiation (Xu *et al.* 1999; Zhou *et al.* 1999). There might be functional difference between B-cells that can replicate and those that cannot. Adult B-cells are functionally heterogeneous, but this heterogeneity has not been correlated to replicative ability or age. It has been suggested that those B-cells that replicate might dedifferentiate and transiently lose function as they replicate (Bonner-Weir 2000 b).

Turnover of B-cells

With mathematical modeling of the B-cell mass, normal turnover of B-cells became evident. The B-cell mass in adult rodent pancreas can double within about one month, due to a 2-3% / 24 hour replication of B-cells. Between 1-2 months and 2-3 months of age, the B-cell mass does almost double, thereafter it remains rather stable due to increased apoptosis which approaches the replication rate. Therefore, complete replacement of the B-cell population could occur in about one month for a rat (Finegood *et al.* 1995). The frequency of apoptotic B-cells was found to be 0.5% in the adult rat. As the steady-state replication rate is just over 2% per day, the lifespan of a rat B-cell can be estimated as ~58 days (Bonner-Weir 2000 b; Finegood *et al.* 1995).

In the neonatal rat pancreas, the B-cell mass does not increase between 1-3 weeks of age, even though the replication rate observed was higher than in the adult. The B-cell replication rate was found to be decreased (Scaglia *et al.* 1997) and the incidence of apoptotic nuclei in that period was significantly increased as compared to slightly younger and older rats (Scaglia *et al.* 1997; Trudeau *et al.* 2000). The apoptotic index peaks at 12-14 days of age in Sprague-Dawley and Wistar rats and at about 11-13 days of age in BALB/c and NOD mice (Trudeau *et al.* 2000). These findings suggest a neonatal wave of neogenesis of B-cells to maintain a constant B-cell mass (Scaglia *et al.* 1997; Trudeau *et al.* 2000). The simultaneous high levels of apoptosis and replication of B-cells coincided with a marked change in both insulin-like growth factor I (IGF-I) and IGF-II as well as IGF-binding proteins (IGFBP) 1 and

2, suggesting that the remodeling resulted from an inadequacy of available survival factors (Petrik *et al.* 1998; Scaglia *et al.* 1997). This hypothesis was supported by the suppression of the normal neonatal apoptosis by increased persistent IGF-II in transgenic mice (Hill *et al.* 2000). A dysregulation of this process could be detrimental, as a fine balance between cell renewal and cell death determines the pancreatic B-cell mass. This concept has been supported by two studies, one of which showed a low protein diet during pregnancy to increase apoptosis, reduce replication of B-cells, reduce pancreatic IGF-II and B-cell mass (Petrik *et al.* 1999 b). Furthermore, the ablation of insulin receptor substrate-2 (IRS-2) resulted in reduced B-cell mass, owing to decreased survival of differentiating B-cells mediated by the IGF-I receptor (Bonner-Weir *et al.* 1999; Withers *et al.* 1999; Withers *et al.* 1998).

Loss of B-cell mass has been observed in the post partum pancreas, in a rat model of transplantable insulinomas, after cessation of glucose infusion in db/db mice and in clinical reports as atrophy of islet tissue in pancreas neighboring insulinomas. The mechanisms involved varied with the model used; when insulinomas were transplanted, the B-cell mass decreased due to increased apoptosis. After stopping glucose infusion, the return from B-cell hypertrophy takes one week, whereas the cell function reverts within 24 hours. In the post partum rat pancreas, both increased apoptosis and decreased replication rate and a reduction in cell size contributes to involution (Bonner-Weir 2000 c; Bonner-Weir *et al.* 1989; Scaglia *et al.* 1995).

Islet cell renewal: precursor and stem cells

Different areas of the ducts and smaller ductular elements have been suggested to harbor *stem cells*, since islet cell budding from ductal structures is present during embryogenesis and during postnatal growth or regeneration (Bouwens & Kloppel 1996; Slack 1995). By definition, stem cells should resemble embryonic cells, the so-called “proto-differentiated” pancreatic cells that have not yet differentiated into exocrine or endocrine tissue. In order to identify such cells, the characteristics of proto-differentiated cells described in fetal pancreas have to be looked at. In case of the rat pancreas, GLUT2, PDX-1 and vimentin are markers that could allow discrimination between proto-differentiated and differentiated duct-lining cells (Bouwens 1998; Madsen *et al.* 1997; Pang *et al.* 1994). However, a proto-differentiated cell population has not yet been found in the duct compartment of normal postnatal rat pancreas and therefore, there is no evidence that stem cells exist in the pancreas (Bouwens 1998).

Furthermore, it is doubtful that stem cells would be involved in normal pancreatic growth or regeneration after injury such as pancreatectomy (Bonner-Weir 2000 c). In this model, expansion and differentiation of the duct cells give rise to the substantial regeneration (further details are discussed below) (Bonner-Weir 2000 b).

Another mechanism for tissue regeneration is *trans-differentiation*. Trans-differentiation is different from stem cell neogenesis in that it involves differentiated cells instead of undifferentiated ones. This mechanism consists of re-programming of gene-expression, which generally occurs via an intermediate stage of “de-differentiation”. Thus, certain terminally differentiated cells retain the capacity to switch off a number of genes and switch on others resulting in a phenotypic switch. Importantly, budding of new B-cells and other hormone positive islet cells has been observed in cells of the ductal complex. Transitional forms were noticed that co-expressed cytokeratin 20 (a ductal characteristic) and insulin as also occurs in the fetal and neonatal pancreas (Bouwens *et al.* 1994). Others reported about “intermediate” or “transitional” cells that co-expressed insulin and amylase even within the same secretory granule. These observations support the hypothesis that trans-differentiating acinar and ductal cells can generate new B-cells (Bouwens 1998). The most likely source of *precursor cells* would be pancreatic ducts because the adult duct epithelium retains the ability to give rise to all differentiated cell types of the pancreas (Bonner-Weir 2000 c). From studies of pancreatic regeneration in rats, the impressive capacity of pancreatic duct cells to expand and differentiate has been shown (Bonner-Weir *et al.* 1993). PDX-1 expression has been observed after rapid replication of duct cells in pancreatectomized rats and therefore, it was hypothesized that adult duct cells have a potential to lose their phenotype with replication, reverting into pluripotent stem cells that can differentiate into islet cells with appropriate stimuli (Sharma *et al.* 1999). In normal rodent and human pancreas, single B-cells or small extra-islet B-cell clusters (isolated B-cells) occur as a portion of the endocrine component of the pancreas. These clusters differ from islets in not being associated with the islet sinusoidal vascular system, and by the lack of intercellular contacts with non-B endocrine cells. In normal rat pancreas, single B-cells account for 0.9% of the total insulin-immunoreactive area. In normal human pancreas, these isolated B-cells occur much more frequently; they represent 9% of the total insulin-immunoreactive area (Bouwens & Pipeleers 1998). In the rat, the appearance of single B-cells can be activated under different experimental conditions. Since there is no other way of explain-

ing the presence of single B-cells, those cells have been considered as indirect evidence that B-cell neogenesis occurs normally in human and rodent pancreas (Bouwens 1998).

B-cell replication and hyperglycemia

Glucose is one of the best stimuli for B-cell replication *in vitro* and *in vivo* (Bonner-Weir *et al.* 1989). It has been suggested that glucose is the driving force for B-cell compensation. Mild hyperglycemia, due to inadequate plasma insulin or insulin resistance could signal the B-cell to compensate, including functional adaptation as well as enhanced B-cell replication and hypertrophy (Bonner-Weir 2000 c). In contrast to mild acute hyperglycemia, chronic or severe hyperglycemia is detrimental. The term "glucose toxicity" has been used to describe detrimental effects, such as B-cell death. In chronic hyperglycemia, oxidative stress is increased and can lead to apoptosis, which can be prevented by administration of an antioxidant (Bonner-Weir 2000 b). Additionally, B-cells exposed to high glucose accumulate intracellular proteins modified with O-linked monosaccharide N-acetylglucosamine (O-Glc-Nac). The accumulation of such modified proteins has been suggested to cause hyperglycemia induced B-cell apoptosis (Bonner-Weir 2000 b). Further secondary effects of a hyperglycemic environment include loss of glucose-induced insulin secretion (Leahy *et al.* 1992) and loss of specific B-cell differentiation (Jonas *et al.* 1999). The loss of glucose induced insulin secretion is a reversible process, involving a reduction of glucose transporter 2 (GLUT2) protein in the B-cells due to reduced GLUT2 expression (Zangen *et al.* 1997). However, the role of the lowered transporter protein in loss of glucose-induced insulin secretion is unknown (Leahy *et al.* 1992). In the pancreatectomized rat model, where animals developed a stable chronic hyperglycemia, a reduction of several islet transcription factors involved in B-cell development and differentiation has been observed (Jonas *et al.* 1999). The changes in transcription factor mRNA levels included a decrease in PDX-1, Nkx6.1 and PAX6 mRNA. The examination of mRNA levels of genes involved in glucose metabolism showed a decrease of GLUT2, glycerol-phosphate dehydrogenase, pyruvate carboxylase and glucokinase. These global alterations observed in pancreatectomized rat islets were proposed to alter the preferential stimulation of oxidative metabolism by glucose and thus adversely influence glucose stimulated insulin release. In addition, islets of partially pancreatectomized rats were markedly hyperplastic and individual B-cells were also hypertrophic, a

common feature of many rodent models of type 2 diabetes (Jonas *et al.* 1999). Protection from apoptosis in these animals might result from the induction of a variety of stress-survival genes, such as those encoding heme oxygenase, Mn-superoxide dismutase, glutathion peroxidase, and fatty acid synthetase (FAS) (Laybutt *et al.* 2000).

2.3.5 Incretin hormones and pancreas development

Several hormones have been implicated in pancreas growth and development, including the insulinotropic hormones glucagon-like peptide-1 (GLP-1) and glucose-dependent insulinotropic polypeptide (GIP).

Glucagon-like peptide-1 (GLP-1) is a gut-derived hormone, which stimulates post-prandial insulin secretion and insulin gene transcription (see chapter 2.4.). Due to its capability of stimulating the cAMP/protein kinase A transduction system (see chapter 2.4.) and the induction of immediate early response genes (IEG), which are known to be implicated in B-cell growth and differentiation, B-cell growth promoting actions of GLP-1 are considerable (Buteau *et al.* 1999). Buteau *et al.* (1999) showed that both GLP-1 and glucose stimulate DNA synthesis in beta (INS-1) cells, as assessed by the measurement of tritiated thymidine incorporation. GLP-1 could promote maximum cell growth, even at low glucose levels. The fact that glucose and GLP-1 did not act additively led the authors to suggest that the two agents act through a common mechanism. *In vitro* studies using CHO (Chinese hamster ovary) cells, which stably expressed the rat GLP-1 receptor (CHO/GLPR), demonstrated that the activation of p38 MAP (mitogen activated protein) kinase was triggered by the GLP-1 receptor (Montrose-Rafizadeh *et al.* 1999). MAP kinases are cytoplasmatic serine/threonine kinases that transmit extracellular signals to the nucleus via phosphorylation of transcription factors and other signaling molecules (Cobb & Goldsmith 1995). MAP kinases are activated by a number of external stimuli, including growth factors that interact with cell surface receptor tyrosine kinases (Cobb & Goldsmith 1995). A number of receptors that couple to heterotrimeric G proteins have recently been shown to stimulate the activity of two members of the MAP kinase superfamily, which includes the extracellular signal-regulated kinase (ERK) and p38 MAP kinase (Faure *et al.* 1994; Frodin *et al.* 1995; Yamauchi *et al.* 1997). The activation of MAP kinase path-

ways best explains the growth-promoting actions of GLP-1 on pancreatic islets (Stoffers *et al.* 2000), since p38 MAP kinase is known to play an important role in various cellular functions, such as phosphorylation of transcription factors, control of apoptosis and cell cycle-mediated events (Montrose-Rafizadeh *et al.* 1999). In a recent study by Trümper *et al.* (2001 c), the GLP-1- and glucose-induced cell proliferation, prevention of apoptosis and stimulation of phosphatidylinositol 3-kinase (PI3K) associated with insulin receptor substrate (IRS) isoforms was shown. PI3K is an enzyme that has been implicated in cell growth and differentiation (Withers & White 2000). Inhibition of the GLP-1 induced PI3K activation, using the PI3K inhibitors LY294003 and wortmannin, led to the conclusion that the growth promoting action of both glucose and GLP-1 on beta (INS-1) cells involves the PI3K signal transduction pathway (Buteau *et al.* 1999). Further, activation of protein kinase (PK) B alpha and PKB beta isoforms and also of glycogen synthase kinase-3 and forkhead transcription factor (FKHR) was demonstrated. Therefore, pleiotropic activation of PI3K/PKB at the level of IRS-molecules, PI3K and PKB isoforms was found to occur following GLP-1 stimulation in beta (INS-1) cells. Signaling pathways of glucose metabolites, MAP kinase and protein kinase A converge at PKB, which plays a central role in mitogenic and anti-apoptotic regulation of B-cells (Trümper *et al.* 2000 a; Trümper *et al.* 2001 c). Wang *et al.* (1999) examined the influence of GLP-1 on the B-cell specific transcription factor PDX-1. The authors could show that GLP-1 increases PDX-1 DNA binding activity, an effect that could be inhibited by LY294002 (Buteau *et al.* 1999). The peptide was also found to increase PDX-1, GLUT2, glucokinase, and insulin mRNA expression (Buteau *et al.* 1999; Wang *et al.* 1999). These data suggest that GLP-1 acts as a growth factor in isolated rat islet tissue and therefore, the peptide could be important for B-cell mass expansion under conditions of increased insulin demand. Recent *in vivo* studies further confirmed some of the results obtained from beta (INS-1) cells. Both GLP-1 and exendin-4 induced an increase in PDX-1 protein levels in pancreata from healthy C57Bl/6 mice, an effect that was abolished by co-administration of the GLP-1 antagonist exendin 9-39. Administration of exendin-4 to GLP-1 receptor knockout mice (Scrocchi *et al.* 1996) did not increase the level of PDX-1 protein, which confirms that exendin-4 acts solely through the GLP-1 receptor. Morphometric analysis of islets in exendin-4 treated animals showed an increase in islet size as compared to a saline treated control group (Stoffers *et al.* 2000). In exendin-4 treated rats, the B-cell mass expanded due to both increased

replication and neogenesis (Xu *et al.* 1999). Similarly, GLP-1 administration to young normoglycemic Umeå mice stimulated islet growth (Edvell & Lindstrom 1999). Recent morphometric studies concerning alterations of the endocrine pancreas of GLP-1R knockout mice showed a change of the topography of the islets cells, with A-cells being located more centrally in the islets. Furthermore, the absence of GLP-1R signaling leads to a shift from large to small and medium-sized islets (Ling *et al.* 2001). Only very few data are available concerning the effect of *glucose-dependent insulinotropic polypeptide* (GIP, see chapter 2.4.) on pancreatic B-cell proliferation and survival. It was shown that GIP induces cellular proliferation and inhibits glucose- and starvation-induced apoptosis in beta (INS-1) cells by activation of pleiotropic signaling pathways (Trümper *et al.* 2001 b). GIP stimulates PKA/cAMP responsive element binder (CREB), MAP kinase and PI3K in a dose-dependent manner synergistically with glucose. Activation of PI3K was associated with IRS isoforms and PI3K isoforms. Downstream of PI3K, GIP stimulated PKB alpha and PKB beta isoforms, glycogen synthase kinase, FKHR and p70^{S6K}, a regulator of translation. The data indicate that mitogenic effects of glucose and GIP in B-cells may not only be caused by activation of transcription but also by initiation of protein translation. Signaling modules activated by GIP were dependent on glucose metabolism and calcium influx and were tightly linked by multiple converging pathways (Trümper *et al.* 2001 a; Trümper *et al.* 2001 b; Trümper *et al.* 2000 b). Therefore, both currently known incretin hormones influence growth and survival of the pancreatic B-cell mass.

2.4 The enteroinsular axis

2.4.1 Definition

The term *enteroinsular axis* has been introduced by Unger and Eisentraut and it comprises hormonal, neural and substrate stimulation, i.e., all signals originating from the gut that reach the endocrine pancreas to stimulate, reduce or modify the secretion of insulin, glucagon, somatostatin and PP (Creutzfeldt 1997; Creutzfeldt & Nauck 1992; Unger & Eisentraut 1969).

2.4.2 Components of the enteroinsular axis

2.4.2.1 Neural components

Activation of the vagus following ingestion of nutrients is thought to augment insulin output via cephalic, gastropancreatic and enteropancreatic vagovagal reflexes. Several gastrointestinal neuropeptides with insulinotropic inhibitory or stimulating action have been demonstrated in pancreatic nerves, e.g. VIP (vasoactive intestinal polypeptide), GRP (gastrin releasing peptide), somatostatin and NPY (neuropeptide tyrosine) (Creutzfeldt 1997; Creutzfeldt & Nauck 1992).

2.4.2.2 Hormonal components (incretin candidates)

The term *incretin effect* denotes the phenomenon that glucose elicits a higher B-cell secretory response when administered via the gut as compared to the intravenous route. In the 1930's, the name incretin was introduced for an insulinotropic gut factor when insulin was the only known pancreatic hormone (LaBarre & Still 1930). *Incretin hormones* today are defined as endocrine insulinotropic factors released from the gut in response to nutrient or more strictly glucose ingestion (Creutzfeldt & Nauck 1992). Under experimental conditions, a large number of peptides have been found to modify (stimulate or inhibit) the function of the endocrine pancreas. Gut factors, such as cholecystokinin, gastrin and secretin have been shown to stimulate insulin secretion only in pharmacological doses and are therefore considered to be of no or only minor importance as incretin hormones. To qualify as incretin candidate, an insulinotropic gut hormone must release insulin glucose dependently at plasma concentrations achieved by glucose or nutrient ingestion. Currently, there are only two gut hormones that fulfill the required characteristics for incretin hormones: GIP (glucose-dependent insulinotropic polypeptide) and GLP-1 (glucagon-like peptide-1) (Creutzfeldt & Nauck 1992).

2.4.3 Glucagon-like peptide-1

GLP-1 has first been described in the late 1980's (Göke *et al.* 1991; Göke *et al.* 1988) and was considered an incretin hormone with powerful insulinotropic effects

(Fehmann *et al.* 1995). GLP-1 (7-36 amide) is the predominant product of intestinal processing of proglucagon and is localized in enteroendocrine L-cells that are mainly found in the lower gut. Indirect stimulation by the cholinergic enteric nervous system and hormonal signals from the upper gut have been discussed to play a role in the secretion of this incretin hormone. *In vitro* studies, using fetal rat intestinal mucosa cells as well as perfused rat intestine, demonstrated that GIP is a secretagogue for GLP-1. In contrast, exogenous GIP does not lead to an increment in plasma GLP-1 in humans. The exact mechanisms that control GLP-1 release still need to be evaluated. This incretin hormone stimulates the insulin secretion of pancreatic B-cells in the presence of elevated glucose levels and enhances proinsulin gene expression (Fehmann *et al.* 1995; Gefel *et al.* 1997; Holst 1994; Thorens 1995). In low concentrations, GLP-1 releases somatostatin from pig and rat pancreata. At physiological glucose levels, GLP-1 inhibits glucagon secretion in various animal species; this effect is more pronounced at low than high glucose levels. It was suggested that the effect of GLP-1 on insulin and somatostatin release is direct, while the effect on glucagon secretion is indirect, possibly mediated by a paracrine effect on the somatostatin cells. This agrees with the concept of intraislet interactions in which both insulin and somatostatin are known as inhibitors of glucagon secretion. GLP-1 has several extrapancreatic effects on different organs, which are discussed elsewhere in detail (Fehmann *et al.* 1995). GLP-1 is degraded by dipeptidyl peptidase present in serum (Holst 1994).

Specific receptors for GLP-1 were first detected on RINm5F cells and consecutively on several other insulinoma cell lines. Furthermore, the receptor was found on somatostatin secreting cells. The GLP-1 receptor shares sequence homology with the receptors for VIP, secretin, GHRH (growth hormone releasing hormone), PTH (parathormone), calcitonin, and glucagon. All of these receptors, including the GLP-1 receptor, are coupled to G proteins. There is evidence that the GLP-1 receptor is functionally coupled to the adenylate cyclase system by a stimulatory G protein. GLP-1 enhances intracellular cAMP in pancreatic islet cells and several insulinoma cell lines. It also depolarizes cells and induces a rise in free cytosolic Ca^{2+} concentration, followed by an increase of the glucose-induced insulin release in rat pancreatic B-cells. After binding to its receptor, GLP-1 is internalized into B-cells; it is currently unknown, whether the receptor protein itself is being internalized after ligand binding (Fehmann *et al.* 1995).

2.4.4 Glucose-dependent insulintropic polypeptide

GIP was first isolated and identified by Brown and co-workers (Brown *et al.* 1969). In man, the peptide is solely expressed in endocrine K-cells of the upper small intestine and in rats, expression of the GIP mRNA is found both in K-cells of the small intestine and the submandibular gland (Buchan *et al.* 1978; Fehmann *et al.* 1995; Tseng *et al.* 1993). GIP (rat, human, porcine and bovine) is a 42 amino acid polypeptide (GIP(1-42)), which is derived from proteolytic processing of its preprohormone precursor (Gallwitz *et al.* 1996). GIP is released into the blood stream in response to nutrient absorption, or more strictly, mainly by carbohydrate and fat absorption. The degree to which fat or glucose stimulate GIP release is species dependent. In rodents and pigs, whose diets usually contain less than 10% energy as fat, carbohydrates are more potent than fat in stimulating GIP release. In contrast, in man, who normally consumes a diet relatively high in lipid content, fat is the more potent stimulator of GIP release (Yip & Wolfe 2000). Moreover, the postprandial level of circulating GIP is dependent on meal size, and the contribution of the enteroinsular axis (see chapter 2.5) is proportionately greater after a large meal. The half-life of human GIP has been estimated at roughly 20 minutes as measured by radioimmunoassay (Brown *et al.* 1975; Elahi *et al.* 1979; Nauck *et al.* 1989; Yip & Wolfe 2000). GIP is degraded by dipeptidyl peptidase IV present in serum (Morgan 1996).

2.4.5 GIP receptor

After being released from enteroendocrine K-cells, GIP reaches the specific GIP receptor via the blood stream. The structure, signal transduction and receptor-mediated functions will be discussed in the following chapter.

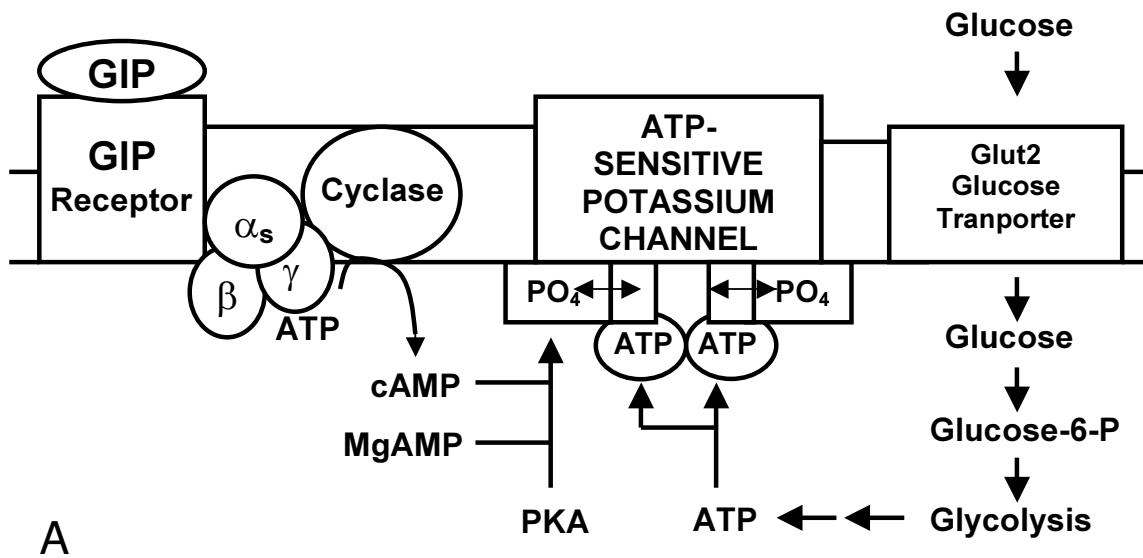
2.4.5.1 GIP receptor structure

Usdin *et al.* first cloned the rat GIP receptor in 1993; subsequently, cloning of the hamster and human GIP receptor has been performed (Gremlich *et al.* 1995; Usdin *et al.* 1993; Volz *et al.* 1995; Yasuda *et al.* 1994). GIP receptor mRNA is present in pancreas, stomach, intestine, adrenal cortex, heart, lung, brain, endothelium of major blood vessels and adipose tissue of the rat (Usdin *et al.* 1993). The receptor is a gly-

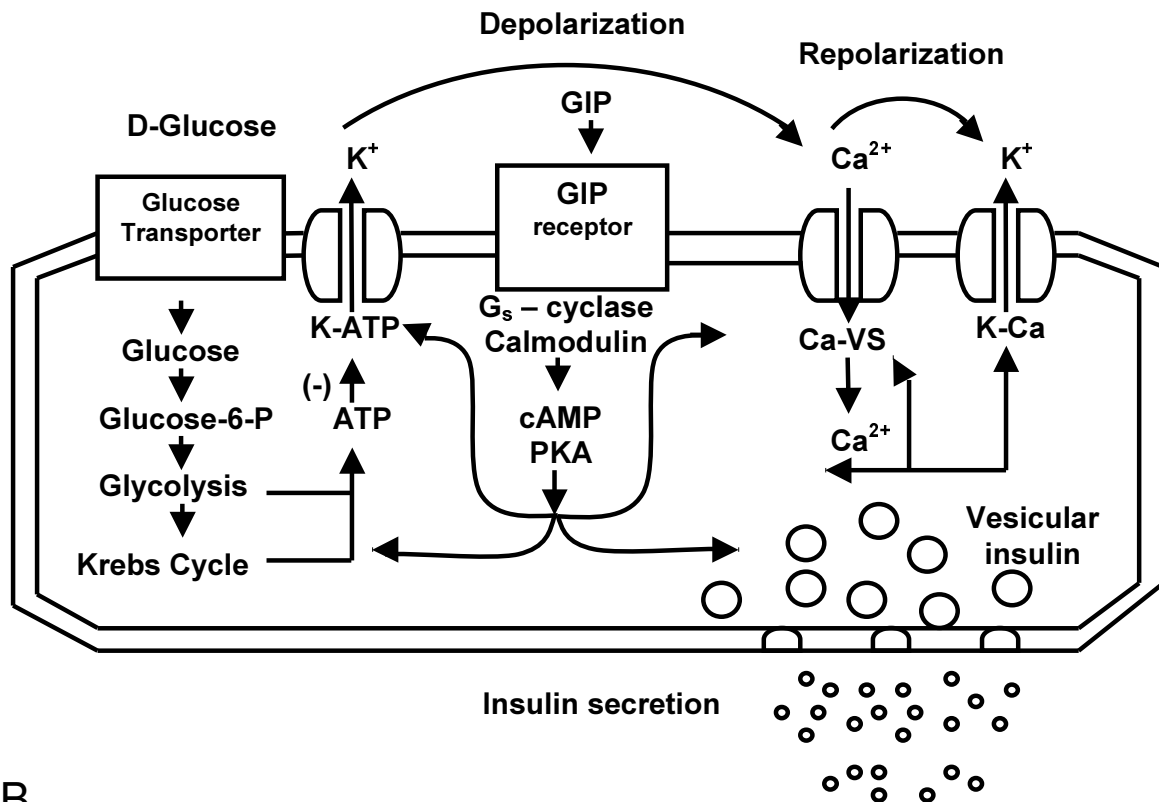
coprotein belonging to the secretin/VIP (vasoactive intestinal polypeptide) family of receptors, a seven transmembrane G protein-coupled receptor family that includes receptors for e.g. secretin, VIP, glucagon, GLP-1, GHRH (growth hormone releasing hormone) and PACAP (pituitary adenylyl cyclase-activating polypeptide). The ligands in this receptor family are bound by their large N-terminal domain, where the first 222 amino acids are necessary for ligand binding and receptor coupling to cAMP production (Gelling *et al.* 1997; Wheeler *et al.* 1995).

2.4.5.2 GIP receptor signal transduction

GIP binding to its receptor activates a heterotrimeric stimulatory G-protein, which in turn activates adenylate cyclase. The resulting cAMP and a subsequent increase in Ca^{2+} influx via voltage-gated calcium channels (Ca-VS) are thought to represent the major signaling pathways by which GIP exerts its insulinotropic effect on pancreatic B-cells (Lu *et al.* 1993 a; Lu *et al.* 1993 b; Wheeler *et al.* 1995). GIP presumably initiates activation of protein kinase A, which in turn may modify the gating properties of the potassium channels, whereas glucose operates via glycolysis-generated adenosine triphosphate, which is known to close the channels. The resulting depolarization causes an opening of voltage-gated calcium channels whereby the intracellular calcium concentration increases. This in turn starts insulin exocytosis (Figure 2.1 A/B). Recently, an additional but distinct signal transduction pathway for GIP was described via PI3K mechanism (Yip & Wolfe 2000). The receptor undergoes rapid and reversible homologous receptor desensitization, typical for G protein coupled receptors (Fehmann *et al.* 1991; Tseng *et al.* 1996 a).



A



B

Figure 2.1 (A) Proposed interaction of GIP with isolated B-cells. After binding and activation of GIP to its receptor, elevated cyclic adenosine monophosphate levels activate protein kinase A, which in turn phosphorylates regulatory sites on the adenosine triphosphate-sensitive potassium channel. Concomitantly, glucose regulates the potassium channels via adenosine triphosphate generated in glycolysis (Holst 1994).

Figure 2.1 (B) Proposed mechanism of stimulation of insulin release by GIP. After closure of the adenosine triphosphate-sensitive potassium channels (K-ATP) by the joint action of glucose and GIP, the B-cell depolarizes, which causes voltage-sensitive calcium channels (Ca-VS) to open. This leads to an increase in free intracellular calcium levels, which in turn induces exocytosis of insulin. Repolarization is achieved by opening of calcium-sensitive potassium channels (K-Ca) (Holst 1994).

2.4.5.3 GIP receptor mediated functions

Extrapancreatic function of GIP

When GIP was first isolated, the peptide was named “gastric inhibitory polypeptide” according to its inhibiting effect on gastric acid secretion. Since this effect was not observed under physiological conditions, the peptide has been renamed “glucose-dependent insulinotropic polypeptide”, due to its main physiologic property (Morgan 1996; Yip & Wolfe 2000). Yip *et al.* have first described functional GIP receptors present on adipose tissue in 1998. GIP can increase fatty acid incorporation, glucose uptake and lipoprotein lipase synthesis and release in adipose tissue. It further inhibits glucagon-induced lipolysis and increases insulin-binding affinity in adipocytes (Yip *et al.* 1998).

GIP reduces glucagon-stimulated hepatic glucose production, an effect, which is more pronounced in the presence of insulin (Fehmann *et al.* 1995). GIP receptor mRNA could not be detected in the liver, using *in situ* hybridization and therefore, the effect might be indirect. GIP receptor mRNA has been detected in the brain but a putative effect of GIP is yet unknown, although a possible transmitter role has been discussed (Morgan 1996). A role for GIP in regulation of adrenal steroid release has been suggested from finding GIP receptor mRNA in the inner layers of the rat adrenal cortex (Yip & Wolfe 2000).

Pancreatic function of GIP

GIP has insulinotropic function on pancreatic B-cells; the peptide stimulates insulin secretion in the presence of elevated glucose levels and enhances proinsulin gene transcription. Pre-exposure of B-cells to GIP enhances the insulin secretory response during a subsequent stimulation with glucose or other secretagogues (“priming effect”) (Fehmann *et al.* 1995). Recent studies also revealed a mitogenic and anti-

apoptotic effect of GIP on B-cells via pleiotropic signaling pathways (see 2.3.5) (Trümper *et al.* 2001 a; Trümper *et al.* 2001 b).

GIP stimulates glucagon secretion but only in the presence of 5 mmol/l glucose or lower. Therefore, GIP does not influence A-cells under physiological conditions.

GIP is a weak stimulator of somatostatin secretion in the perfused pancreas of the rat (Fehmann *et al.* 1995).

2.4.6 Neural mediation of the incretin effect

In man, the nervous system does not contribute much to the incretin stimulation of insulin secretion after oral glucose. In some animal species (e.g. rat, mouse), sweet tasting nutrients or mixed meals provoke a rapid, pre-absorptive burst of insulin secretion. Therefore, gastric instead of oral glucose administration reduces glucose tolerance for example in rats, which underlines the importance of the cephalic phase of insulin release in this species (Creutzfeldt 1997; Creutzfeldt & Nauck 1992).

2.4.7 Quantification of the incretin effect

McIntyre *et al.* (1964) and Elrick and coworkers (Elrick *et al.* 1964) first evidenced the difference in B-cell secretory response to oral and intravenous glucose. Three years later, another workgroup found the plasma insulin response to isoglycemic intravenous glucose to be only 30-40% of that seen after oral glucose ingestion (Perley & Kipnis 1967). The incretin effect has been quantified in several investigations (Creutzfeldt & Nauck 1992; Nauck *et al.* 1986 b). Its contribution was 20-60% of the C-peptide response after glucose ingestion, depending on the size of the glucose load (Nauck *et al.* 1986 b). GIP has been considered to be the more potent incretin hormone than GLP-1 (Creutzfeldt & Nauck 1992; Nauck 1999; Nauck *et al.* 1993 a). Studies using a GIP-receptor antagonist revealed a 72% reduction of the postprandial insulin response in rats (Tseng *et al.* 1996 b) and therefore, GIP seems to play a dominant role in mediating postprandial insulin release.

2.4.8 Pathophysiology of the enteroinsular axis in diabetes

Besides insulin resistance, impaired insulin secretion is a characteristic of type 2 diabetes mellitus. The total volume of pancreatic islets can be reduced up to 60-70% in type 2 diabetics as compared to weight-matched normal subjects (Rahier *et al.* 1989). Taking into account that the islet reduction has to approach 90% before metabolic consequences occur, functional defects may also play a role in type 2 diabetic subjects (Eisenbarth 1986). Comparison of the B-cell response to oral and isoglycemic intravenous glucose revealed a clearly reduced incretin effect in type 1 and 2 diabetic patients (Nauck *et al.* 1986 a; Suzuki *et al.* 1990; Tronier *et al.* 1985). The effects of the incretin hormones GIP and GLP-1 in diabetic patients and animal models of both type 1 and 2 diabetes have been studied separately and it was evidenced that the GLP-1 effect is preserved in diabetes whereas GIP administration had no effect on the insulin response (Creutzfeldt *et al.* 1996; Elahi *et al.* 1994; Linn *et al.* 1996; Nauck *et al.* 1993 c; Nauck *et al.* 1993 b; Young *et al.* 1999). Several mechanisms contributing to the reduced insulinotropic action of GIP have been discussed. Firstly, the homologous desensitization of the GIP receptor has been proposed from findings in diabetic rats, which exhibited largely elevated GIP serum levels and significantly higher duodenal GIP mRNA expression as compared to normal rats (Tseng *et al.* 1996 a). *In vitro* studies using LGIPR2 cells exposed to elevated GIP levels revealed a reduction in GIP-stimulated cAMP formation and therefore, the chronic desensitization of the GIP receptor by its ligand was proposed (Tseng *et al.* 1996 a). Further, *in vitro* studies revealed a higher expression of RGS2 (regulator of G protein signaling) after GIP stimulation and showed an interaction of RGS2 and the α subunit of the G protein complex (Tseng & Zhang 1998). Agonist induced stimulation of RGS2 expression is therefore thought to result in a feedback desensitization of the stimulated receptor. Secondly, Holst *et al.* (1997) discussed the possibility of a reduced or defective expression of the GIP receptor in diabetics. Actually, a more recent study revealed a decreased receptor expression in diabetic fatty Zucker rats, which was suggested to explain the decreased effectiveness of GIP administration on insulin release (Lynn *et al.* 2001). So far, no mutations of the GIP receptor gene have been found to correlate with the development of diabetes mellitus but geneticists were encouraged to look in the GIP receptor gene or gene regulation to investigate this possibility (Holst *et al.* 1997). Miyawaki *et al.* (1999) generated GIP receptor defi-

cient mice, which only exhibited mild glucose intolerance. Some investigators have assumed adaptive developmental mechanisms to compensate for the loss of one incretin hormone receptor early in development (Baggio *et al.* 2000; Lewis *et al.* 2000). In mice, lacking GLP-1 receptor function (Scrocchi *et al.* 1996), elevated GIP serum levels were observed and considered to play a role as such compensatory factor (Pederson *et al.* 1998).

2.5 Generation of GIPR^{dn} transgenic animals

The generation of transgenic mice, expressing a dominant negative GIP receptor has been described in detail by Volz (1997). The following shall only give a brief review of the methods and results presented by Volz (1997).

2.5.1 Targeted mutation of the human GIP receptor

The targeted mutation of the human GIP receptor was supposed to result in a sustained GIP binding affinity but a loss in its ability to induce signal transduction (dominant negative GIP receptor, GIPR^{dn}).

The third intracellular G-protein coupling loop of the GIP receptor is essential for signal transduction. Therefore, the cDNA of the human GIP receptor was mutated in the region, coding for the third intracellular loop by introducing a point mutation at nucleotide position 1018-1020 (amino acid position 340) (Ala → Glu) and a deletion of 24 base pairs/8 amino acids (nucleotide position 955-978/ amino acid position 319-326), using oligonucleotides containing the specific mutations.

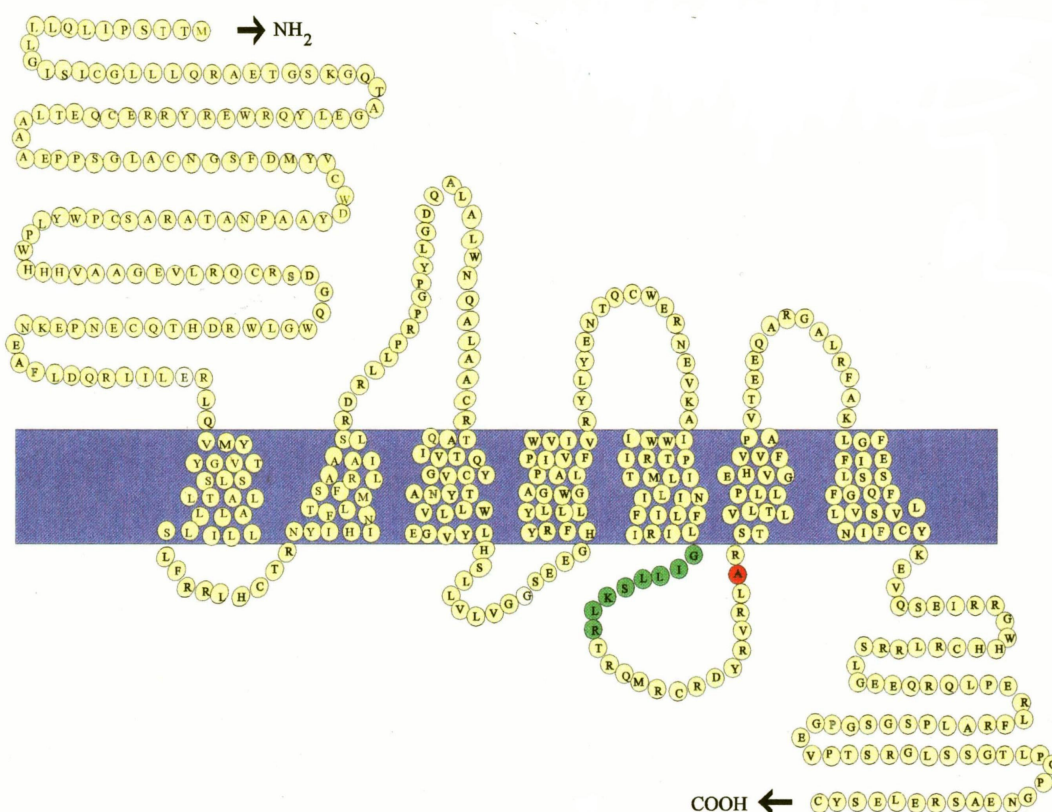


Figure 2.2 Amino acid sequence of the human GIP receptor and areas where targeted mutations have been performed. The cDNA of the human GIP receptor was mutated in the region coding for the third intracellular loop by introducing a point mutation at amino acid position 340 (Ala → Glu, red) and a deletion of 8 amino acids at position 319-326 (green) (Volz 1997).

2.5.2 *In vitro* analysis of the mutated GIP receptor

Stably transfected CHL (Chinese hamster leucoblastom) cells were used for comparing the affinity of GIP to the wildtype and the mutated GIP receptor. The binding affinity of GIP has been shown to be nearly equal for both receptors (K_D wildtype : K_D GIPR^{dn} = $0.22 \cdot 10^{-9}$ M : $0.35 \cdot 10^{-9}$ M). Furthermore, cAMP production following GIP stimulation has been compared in CHL-cells expressing the wildtype and the mutated GIP receptor. In CHL-cells expressing the wildtype GIP receptor, the cAMP concentration rose with increasing GIP concentration (between 10^{-12} and 10^{-8} M hGIP(1-42)). In contrast, CHL-cells expressing the mutated GIP receptor do not exhibit an increase in intracellular cAMP concentration following GIP stimulation. Therefore, the

mutated GIP receptor carries the desired properties of a dominant negative receptor: normal binding affinity to its ligand but loss of cAMP induced signal transduction.

2.5.3 Generation of mutant mice

The mutated cDNA of the human GIP receptor was cloned into the *XbaI/HindIII* site of the RIP1 vector (Hanahan 1985), which includes the rat proinsulin gene promoter II. This vector has been successfully used to achieve B-cell specific expression of cDNA constructs in transgenic mice (Hanahan 1985; Kato *et al.* 1994). Parts of the vector were released by *Sall/Sspl* digestion and the resulting fragments were separated using an ethidiumbromide-free gel. After further purification and dialysis, the RIP1-GIPR^{dn} cDNA construct was injected into the male pronucleus of mouse zygotes (CD-1 females) at a final concentration of 400 copies/pl. The zygotes were then transferred into cycle-synchronized females. Twelve out of 57 offspring were identified GIPR^{dn} transgenic by PCR analysis (see 3.1).

3. Research Design and Methods

3.1 Transgenic animals

Transgenic animals were generated as previously described by Volz-Peters *et al.* (2000) and Volz (1997) (Model patent number: DE/11.08.99/19836382). Transgenic males were bred onto a CD1 background (Charles River-Wiga, Germany). Animals investigated in the present study were hemizygous male and female transgenic mice and age- and sex-matched non-transgenic littermate controls. Mice were maintained on a 12-h light, 12-h dark cycle and fed standard rodent chow (Diet 1: Altromin C1324, Germany, Table 3.1) and tap water ad libitum. For determination of urine glucose excretion, a total number of 112 animals were investigated. 24 animals were included in monthly blood glucose and body weight determination. At the age of ten, 30 and 90 days, blood/serum glucose and serum insulin levels of 48 animals were measured. Serum glucose and insulin values were determined in 23 animals at eight months of age. HbA_{1c} levels were measured in the same animals at four months of age. For OGTT, a total number of 20 animals were investigated. Food and water intake was determined in 25 animals. The total number of animals for morphometric analysis of the pancreas in each age group (10, 30 and 90 days) was 16 (four male and four female GIPR^{dn} transgenic as well as four male and four female non-transgenic mice). For morphometric analysis of the kidneys, 23 animals were studied altogether. 54 animals were included in the determination of the 12-month survival rate. In order to investigate the influence of carbohydrate intake on the metabolic state, a separate group of mice was fed a carbohydrate-restricted diet (Diet 2: Altromin C1009, Germany, Table 3.1) from weaning until four months of age, afterwards they were fed the standard rodent chow. 38 animals were included in monthly blood glucose and body weight determination. HbA_{1c} levels were measured in 31 animals at four months of age. Food and water intake was determined in 26 animals. 43 animals were included in the 12-month survival study.

The numbers of animals studied in the different investigations are listed in Tables and Figures according to their age, sex and transgenity.

Table 3.1 Composition of the different diets

	Diet 1: Altromin C1324	Diet 2: Altromin C 1009
Protein (%)	18.5	17.0
Fat (%)	3.8	7.0
Fiber (%)	6.0	34.0
Ashes (%)	6.8	8.0
Disaccharides (%)	5.3	1.3
Energy (kcal/kg)	2,473.7	1,343.6

PCR-Analysis

Transgenic mice were identified by polymerase chain reaction using 5'-ACA GNN TCT NAG GGG CAG ACG NCG GG-3' sense (Tra1) and 5'-CCA GCA GNT NTA CAT ATC GAA GG-3' antisense (Tra3) oligonucleotides. These primer sequences bind to both the human cDNA of the mutated GIP receptor and the endogenous murine GIP receptor (Figure 3.1). Since the sequence of the murine GIP receptor has not been evaluated yet, oligonucleotides were chosen in areas where the known sequences of the human, rat and hamster GIP receptor are highly conserved. In case of sequence variation within these animals, oligonucleotide synthesis was performed allowing all nucleotides ("N" in primer sequence) to integrate (Volz 1997).

Figure 3.1 PCR result

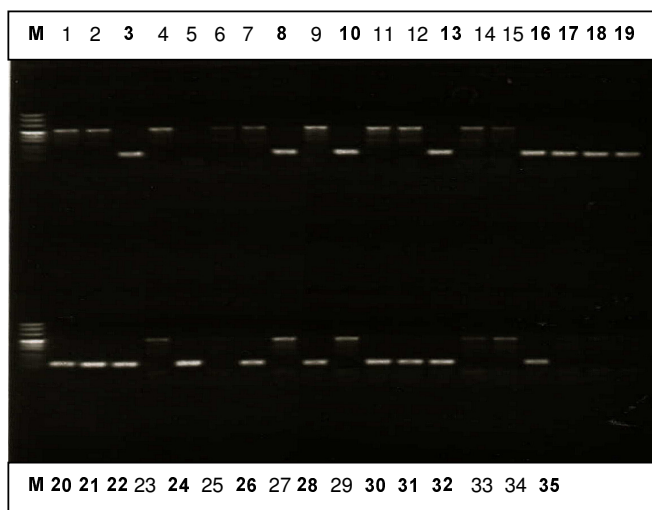


Figure 3.1 shows a PCR result of GIPR^{dn} transgenic and control mice. At the beginning of each row, the PUC Mix Marker #8 (M) is shown. Probes from control animals show a DNA fragment of 500 base pairs (endogenous GIP receptor). Transgenic animals exhibit a DNA-fragment of 140 base pairs (mutated GIP receptor, GIPR^{dn}). The number of the animals is shown underneath the PCR printout, transgenic animals are written in bold numbers.

a) Method

Materials used are listed under 3.1.b.

Tail tip biopsies were taken at weaning and stored at -80°C until assayed. DNA was extracted from tail tips as previously described (Hoeflich *et al.* 1999); the tail tip of approximately 0.4 cm length was digested over night in 200 μl Kawasaki buffer and 12 μl proteinase K (20 mg/ml). Subsequently, proteinase K was inactivated by heating for 15 minutes at 95°C . Large components were separated by centrifugation (2 min/10000xg) and the supernatant was diluted 1:5 in sterile redistilled water.

19 μl of the Master Mix and 1 μl of the 1:5 diluted digest were mixed carefully in PCR-analysis cups (Eppendorf, Germany), which were then placed in a Mastergradient thermocycler (Eppendorf, Germany) and the program was run. In the meantime, a 2% agarose solution containing 2 μl ethidium bromide per 100 ml was casted in a gel-casting chamber (Easy CastTM, PeqLab, Germany). After the gel was polymerized, the tray was put into the Easy CastTM gel chamber (PeqLab, Germany) and the chamber was filled with 1*TAE buffer.

After amplification, 4 μl loading dye (MBI Fermentas, Germany) was added to each sample and then transferred into the sample wells of the agarose gel. At the beginning of each row, 12 μl PUC Mix Marker #8 (MBI Fermentas, Germany) was placed in a well in order to allow estimation of amplified fragment size. Electrophoresis was run for approximately 45 min at 90 volt. Subsequently, the gel was placed on an Ultraviolet Transilluminator and a Polaroid picture (AGS, Germany) was taken for result documentation.

b) Material

Proteinase K (Roche, Germany): 20 mg/ml diluted in redistilled water

Kawasaki buffer: 30 mg $\text{MgCl}_2 \cdot 6 \text{H}_2\text{O}$ (Sigma, Germany)

186 mg KCl (Sigma, Germany)

500 μl Tween 20 (Sigma, Germany)

diluted in 100 ml 20 mM Tris/HCl pH 8.3 (Roth, Germany)

Primer concentration (Tra1, Tra3) 10 pmol/ μl each (Genzentrum/DNSynthese, Germany)

dNTP (Eppendorf, Germany): dATP, dGTP, dTTP, dCTP, 100 mM each

Master Mix: PCR-KIT (Quiagen, Germany)

dNTP 1mM	4 μl
10*Buffer	2 μl
MgCl_2	1.25 μl
Primer sense (Tra1)	1 μl
Primer antisense (Tra3)	1 μl
Redistilled water	5.7 μl
Q-solution	4 μl
Taq polymerase	0.125 μl

EDTA 0.5 M pH 8.0 (stock solution)

186.1 g EDTA (Roth, Germany)

800 ml distilled water

add approximately 20 g sodium hydroxide pellets (Merck, Germany) diluted in 50 ml distilled water until pH 8.0 is reached

50* TAE stock solution:

- 121 g Tris base (Roth, Germany)
- 28.55 ml glacial acetic acid (Sigma, Germany)
- 50 ml 0.5 M EDTA pH 8.0 (Roth, Germany)
- ad 500 ml distilled water

Agarose gel (GIBCO BRL, Germany):

- 2 g Agarose/100 ml 1*TAE buffer, add 2 μ l
- ethidium bromide (Merck, Germany)

Program for DNA amplification

- a) 4 min 94°C
- b) 1 min 94°C
- c) 1 min 60°C
- d) 2 min 72°C
- e) 10 min 72°C
- f) Hold on 4°C

Steps b) - d): 35 cycles

3.2 Urine glucose

In order to determine the onset of diabetes, urine glucose was measured at 14, 21 and 30 days of age in 86 mice (25 male and 16 female control mice, 18 male and 27 female transgenic mice). In addition, a separate group of 10-day-old mice, including nine male and nine female transgenic and four male and four female control mice, was screened for urinary glucose excretion. Up to 21 days of age, urine was collected onto the test stripe by gently rubbing the vulva/preputium. In older animals, spot urine samples were taken by carefully squeezing the bladder with two fingers if no spontaneous urine could be obtained. Urinary glucose excretion was measured semiquantitatively using the glucose-oxidase-peroxidase method (Combi-screen[®] Glucose, ANALYTICON, Germany).

Furthermore, spot urine samples were taken from 110 and 140 days old animals of the different diet groups both after a twelve-hour fasting period and two hours after refeeding.

3.3 Blood/serum glucose and serum insulin values

Blood was collected from the retroorbital plexus under ether anesthesia in fed 10-day-old mice and 1-, 3-, and 8-month-old mice. The number of animals included four male and four female controls and four male and four female transgenic mice each at ten days and one and three months of age. At eight months of age, eleven male controls, six male transgenic mice and three female controls and three female transgenic animals were investigated. From the age of three months onwards, the animals were starved over night (twelve hours) and fed for two hours prior to sampling. Serum was separated by centrifugation (ten minutes, 10,000 x g) and stored at -80°C until assayed. In 10-day-old animals, blood glucose was determined immediately using the Precision QID System (Medisense, Germany). Serum glucose of 1-, 3-, and 8-month-old mice was measured using a Hitachi 717 autoanalyzer and adapted reagents from Roche (Germany). Serum insulin in mice from all age groups was quantified using the Ultrasensitive Mouse-Insulin ELISA kit (Merckodia, Sweden).

Twelve-hour fasting blood glucose levels were determined from two groups of animals fed different diets (see 3.1) in monthly intervals between 80 and 230 days of age. The number of animals investigated is listed in Figures 4.1 and 4.2. Blood samples (4 μl) were directly placed onto a sensor electrode from a small incision of the tail tip. Blood glucose was determined using the Precision Q.I.D. system (Medisense, Germany).

3.4 Glycated hemoglobin (HbA_{1c})

Glycated hemoglobin (HbA_{1c}) levels were measured in 4-month-old mice using freshly hemolyzed blood samples. Reagents were obtained from Recipe Chemicals and Instruments (Germany); measurements were performed on a modular automated analyzing system (Merck, Germany), which was kindly provided by Recipe Chemicals and Instruments. The numbers of animals investigated in both diet groups are shown in Figure 4.4 and 4.5.

3.5 Oral glucose tolerance test (OGTT)

An oral glucose tolerance test (OGTT) was performed at four months of age in seven male controls and seven male transgenic mice as well as six female controls and four female transgenic mice constantly fed standard rodent chow. Animals were fasted twelve hours and a basal blood sample was collected from the nicked tail tip for determination of serum insulin and blood glucose (t=0 minutes). Mice were then gently fixed and 1.5 mg glucose per gram body weight was administered orally. Further blood samples were collected at 10, 20, 30, 60, 90 and 120 minutes for determination of blood glucose, and at 45 and 120 minutes for determination of serum insulin levels. During glucose challenge, blood glucose was determined in freshly hemolyzed samples (Kabe, Germany) by automated analyzer technique (Merck, Germany).

For the determination of serum insulin, blood was collected from the nicked tail tip by gently stripping the tail and collecting the blood in heparinized capillary tubes. Serum was separated from cellular components by centrifugation (10 min, 10,000 x g), collected and stored at -80°C until assayed. Serum insulin levels were determined using a RIA kit (Linco Research, USA).

3.6 Subcutaneous glucose tolerance test (SCGTT)

The subcutaneous glucose tolerance test (SCGTT) was performed at 4 months of age in 24 animals (six male and six female controls and six male and six female transgenic mice) constantly fed standard rodent chow. In the first experiment, 130 μl of a 2 M glucose solution in 0.9% NaCl was administered subcutaneously. After a 7-day-recovery period, the same animals were used in a second experiment where 130 μl of a 2 M glucose solution in 0.9% NaCl with 8% GIP (Bachem, Germany) was administered. The third experiment followed another 7-day-recovery period using 8% GLP-1 (Bachem, Germany) in a 2 M glucose solution in 0.9% NaCl. The test procedure was equal within experiments: After a 15-hour fasting period, a basal blood sample for the determination of fasted serum insulin levels and blood glucose was collected from the tail tip as described in 3.5. Further blood samples were collected at 10, 20, 30, 60, 90 and 120 minutes after subcutaneous administration of the glucose solution for determination of blood glucose, using the Precision QID System (Medisense, Germany). At 10 minutes, a blood sample (100 μl) was collected for the

determination of serum insulin levels. The serum was separated and insulin measured as described in 3.5. The area under the glucose curve (AUC glucose) was calculated using the basal blood glucose values as a baseline under the curve that resulted from the different glucose values after administration of the glucose solutions. The program GraphPad Prism 3.0 (GraphPad Software, USA) was used for the calculation of the AUC glucose.

3.7 Daily food and water intake, urine volume

Daily food and water intake was surveyed five times in a two-day interval, both at four and seven months of age in animals fed the different diets (see 3.1). In addition, the 24-hour urine volume was determined using metabolic cages (Tecniplast, Germany) at the age of seven months. The numbers of animals investigated are shown in Table 4.5 and 4.6.

3.8 Serum parameters

Blood was collected under ether anesthesia, by puncture of the retroorbital plexus. Serum was separated by centrifugation (10 min, 10,000 x g) and stored at -80°C until assayed. Various serum parameters, including sodium, chloride, creatinine, urea, cholesterol, triglycerides, total protein and albumin were determined at three months of age in four male controls, four male transgenic mice, four female controls and four female transgenic mice, using a Hitachi 717 autoanalyzer (Boehringer, Germany) and adapted reagents from Roche (Germany).

3.9 Body and organ weights

The same animals that were used for determination of fasted blood glucose levels were weighed in monthly intervals between 80 and 230 days of age after the twelve-hour fasting period. Organ weights were determined at 90 days of age as described elsewhere in detail (Hoeflich *et al.* 1999); briefly, organs were removed, carefully separated from adjacent tissues and weighed to the nearest mg. For the calculation of gastric and intestinal content, the gastrointestinal tract was weighed before and after removal of the contents. At the age of 10, 30 and 90 days, body weight was de-

terminated in fed mice to the nearest 0.1 g. In 30- and 90-day-old animals, the body weight was corrected for gastric and intestinal content. The numbers of animals investigated are shown in Table 4.8.

3.10 Pancreas preparation and morphometric analysis

Morphometric analysis of the pancreas was performed at the age of 10, 30 and 90 days. The number of animals investigated at each age group was four male controls, four male transgenic mice, four female controls and four female transgenic mice.

Mice were killed by exsanguination under ether anesthesia and blood was collected for determination of glucose and insulin levels as described above. The pancreas was removed immediately, carefully separated from adjacent tissues, weighed to the nearest mg, placed in a tissue capsule on a piece of foam-rubber sponge to avoid distortion and fixed in 10% neutral buffered formalin. For the 10-day age group, an *in situ* fixation was performed before removal of the pancreas to protect the organ from damage. After fixation at room temperature for 24 hours the pancreas was routinely processed and embedded in paraffin. The pancreas was sectioned perpendicular to its longitudinal axis into parallel slices of 1 mm thickness, with the first cut positioned randomly within an interval of 1 mm length at the splenic end of the pancreas. Slices were placed in tissue capsules with the right cut surface facing downward, and paraffin embedding was finished. Approximately 5 μm thick serial sections for histology were cut with a HM 315 microtome (Microm GmbH, Germany) and mounted on 3-aminopropyltriethoxy-silane-treated glass slides. Photographs of hematoxylin and eosin (H&E) stained sections, showing the complete cut surface of all pancreas slices, were taken at a final magnification of 11x using a Wild M 400 photomicroscope (Wild, Switzerland). At the beginning of each set, an object micrometer was photographed under the same conditions for calibration; prints of all negatives were made at a constant setting of the enlarger. Morphometric evaluation was carried out on a Videoplan[®] image analysis system (Zeiss-Kontron, Germany) attached to a microscope by a color video camera. The cross-sectional area of the pancreas was determined planimetrically by circling the cut surface on the prints. Measurements of islet profiles and the various endocrine cell types were carried out on immunohistochemically stained sections (see below). Images were displayed on a color monitor at an 850x final magnification, and the profiles of islets or endocrine cells were meas-

ured planimetrically by circling their contours with a cursor on the digitizing tablet of the image analysis system. Cavalieri's principle was used to estimate the volume of the embedded, i.e. shrunken pancreas ($V_{(\text{Pan})\text{s}}$) as well as the volume of pancreatic islets ($V_{(\text{Islet},\text{Pan})\text{s}}$) (Gundersen & Jensen 1987; Wanke *et al.* 1994). The volume of pancreas ($V_{(\text{Pan})}$) before embedding was calculated from the pancreas weight divided by the specific weight of mouse pancreas ($1,08 \text{ mg/mm}^3$) (Wanke *et al.* 1994). A correction factor for tissue shrinkage due to histological processing was calculated for each organ by dividing the volume of the pancreas before embedding by the volume of the embedded pancreas. Assuming the same extent of shrinkage for islets and the whole organ, the total volume of pancreatic islets ($V_{(\text{Islet},\text{Pan})}$) was calculated as the product of $V_{(\text{Islet},\text{Pan})\text{s}}$ and the individual correction factor. The volume density of the islets in the pancreas ($Vv_{(\text{Islet}/\text{Pan})}$) was calculated dividing the $V_{(\text{Islet},\text{Pan})}$ by the $V_{(\text{Pan})}$. The volume density of the various endocrine cells in the islets ($Vv_{(\text{X-cell}/\text{Islet})}$) was calculated by division of the sum of cross-sectional areas of A-, B-, D- and PP-cells, respectively, by the sum of cross-sectional areas of all islet profiles (Weibel 1979). The total volume of the various endocrine cell types ($V_{(\text{X-cell},\text{Islet})}$) was obtained from the product of the volume density of the endocrine cell-type in the islets and the total islet volume.

Isolated B-cells (insulin positive single cells and small clusters of insulin positive cells that were not contained within established islets) were quantified separately as an index for islet neogenesis (Petrik *et al.* 1999 a; Xu *et al.* 1999). The volume density of isolated B-cells in the pancreas was obtained by dividing the sum of cross-sectional areas of isolated B-cells by the sum of cross-sectional areas of whole pancreas. The total volume of isolated B-cells was obtained from the product of their volume density in the pancreas and the total volume of the pancreas.

3.11 Immunohistochemistry of pancreatic tissue

The indirect immunoperoxidase technique (Nakane & Pierce 1967) was applied to localize insulin, glucagon, somatostatin and pancreatic polypeptide (PP) containing cells. All required antisera were purchased from DAKO Diagnostika (Germany). Sections were deparaffinized in xylene, rehydrated in a descending ethanol series and washed in distilled water. Sections were then incubated in 1% hydrogen peroxide in phosphate-buffered saline (PBS) (pH 7.4) for 15 minutes to block endogenous per-

oxidase activity, followed by a 10-minute washing in PBS (pH 7.4). Tissue sections were then pre-incubated with normal rabbit serum (detection of insulin) or normal swine serum (detection of glucagon, somatostatin and PP) for 30 minutes to reduce non-specific binding. Subsequently, slides were incubated for two hours with guinea pig anti-porcine insulin (dilution: 1:2,000), rabbit anti-human glucagon (dilution: 1:500), rabbit anti-human somatostatin (dilution: 1:300) or rabbit anti-human pancreatic polypeptide (dilution: 1:700), respectively. All antisera were diluted in PBS (pH 7.4) and incubations were performed at room temperature in a humidity chamber. After a 10-minute washing in PBS, horseradish peroxidase conjugated rabbit anti-guinea pig IgG or porcine anti-rabbit IgG (diluted 1:50 in PBS containing 5% (vol/vol) mouse serum) was applied for one hour. The slides were washed in PBS for 10 minutes and immunoreactivity was visualized using 3,3' diaminobenzidine tetrahydrochloride dihydrate (Fluka Chemie, Germany) as chromogen. Tissue sections were counterstained with Mayer's hemalaun solution, dehydrated in an ascending series of alcohols, cleared in xylene and mounted under glass coverslips using Histofluid® (Superior, Germany).

Specificity controls included substitution of primary antisera with nonimmune serum and omission of the secondary antiserum.

3.12 Urine protein analysis

In order to evaluate clinical features of kidney damage, urine protein analysis was performed. Urine samples of six male controls, six male transgenic mice and three female controls and three female transgenic mice were collected in monthly intervals between 56 and 240 days of age. Urine samples were always taken between two and three o'clock in the afternoon and immediately stored at -80 °C until assayed. The same animals were used for qualitative and quantitative morphologic analysis of the kidneys at the age of 240 days (see below).

3.12.1 Sodium dodecyl sulfate (SDS) polyacrylamide gel electrophoresis (PAGE)

a) Methods

Materials used are listed below.

All urine samples were examined within one week. First, urine creatinine concentration was measured, using an automated analyzer technique (Hitachi, Merck, Germany). Urine samples were then diluted to a creatinine content of 1.5 mg/dl, but at least 1:2 with sample buffer. Subsequently, the diluted samples were heated in a thermoblock TB1 (Biometra, Germany) for 10 minutes at 100°C for denaturation of the proteins. In the meantime, a SDS-12% polyacrylamide gel was casted in a gel-casting chamber (Mini-Protean III, Biorad, Germany) and covered with isopropanol. After polymerization, the stacking gel was casted onto the SDS-12% gel; a comb for forming sample wells was immediately placed in the still fluid stacking gel. When the stacking gel was fully polymerized, the comb was removed and the gel was placed into an electrophoresis cell (Protean III, Biorad, Germany), which was then filled with running buffer to the top of the inside cell. The samples, a broad molecular weight standard (Biorad, Germany) and a mouse albumin standard (Biotrend, Germany) diluted 1:100 in sample buffer were then loaded onto the gel and electrophoresis was run for 60 minutes at 200 volt. The gel was removed from the glass frame and silver staining was performed due to a standard protocol (see 9.1). Clearly visible gel bands were registered and gels were photographed for documentation. Finally, gels were dried according to the manufacturers protocol (see 9.2), using the DryEase™Mini-Gel Drying System (Novex, Germany) for long-term storage.

b) Materials

Sample buffer

Distilled water	: 1 ml
Tris/HCl (Roth, Germany) 0.5 M pH 6.8	: 0.25 ml
Glycerol (Merck, Germany)	: 0.2 ml
SDS (Sigma, Germany) 10%	: 0.4 ml
Bromphenol blue (Sigma, Germany) 0.05%	: 0.125 ml

Tris/HCl 0.5 M pH 6.8

Tris base (Roth, Germany) : 6.075 g
ad 60 ml distilled water, adjust pH using 1N HCl (Merck, Germany)

Running buffer (stock)

Tris base (Roth, Germany) : 30.3 g
Glycine (Merck, Germany) : 144 g
ad 1 l distilled water

Running buffer (ready to use)

Stock solution : 40 ml
SDS (Sigma, Germany), 10% : 4 ml
ad 400 ml distilled water

SDS-12% polyacrylamide gel

Distilled water : 3.5 ml
Tris/HCl (Roth, Germany) 1.5 M, pH 8.8 : 2.5 ml
SDS (Sigma, Germany) 10% : 100 μ l
Acrylamide (Roti Phenol, Germany) : 4.0 ml
Ammonium persulfate
(Biorad, Germany) 10% : 50 μ l
Tetraethylethylenediamine
TEMED (Sigma, Germany) : 5 μ l

Stacking gel

Distilled water : 6.1 ml
Tris/HCl (Roth, Germany) 0.5 M, pH 6.8 : 2.5 ml
SDS (Sigma, Germany) 10% : 100 μ l
Acrylamide (Roti Phenol, Germany) : 1.3 ml
Ammonium persulfate
(Biorad, Germany) 10% : 50 μ l
Tetraethylethylenediamine
TEMED (Sigma, Germany) : 5 μ l

3.12.2 Western blot analysis

In order to clarify whether a lane of approximately 67 kDa in the SDS-PAGE reflects albumin, Western blot analysis was performed from the urine samples of 240-day-old animals.

a) Methods

Materials used are listed below.

For Western blot analysis, a SDS-12% polyacrylamide gel was run as described above. After electrophoresis, gels were placed on a pre-wetted nitrocellulose membrane (Schleicher & Schüll, Germany) between three layers of absorbent paper imbibed with buffer, and fiber pads each side, and the sandwich was set in the gel holder cassette. Two cassettes were placed into the electrode module, which was then inserted in the buffer tank along with a frozen cooling unit (Mini Trans-Blot Cell, Biorad, Germany). After filling the tank with Towbin buffer, the transfer was run overnight at 30 volt. The next day, the membranes were dyed with ponceau S solution (Sigma, Germany) to confirm blotting was achieved. After washing in Tris buffered saline (TBS, pH 8.3), blocking was performed in 1% bovine serum albumin (BSA, Sigma, Germany) for one hour to avoid non-specific binding of the antibody probe to the membrane. Then incubation with rabbit anti-mouse albumin antibody probe (Biotrend, Germany; 1:300 in TBS-Tween and 1% BSA) was performed for three hours. The membrane was then incubated with horseradish peroxidase conjugated swine anti-rabbit antibody (DAKO Diagnostika, Germany; 1:1000 in TBS-Tween and 1% BSA) for one hour. After washing three times in TBS-Tween for ten minutes, immunoreactivity was visualized using 3,3' diaminobenzidine tetrahydrochloride dihydrate (Fluka Chemie, Germany) as chromogen. Membranes were photographed and stored in a light protected cassette.

b) Materials

Towbin buffer (stored at 4 °C)

Tris base (Roth, Germany)	: 3.03 g
Glycine (Merck, Germany)	: 14.4 g
Distilled water	: 800 ml
Methanol (Merck, Germany)	: 200 ml

Tris buffered saline (TBS) 10* stock solution (stored at 4 °C)

Tris base (Roth, Germany)	: 60.6 g
Sodium chloride (Merck, Germany)	: 87.6 g
ad 1 l distilled water, adjust pH 7.5 using 1N HCl (Merck, Germany)	

TBS-Tween

1* TBS (10* TBS stock solution diluted 1:10)
0.05% Tween (Sigma, Germany)

DAB (3,3' diaminobenzidine tetrahydrochloride dihydrate)

DAB (Fluka Chemie, Germany)	: 5 ml
Tris/HCl 50 mM pH 7.3	: 25 ml
Hydrogen peroxide (Merck, Germany), 30%	: 10 µl

3.13 Immunohistochemistry of the kidneys

Kidneys used for immunohistochemistry were fixed by orthograde perfusion as described under 3.14. Instead of glutaraldehyde, a 4% paraformaldehyde in PBS (pH 7.4) was used for perfusion and kidneys were post-fixed *in situ* by immersion in 4% paraformaldehyde for 24 hours. Both kidneys were cut into parallel transversal slices, half of which were embedded in paraffin for immunohistochemistry and the other half was embedded in plastic as described in 3.15.

The indirect immunoperoxidase technique (Nakane & Pierce 1967) served to localize the extracellular matrix proteins collagen IV, laminin and fibronectin. Sections were deparaffinized, rehydrated, and endogenous peroxidase was blocked as described in 3.11. The slides were then washed in tris-buffered saline (TBS) (pH 7.6) for 10 min-

utes and proteinase K (Dako Diagnostika, Germany) was applied for 30 minutes at 37°C to improve the accessibility of the antibodies to target sites within the tissue. After washing the slides in TBS for 10 minutes, tissue sections were pre-incubated with normal swine serum for 30 minutes at room temperature. Subsequently, slides were incubated with rabbit-anti human placental type IV collagen (Quartett, Germany), dilution 1:40 in TBS, rabbit anti-mouse laminin (DCS, Germany), dilution 1:50 in TBS, or rabbit-anti human placental fibronectin (Biocarta, Germany), dilution 1:100 in TBS, in a humidity chamber for two hours at 37°C. After a 10-minute washing in TBS, porcine anti-rabbit IgG (diluted 1:100 in TBS containing 5% (vol/vol) mouse serum) was applied for one hour; incubation took place at 37°C in a humidity chamber. Then slides were washed in TBS for 10 minutes and immunoreactivity was visualized using Sigma fast DAB (3,3' diaminobenzidine; Sigma, Germany) tablets. The DAB tablet and the urea hydrogen peroxide tablet were dissolved in 5 ml of TBS and then the tissue sections were covered with the solution and incubated for 5 minutes. Tissue sections were counterstained with Mayer's hemalaun solution, dehydrated in an ascending series of alcohols, cleared in xylene and mounted under glass coverslips using Histofluid (Superior, Germany).

Specificity controls included substitution of primary antisera with non-immune serum and omission of the secondary antiserum.

3.14 Kidney preparation and morphometric analysis

The numbers of animals investigated at four and eight months of age are listed in Tables 4.13 and 4.14.

For morphometric analysis, kidneys were fixed by orthograde perfusion at constant pressure of 100 mm Hg. The animals were killed by ether inhalation, the abdominal cavity and thorax were immediately opened and a needle to which the perfusion tubes were attached was inserted into the left ventricle of the heart. The vascular system was pre-flushed with PBS (pH 7.4, 37 °C) for 20 seconds and then a 3% glutaraldehyde solution (37 °C) was perfused for five minutes; an incision of the inferior vena cava served as outlet for the perfusate. The kidneys were post-fixed *in situ* by immersion in 3% glutaraldehyde for 2 days before further processing. Both kidneys were then carefully removed and trimmed free of attached tissue before weighing to the nearest mg on a precision balance (Mettler Instrument Corporation, Germany).

The length of each kidney was documented before it was cut into parallel transversal slices of approximately 2 mm thickness, with the first cut positioned randomly in a 1 mm interval from one of the poles. The kidney slices were placed into tissue capsules onto a foam rubber sponge to avoid distortion and routinely processed for plastic embedding in a Citadel 1000 (Shandon, Germany). Embedding in glycolmethacrylate and methylmethacrylate was performed as previously described (Hermanns *et al.* 1981). Approximately 1.5 μm thick sections for histology were cut using a Reichert-Jung 2050 rotary microtome (Cambridge Instruments, Germany). Sections of each kidney slice were stained with H&E, PAS (Periodic Acid Schiff stain) and a modified protocol for a combined PASM-PAS (Periodic acid silver methenamine-PAS) dye, respectively (see attachment). Photographs of PAS stained sections, showing the complete cut surface of all kidney slices, were taken at a final magnification of 15x using a Wild M 400 photomicroscope (Wild, Switzerland). At the beginning of each set, an object micrometer was photographed under the same conditions for calibration; prints of all negatives were made at a constant setting of the enlarger. Morphometric evaluation was carried out on a Videoplan[®] image analysis system (Zeiss-Kontron, Germany) attached to a microscope by a color video camera. The cross-sectional area of the kidney sections was determined planimetrically by circling the cut surface on the prints. Measurement of glomerular profiles was carried out on PASM-PAS stained sections. Images were displayed on a color monitor at an 850x final magnification (25x objective), and the profiles of glomeruli were measured planimetrically by circling their contours with a cursor on the digitizing tablet of the image analysis system. Cavalieri's principle was used to estimate the volume of the embedded, i.e. shrunken kidney ($V_{(\text{Kid})\text{s}}$) (Gundersen & Jensen 1987). The volume of the kidneys ($V_{(\text{Kid})}$) before embedding was calculated from the kidney weight divided by the specific weight of mouse kidney (1.05 mg/mm³). A correction factor for tissue shrinkage due to histological processing was calculated for each organ by dividing the volume of the kidneys before embedding by the volume of the embedded kidneys. Assuming the same extent of shrinkage for glomeruli and the whole organ, the mean glomerular volume ($v_{(\text{Glo})\text{m}}$) was calculated as the product of mean glomerular area, shape coefficient (1.40) and the individual correction factor, divided by the size coefficient (1.04) as described elsewhere in detail (Wanke 1996; Weibel & Gomez 1962).

3.15 Histological techniques

a) Paraffin histology

Organs were fixed by immersion in 10% neutral buffered formalin for 24 hours. After fixation, the organs were sliced and representative parts were placed in tissue capsules. The tissues were routinely processed in a Histomaster 2050/DI (Bavimed, Germany) and embedded in paraffin. Approximately 5 μm thick sections for histology were cut using a HM 315 microtome (Microm GmbH, Germany); sections were transferred into a water bath and mounted on glass slides (Marienfeld, Germany). Routinely, sections were stained with H&E (for paraffin embedded tissue); additional staining was performed if necessary (PAS, Gomori's silver stain).

b) Frozen sections

For determination of lipid, frozen sections were cut using a microtome (Leitz, Germany) and stained with Fat red. Staining protocols are listed in the attachment.

c) Plastic histology

Organs were fixed by immersion in 10% neutral buffered formalin for 24 hours or by perfusion with 3% glutaraldehyde (details are given in chapter 3.14). After fixation, tissue samples were placed in tissue capsules and processed in a Citadel 1000 (Shandon, Germany) for 18 hours. Subsequently, tissue capsules were transferred into a solution containing equal amounts of hydroxymethylmethacrylate (Fluka Chemie, Germany) and methylmethacrylate (Riedel de Haën, Germany); immersion of the tissue pieces in this solution took place at 4°C on a shaker for 18 hours. Tissue capsules were then brought into "solution A", containing 338 mg of benzoylperoxide with 25% water (Merck, Germany), 20 ml methylmethacrylate, 60 ml hydroxymethylmethacrylate, 16 ml ethyleneglycol monobutylether (Merck, Germany) and polyethylene glycol 400 (Merck, Germany). After immersion for four hours at 4°C on a shaker, tissue pieces were placed in plastic cups and embedded, using 60 μl of dimethylanilin (Merck, Germany) in 40 ml of solution A as starter for polymerization. Cups were immediately placed into a water bath (4°C) making sure that the distance between

the cups was at least 3 cm. Polymerization took place at 4°C over night. On the next day, the casted blocks were removed from the cups and approximately 1.5 µm thick sections were cut on a Reichert-Jung 2050 rotary microtome (Cambridge Instruments, Germany). Sections were transferred into a water bath (40-50°C) and mounted on glass slides. Tissue sections were left on a heating stage (60°C) for 30 minutes before staining. Routinely performed staining procedure was H&E; additional staining was performed if necessary (PAS, PASM-PAS). Staining protocols are listed in the attachment.

3.16 Twelve-month survival

Two groups of GIPR^{dn} transgenic and control mice were studied until the age of twelve months, one of them was constantly fed standard rodent chow (Diet 1) and the other was fed the carbohydrate-restricted diet from weaning until four months of age (Diet 2). The time of death was documented for each animal that died within the 12-month period and the cause of death was examined by complete necropsy including paraffin or plastic histology if necessary.

Number of animals studied per group:

Diet 1: male control: 18, male transgenic: 9, female control: 7, female transgenic: 20

Diet 2: male control: 11, male transgenic: 7, female control: 13, female transgenic: 12

3.17 Data Presentation and Statistical Analysis

Statistical significance of differences between two groups (quantitative-stereological kidney findings at four months of age) was calculated by non-parametric Mann-Whitney U test using the SPSS 10.0 program for Windows (Leibniz Rechenzentrum, Germany). If more than two groups were tested, the general linear model procedure (GLM) was used in order to calculate the least squares means (LSM); comparison of the LSM of different groups was performed using the student's t-test (SAS version 6.4, SAS Institute, Germany). P values < 0.05 were considered significant. Morphometric results (kidney, pancreas) were corrected for embedding shrinkage using the individual correction factor. Data are presented as means ± SEM, the SEM was calculated dividing the SD by the square root of the number of animals examined.

4. Results

4.1 Urine glucose

a) Animals receiving standard rodent chow

To determine the onset of diabetes mellitus in GIPR^{dn} transgenic mice, urinary glucose excretion was measured at the age of 10, 14, 21 and 30 days. Animals were weaned at 28 days of age and had free access to standard rodent chow. Urinary glucose excretion was not detectable in any transgenic or control animal at 10 days of age. At two weeks of age, glucose was present in urine samples of 1/18 male and 1/27 female transgenic mice. All transgenic mice demonstrated severe glucosuria (>1,000 mg/dl) at three and four weeks of age. Glucosuria was not detected in controls at any age studied (Table 4.1).

Further, glucose excretion in urine was measured in a group of animals at 110 and 140 of age, including seven male transgenic and three female transgenic animals. All transgenic animals from group Diet 1 showed fasting and postprandial glucosuria (>1,000 mg/dl).

Group (n)	Age (days)			
	10	14	21	30
Co male	0/4	0/25	0/25	0/25
Tg male	0/9	1/18	18/18	18/18
Co female	0/4	0/16	0/16	0/16
Tg female	0/9	1/27	27/27	27/27

Table 4.1 Onset and incidence of diabetes mellitus in GIPR^{dn} transgenic mice. Onset of diabetes in transgenic (tg) mice occurs between 14 and 21 days. Control (co) mice do not show glucosuria at any time point investigated. Data are presented as number of animals showing glucosuria / number of animals investigated in each group.

b) Animals receiving the carbohydrate restricted diet until four months

Urine glucose was measured at 110 and 140 days of age. At 110 days of age, only one third of both male (2/7) and female (4/12) transgenic animals showed fasted glucosuria. Postprandially, all transgenic males and 8/12 transgenic females examined showed glucosuria. After the diet was changed (at 120 days of age), all transgenic males showed fasted and postprandial glucosuria, whereas one third of fasted and all fed female transgenic animals exhibited severe glucosuria (>1,000 mg/dl).

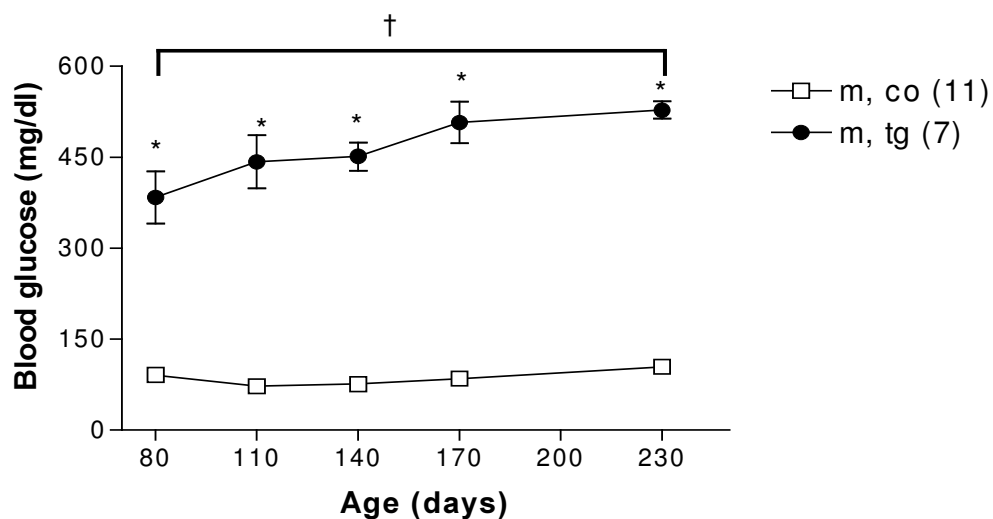
4.2. Blood/serum glucose and serum insulin levels

a) Animals receiving standard rodent chow

Blood and serum glucose levels

From 80 days of age onwards, fasting blood glucose levels were determined in monthly intervals. Glucose values were significantly (> 4-fold) elevated in transgenic mice, as compared to age- and sex-matched littermate controls, irrespective of the age at sampling. From 80 to 230 days of age, blood glucose levels increased in transgenic males ($p < 0.05$) and females (n.s.). Blood glucose levels of control mice remained stable over the period sampled (Fig. 4.1 A/B).

(A) Male animals



(B) Female animals

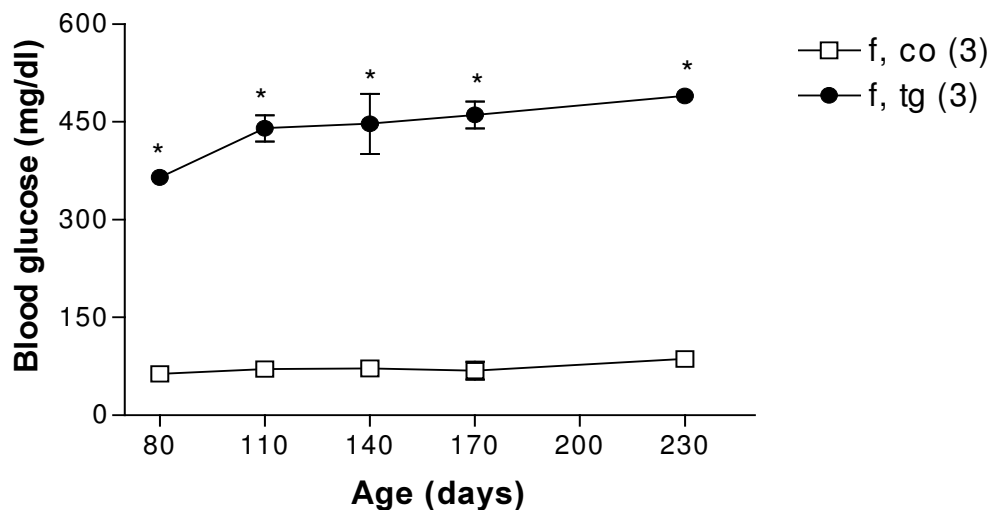


Figure 4.1 (A/B). Blood glucose values of animals receiving Diet 1 between 80 and 230 days of age; (A) male animals, (B) female animals. Blood glucose values of both male (m) and female (f) transgenic (tg) mice are significantly higher than those of sex-matched controls (co). Data are means \pm SEM; (n), number of animals investigated. * $p < 0.05$ vs. control, † $p < 0.05$ vs. previous time point.

In addition, blood glucose levels were determined in fed animals prior to sacrifice. In 10-day-old transgenic mice, blood glucose levels did not differ from those of control mice. Serum glucose concentration was elevated 3.9-fold ($p < 0.05$) in one-month-old male transgenic mice, as compared to male littermate controls and 4.0-fold ($p < 0.05$) in female transgenic mice vs. female littermate controls. At three months of age, postprandial serum glucose was 7.0-fold ($p < 0.05$) elevated in male and 4.4-fold ($p < 0.05$) elevated in female transgenic mice vs. sex-matched controls (Table 4.2).

Group (n)	Age (days)		
	10	30	90
Co male (4)	110 ± 10	205 ± 14	152 ± 18
Tg male (4)	111 ± 7	807* ± 22	1065* ± 39
Co female (4)	114 ± 4	153 ± 9	197 ± 29
Tg female (4)	106 ± 7	616* ± 51	865* ± 33

Table 4.2 Blood and serum glucose concentrations (mg/dl), Diet 1. Values at the age of 10 days represent blood glucose, values at 30 and 90 days of age represent serum glucose levels. From 30 days of age onwards, transgenic (tg) mice exhibit severe hyperglycemia. Data are means ± SEM; (n), number of animals investigated. * p<0.05 vs. control (co).

Two-hour postprandial serum glucose levels were largely elevated in 8-month-old transgenic males and females vs. controls (p<0.05) (Table 4.3).

Group (n)	Serum glucose (mg/dl)	Serum insulin (ng/ml)
Co male (11)	193 ± 6	4.28 ± 0.82
Tg male (6)	1061* ± 51	0.39* ± 0.07
Co female (3)	159 ± 2	4.52 ± 0.44
Tg female (3)	869* ± 64	0.51* ± 0.03

Table 4.3 Postprandial serum glucose and insulin concentrations of 8-month-old mice, Diet 1. Transgenic mice (tg) exhibit severe hyperglycemia and hypoinsulinemia as compared to age- and sex-matched controls (co). Data are means ± SEM; (n), number of animals investigated; * p<0.05 vs. control.

Serum insulin levels

At the age of 10 days, mean serum insulin levels were reduced 1.8-fold in male and 2.2-fold in female transgenic animals as compared to sex-matched littermate controls (n.s.). Insulin values in one-month-old transgenic males were reduced 18.8-fold (p<0.05) and 6.1-fold (p<0.05) in female transgenic mice vs. sex-matched controls. Postprandial insulin levels were significantly reduced in 3-month-old male (6.9-fold)

and female transgenic mice (4.3-fold) vs. control mice (Table 4.4). Further, postprandial serum insulin levels were determined at eight months of age and found to be significantly lower in GIPR^{dn} transgenic males and females, as compared to age- and sex-matched littermate controls (Table 4.3).

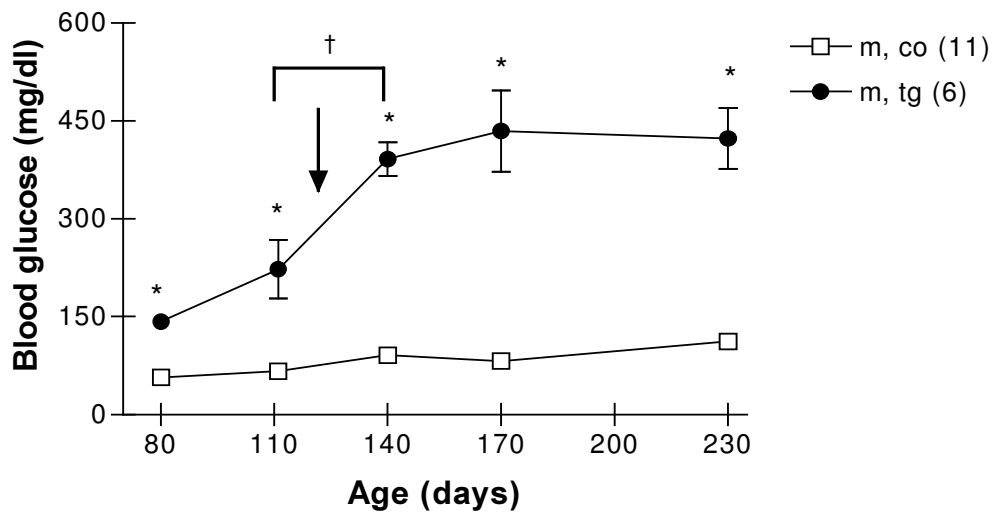
Group (n)	Age (d)		
	10	30	90
Co male (4)	0.14 ± 0.03	5.63 ± 1.74	2.43 ± 1.59
Tg male (4)	0.08 ± 0.01	0.30* ± 0.04	0.35* ± 0.12
Co female (4)	0.60 ± 0.22	3.23 ± 0.39	0.81 ± 0.09
Tg female (4)	0.27 ± 0.13	0.53* ± 0.15	0.19* ± 0.06

Table 4.4 Serum insulin concentrations (ng/ml), Diet 1. Serum insulin levels are lower in transgenic (tg) animals at 10 days of age and are significantly lower in GIPR^{dn} transgenic mice at 30 and 90 days of age vs. age-matched control (co) mice. Data are means ± SEM; (n), number of animals investigated. * p<0.05 vs. control.

b) Animals receiving the carbohydrate restricted diet until 4 months

Fasting blood glucose levels were measured between 80 and 230 days of age in monthly intervals. All transgenic animals exhibited significantly higher blood glucose levels than sex- and diet-matched control mice, irrespective of the age at sampling. In all transgenic animals, blood glucose levels increased significantly between 110 and 140 days of age, the interval when the diet was changed from carbohydrate-restricted to standard diet (Fig. 4.2 A/B). In male and female transgenic animals a 1.8- and 1.3-fold increase was documented, in male and female control mice, the rise of blood glucose levels between 110 and 140 days was not significant (1.4- and 1.2-fold, respectively).

(A) Male animals



(B) Female animals

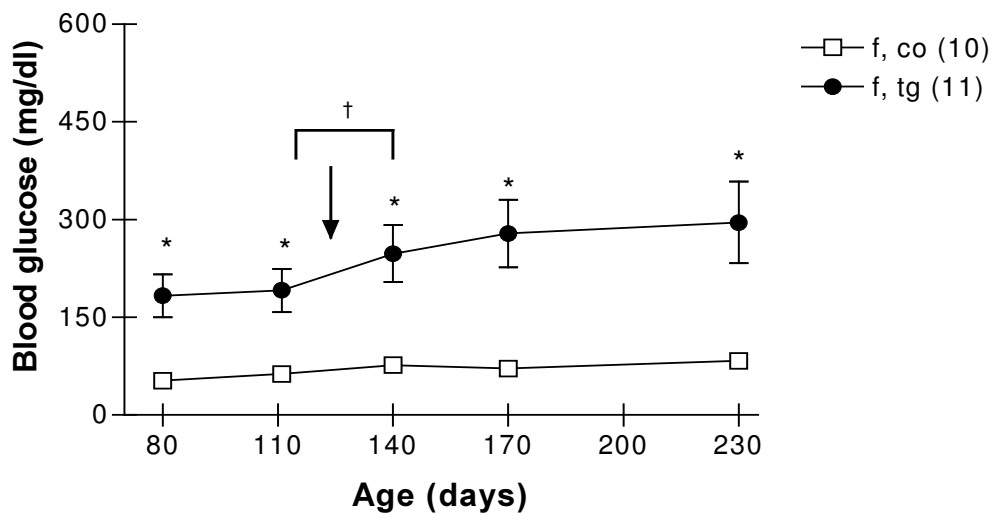
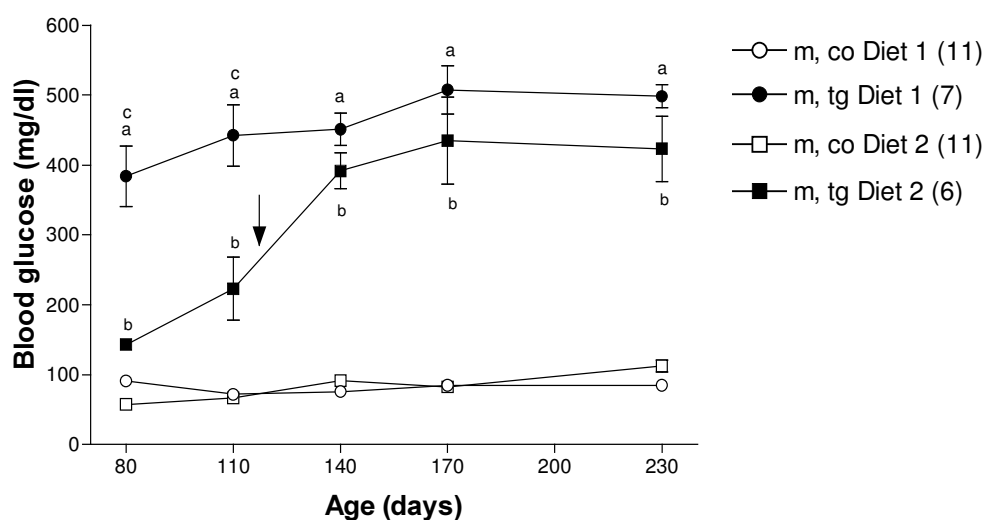


Figure 4.2 (A/B) Blood glucose values between 80 and 230 days of age of animals receiving Diet 2; (A) male animals, (B) female animals. Blood glucose values of both male (m) and female (f) transgenic (tg) mice are significantly higher than those of sex-matched controls (co). Blood glucose values of all transgenic animals increase significantly between 110 and 140 days of age. The time point of diet change is indicated with an arrow. Data are means \pm SEM; (n), number of animals investigated. * $p < 0.05$ vs. control, † $p < 0.05$ vs. previous time point.

c) Comparison of both diet groups

Until 110 days of age, transgenic animals fed standard rodent chow showed significantly higher fasted blood glucose levels than transgenic animals fed the carbohydrate-restricted diet. After the diet was changed, transgenic animals of the group Diet 2 still showed lower fasted blood glucose levels than transgenic animals permanently fed standard rodent chow, however, this difference was not statistically significant (Fig. 4.3 A/B).

(A) Male animals



(B) Female animals

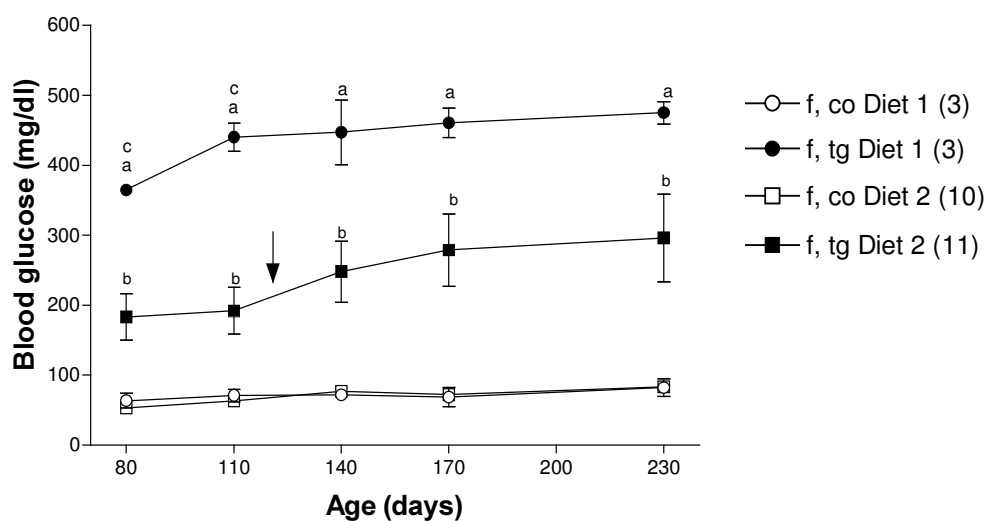


Figure 4.3 (A/B) Comparison of blood glucose values of animals receiving Diet 1 and Diet 2 between 80 and 230 days of age; (A) male animals, (B) female animals. Blood glucose values of both male (m) and female (f) transgenic (tg) mice receiving Diet 1 are higher than those of transgenic animals receiving Diet 2. The time point of diet change is indicated with an arrow. Data are means \pm SEM; (n), number of animals investigated; a-c: $p < 0.05$, a: Diet 1 transgenic vs. control (co), b: Diet 2 transgenic vs. control, c: Diet 1 transgenic vs. Diet 2 transgenic.

4.3 Glycated hemoglobin (HbA_{1c}) levels

In order to evaluate whether high blood glucose levels in transgenic mice are associated with high levels of glycated hemoglobin (HbA_{1c}), HbA_{1c} levels were determined at four months of age.

a) Animals receiving standard rodent chow

HbA_{1c} levels were significantly higher in transgenic males and females as compared to age- and sex-matched control mice (Fig. 4.4).

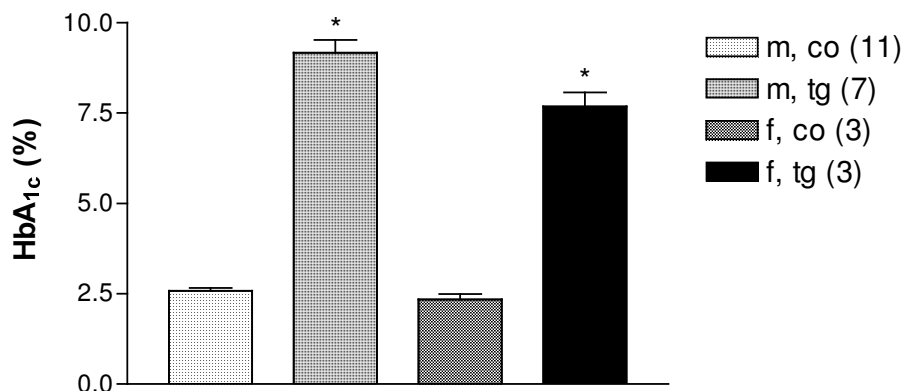


Figure 4.4 Glycated hemoglobin of animals receiving Diet 1. HbA_{1c} levels are significantly higher in transgenic (tg) males (m) and females (f) as compared to age- and sex-matched control (co) mice. Data are means \pm SEM; (n), number of animals investigated. * $p < 0.05$ vs. control.

b) Animals receiving the carbohydrate restricted diet

HbA_{1c} levels were significantly higher in transgenic males and females as compared to age- and sex-matched control mice (Fig. 4.5).

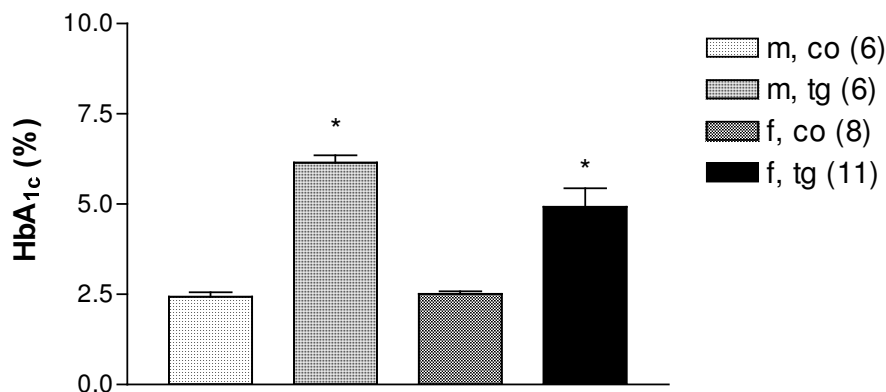


Figure 4.5 Glycated hemoglobin of animals receiving Diet 2. In all transgenic (tg) animals studied, HbA_{1c} levels are significantly higher than those of age- and sex-matched control (co) mice. Data are means \pm SEM; (n), number of animals investigated; m, male; f, female. * $p < 0.05$ vs. control.

c) Comparison of both diet groups

HbA_{1c} levels were significantly higher in transgenic animals permanently fed the standard rodent chow as compared to transgenic animals fed the carbohydrate-restricted diet (Fig. 4.6).

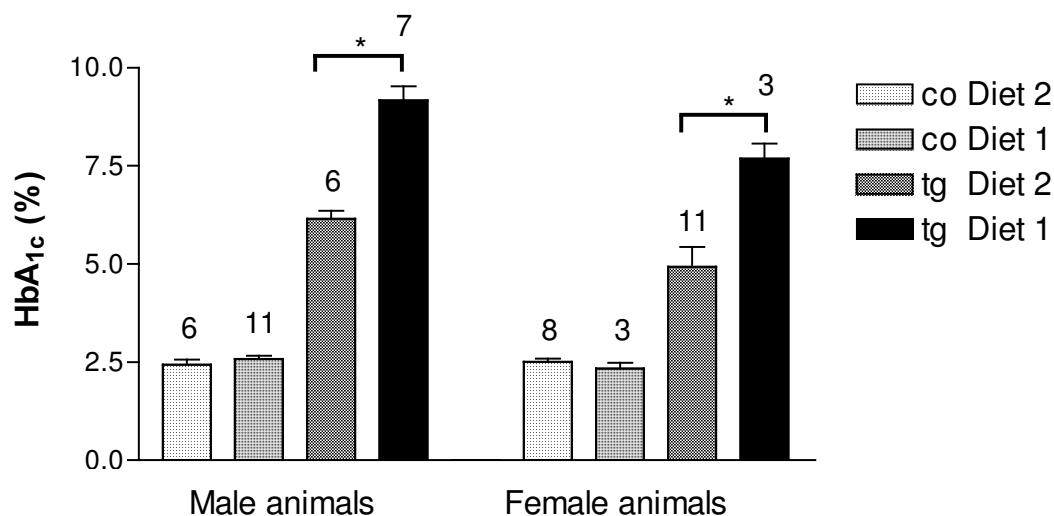
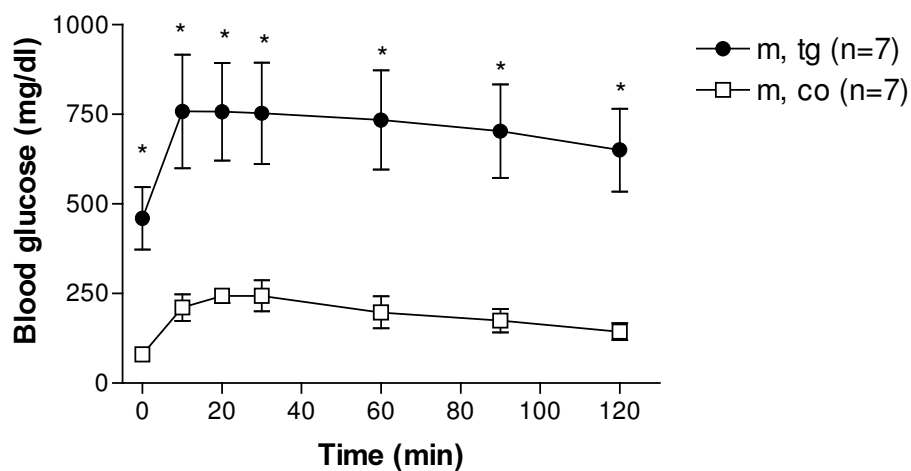


Figure 4.6 Comparison of glycated hemoglobin levels of animals receiving Diet 1 and Diet 2. Both male (m) and female (f) transgenic (tg) animals receiving Diet 1 exhibit significantly higher HbA_{1c} levels than transgenic animals fed Diet 2. Data are means \pm SEM; n, number of animals investigated. * $p < 0.05$.

4.4 Oral glucose tolerance test (OGTT)

In order to clarify whether the diabetic state is due to low insulin secretion or disturbed insulin sensitivity, OGTT was performed in 4-month-old mice receiving Diet 1. Basal blood glucose levels were 459.9 ± 32.8 mg/dl for male and 450.7 ± 74.6 mg/dl for female transgenic mice. In control males, basal blood glucose levels were 80.3 ± 5.9 mg/dl and 76.0 ± 8.3 mg/dl in females, respectively. Blood glucose levels of transgenic mice were significantly elevated at all time points examined and showed only a slight decrease 120 min after oral glucose challenge, whereas control mice reached near basal levels after 120 min (Fig. 4.7 A/B). These findings clearly show that $GIPR^{dn}$ transgenic mice are glucose intolerant.

(A) Male animals



(B) Female animals

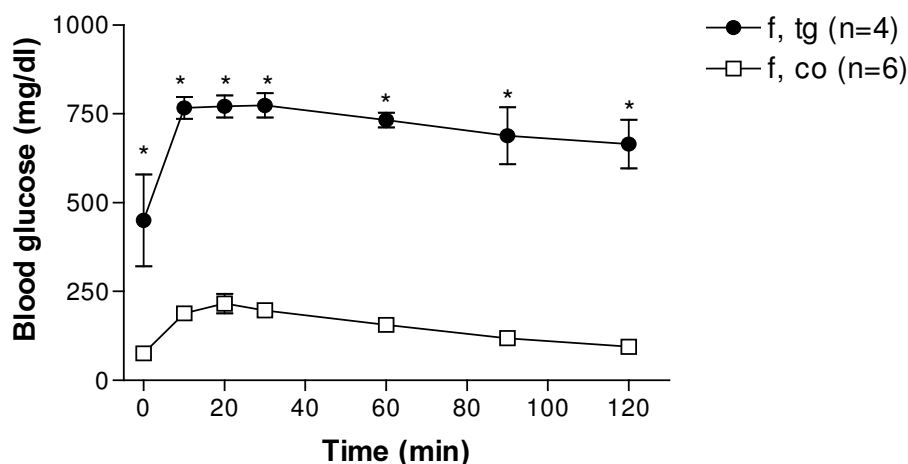
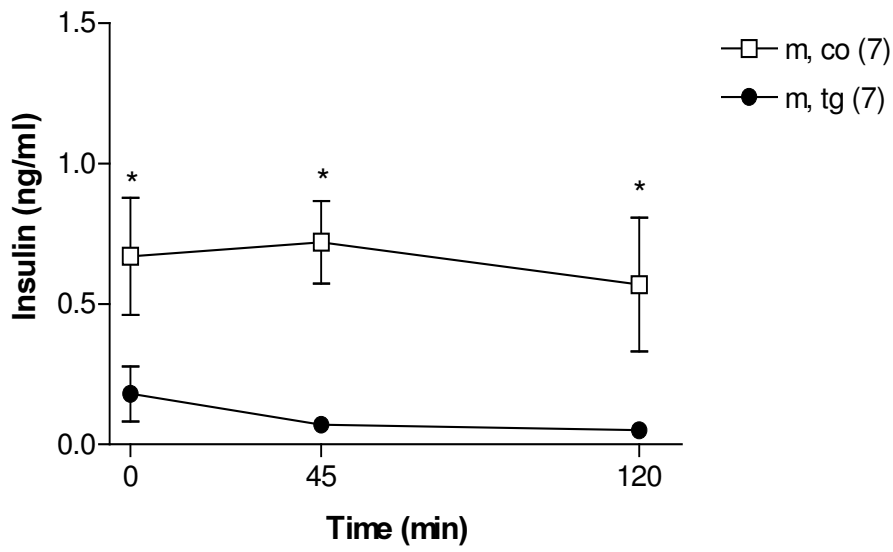


Figure 4.7 (A/B) Oral glucose tolerance test of animals receiving Diet 1, (A) male animals; (B) female animals. Transgenic (tg) male (m) and female (f) animals exhibit significantly higher glucose values after oral glucose challenge than sex-matched controls (co). Data are means \pm SEM; (n), number of animals investigated. * $p < 0.05$ vs. control.

Serum insulin levels were determined during the oral glucose tolerance test at 0, 45 and 120 minutes. In male $GIPR^{dn}$ transgenic mice, serum insulin values were significantly lower than those of control mice at the basal state (3.7-fold), at 45 min (10.3-fold) and at 120 minutes (11.4-fold). Whereas insulin levels of control males showed a slight increase from basal levels at 45 minutes, serum insulin values of $GIPR^{dn}$ transgenic males were 2.6-fold decreased. At 120 minutes, serum insulin concentrations had returned to basal levels in control males and were 3.6-fold lower than fasted levels in transgenic males, respectively. In female transgenic mice, basal insulin levels were 4.7-fold lower than those of control mice. Values at 45 minutes were 14.6-fold lower ($p < 0.05$), and at 120 min after oral glucose load serum insulin concentrations were 5-fold lower than those observed in female controls. Insulin levels rose markedly from 0 to 45 min and decreased to near basal levels between 45 and 120 min in female control mice, whereas in female transgenic mice insulin levels remained at basal levels over the period sampled (Fig. 4.8 A/B).

(A) Male animals



(B) Female animals

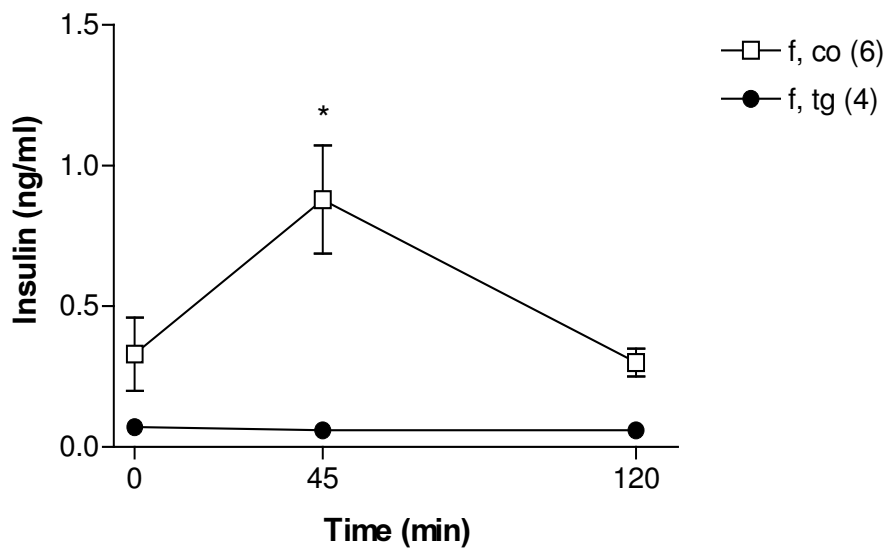


Figure 4.8 (A/B) Serum insulin levels during an oral glucose tolerance test of animals receiving Diet 1; (A) male animals, (B) female animals. Serum insulin levels of transgenic (tg) male (m) and female (f) animals are lower than those of sex-matched controls (co). Data are means \pm SEM; (n), number of animals investigated. * $p < 0.05$ vs. control.

4.5 Subcutaneous glucose tolerance test (SCGTT)

The SCGTT was performed in order to clarify whether the diabetic phenotype results from the disruption of GIP receptor signaling by the mutated receptor or a non-specific affection of further B-cell associated G protein-coupled receptors. Since the GLP-1 receptor is also G protein-coupled, GLP-1 was used as an example to show the specificity of the alterations to the mutated receptor. The area under glucose curve (AUC glucose) was significantly elevated in transgenic animals receiving the 2 M glucose solution in 0.9% NaCl as compared to sex-matched controls. The concomitant administration of 8% GIP had no effect on the AUC glucose in transgenic animals, whereas in controls, an at least 42% reduction of the AUC glucose was observed as compared to animals receiving glucose without GIP (Fig. 4.9). The application of GLP-1 during SCGTT had the same effects on the AUC glucose of transgenic and control animals: The GLP-1-induced reduction of the AUC glucose was between 48-56% as compared to SCGTT without GLP-1 (Fig. 4.10).

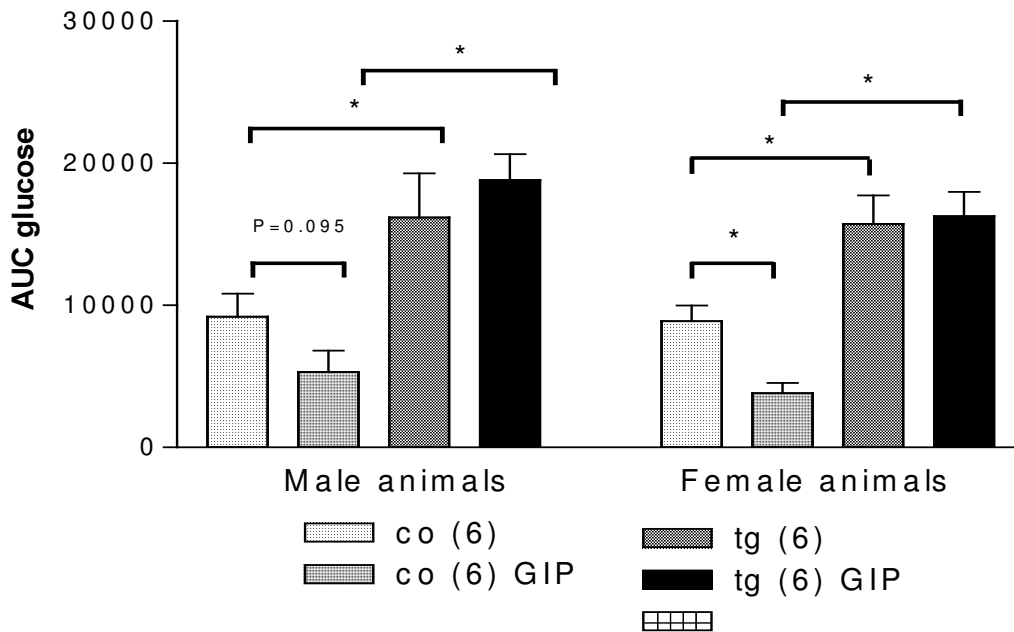


Figure 4.9 AUC glucose during SCGTT with and without application of 8% GIP. During SCGTT, the AUC glucose of transgenic (tg) male (m) and female (f) animals is significantly higher than that of sex-matched controls (co). The application of GIP has no effect on the AUC glucose in transgenic animals. In controls, an at least 42% GIP-induced reduction of the AUC glucose can be

observed as compared to SCGTT without GIP. Data are means \pm SEM; (n), number of animals investigated. * $p < 0.05$ vs. control.

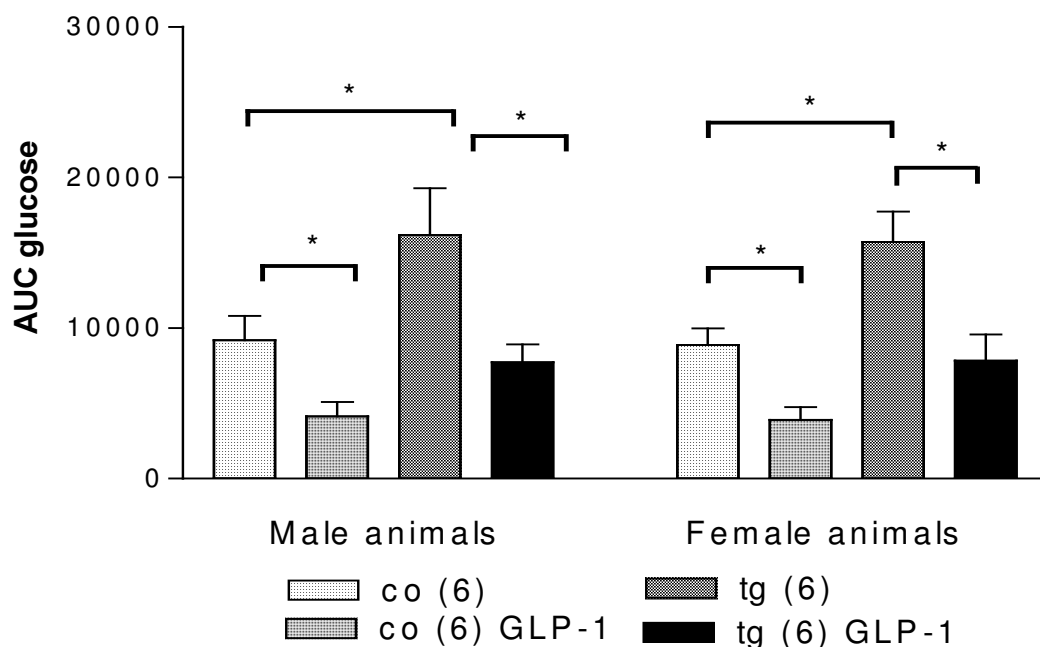


Figure 4.10 AUC glucose during SCGTT with and without application of 8% GLP-1. The application of GLP-1 has the same effect on the AUC glucose in transgenic and control animals. An at least 48% reduction of the AUC glucose can be observed in all animals receiving GLP-1 as compared to SCGTT without GLP-1. Data are means \pm SEM; (n), number of animals investigated. * $p < 0.05$ vs. control.

The increase of insulin secretion was calculated from the basal and 10-minute insulin values during SCGTT. Glucose alone induced an at least 2.1-fold increase of serum insulin levels in controls, whereas in transgenic mice, no glucose-induced increase of insulin levels was observed. The concomitant application of GIP during SCGTT induced a 6.3-fold increase of insulin levels in male controls and a 2.6-fold increase in female controls, respectively. In transgenic animals, GIP was not capable to augment the glucose-induced insulin secretion. GLP-1 induced a 4.9-fold increase of insulin levels in male and a 3.9-fold increase in female controls, respectively. GLP-1 did not augment the 10-minute insulin levels in transgenic mice (Fig. 4.11).

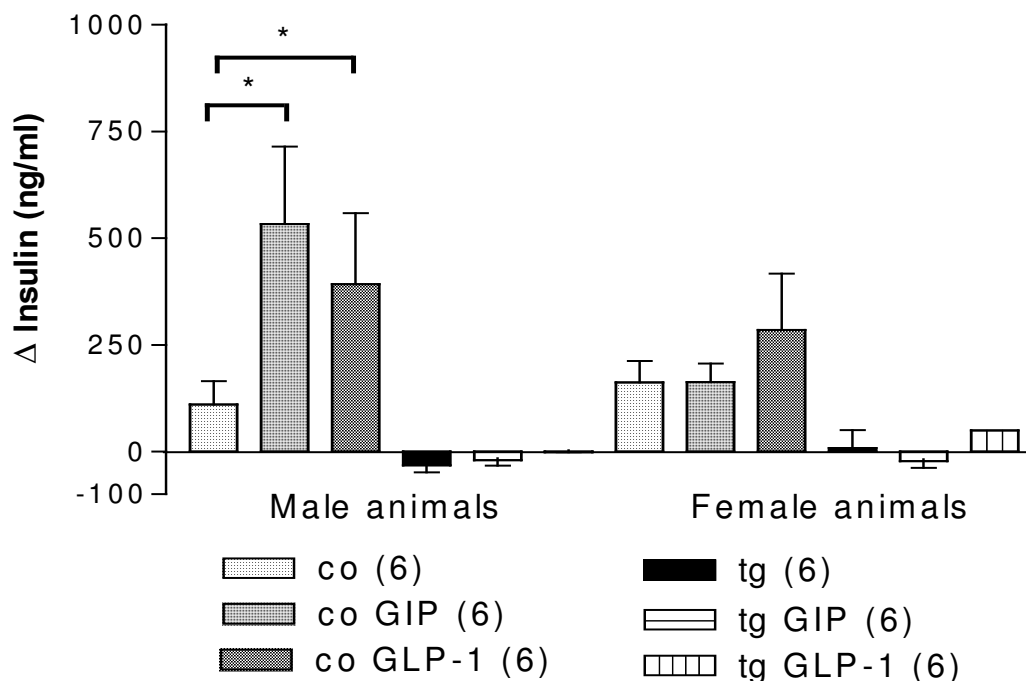


Figure 4.11 Increase of serum insulin levels during SCGTT without and with GIP and GLP-1. Glucose alone induced an increase of the insulin levels in controls (co) but not in transgenic (tg) animals. GIP and GLP-1 further augmented the glucose induced insulin secretion in male (m) controls. In female (f) controls and transgenic animals, the peptides did not significantly increase the glucose-induced insulin secretion. Data are means \pm SEM; (n), number of animals investigated. * $p < 0.05$ vs. control.

4.6 Daily food and water intake, urine volume

To investigate the effect of the metabolic state on feeding behavior, food and water intake was measured in two groups of mice fed different diets at four and seven months of age. To evaluate whether polydipsia correlates with polyuria, the 24-hour urine volume was measured from the same group of mice at seven months of age.

a) Animals receiving standard rodent chow

Irrespective of the age at sampling, food intake was over 2.3-fold elevated in male transgenic mice vs. control males and more than 2.1-fold in transgenic females vs. control females, respectively ($p < 0.05$) (Table 4.5). These findings indicate severe hyperphagia in GIPR^{dn} transgenic mice.

Water intake of male and female transgenic mice was more than 8.4-fold higher vs. control mice, at both four and seven months of age ($p < 0.05$) (Table 4.5). These results show that the metabolic state in GIPR^{dn} transgenic animals is accompanied by severe polydipsia.

The urine volume was more than 18-fold elevated in male and female GIPR^{dn} transgenic mice vs. sex-matched littermate controls (Table 4.5). This finding demonstrates severe polyuria in GIPR^{dn} transgenic mice.

Group (n,n)	Food intake (g/g body weight/day)		Water intake (g/g body weight/day)		Urine volume (ml/day)
	4 months	7 months	4 months	7 months	7 months
Co male (8,8)	0.13 ± 0.01	0.10 ± 0.01	0.19 ± 0.02	0.17 ± 0.01	1.69 ± 0.28
Tg male (7,7)	0.30* ± 0.02	0.27* ± 0.01	1.61* ± 0.08	1.43* ± 0.14	44.86* ± 2.49
Co female (6,3)	0.13 ± 0.01	0.15 ± 0.02	0.20 ± 0.01	0.21 ± 0.05	2.97 ± 0.55
Tg female (5,3)	0.32* ± 0.04	0.32* ± 0.02	1.67* ± 0.36	1.88* ± 0.13	52.67* ± 7.22

Table 4.5 Daily food and water intake and daily urine volume of animals receiving Diet 1. All transgenic animals show polydipsia, polyuria and hyperphagia. Data are means ± SEM; (n,n), number of animals investigated at four and seven months of age; (co), control; (tg), transgenic. * $p < 0.05$ vs. control.

b) Animals receiving the carbohydrate-restricted diet

Data are presented in Table 4.6. Transgenic animals receiving the carbohydrate restricted diet showed significantly higher food and water intake as compared to age-, sex-, and diet-matched control mice, irrespective of the age at sampling. At 4 months of age, food intake was 1.2-fold higher in both male and female transgenic mice as compared to sex-matched controls. Water intake was 1.4-fold higher in male and 1.5-fold elevated in female transgenic mice, respectively ($p < 0.05$). When fed standard rodent chow for three months (at seven months of age), food intake was 1.4-fold higher in male ($p < 0.05$) and 1.5-fold higher in female transgenic mice ($p < 0.05$) as compared to sex-matched controls. Water intake was 9.2-fold elevated in male ($p < 0.05$) and 6.1-fold elevated in female transgenic mice ($p < 0.05$) as compared to controls. Water intake increased significantly between four and seven months of age in both male and female transgenic animals. At seven months of age, the 24-hour

urine volume was significantly higher in both male and female transgenic animals as compared to controls.

Group (n,n)	Food intake (g/g body weight/day)		Water intake (g/g body weight/day)		Urine volume (ml/day)
	4 months	7 months	4 months	7 months	7 months
Co male (4,4)	0.33 ± 0.01	0.25 [†] ± 0.02	0.49 ± 0.04	0.19 ± 0.03	1.69 ± 0.11
Tg male (6,6)	0.40 [*] ± 0.02	0.36 [*] ± 0.01	0.71 [*] ± 0.07	1.75 [†] ± 0.10	44.86 [*] ± 1.78
Co female (4,4)	0.36 ± 0.01	0.28 ± 0.02	0.50 ± 0.03	0.23 ± 0.02	2.97 ± 0.24
Tg female (13,11)	0.42 [*] ± 0.01	0.38 [*] ± 0.02	0.76 [*] ± 0.05	1.40 [†] ± 0.25	52.67 [*] ± 6.21

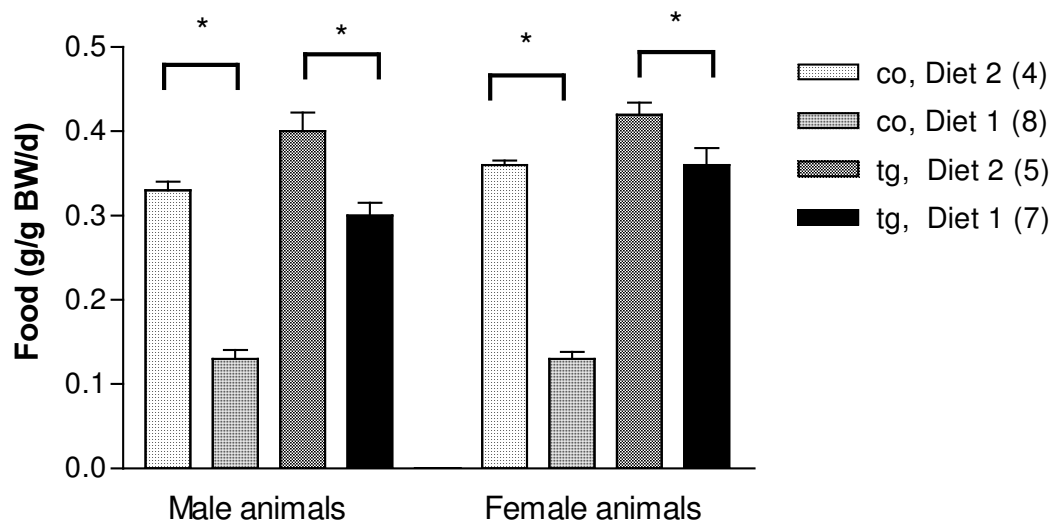
Table 4.6 Daily food/water intake and urine volume of animals receiving Diet 2. Transgenic animals investigated show significantly higher food and water intake as well as 24-hour urine volume. Data are means ± SEM; (n,n), number of animals investigated at four and seven months of age; (co), control; (tg), transgenic. * p<0.05 vs. control; † p<0.05 vs. previous time point.

c) Comparison of both diet groups

At four months of age, both control and transgenic mice receiving the carbohydrate-restricted diet (Diet 2) showed a significantly higher food intake than control and transgenic mice receiving standard rodent chow. At the same age, controls fed Diet 2 showed a higher water intake than controls fed Diet 1 (n.s.). Transgenic animals fed Diet 2 exhibited a significantly lower water intake than transgenic animals fed Diet 1 (Fig. 4.12 A/B).

At seven months of age, food intake of all animals previously fed the carbohydrate-restricted diet was significantly higher than that of animals constantly fed standard rodent chow (Fig. 4.13 A/B). Water intake and the 24-hour urine volume were nearly identical comparing the two diet groups (Fig. 4.13 C).

(A) Food intake, four months of age



(B) Water intake, four months of age

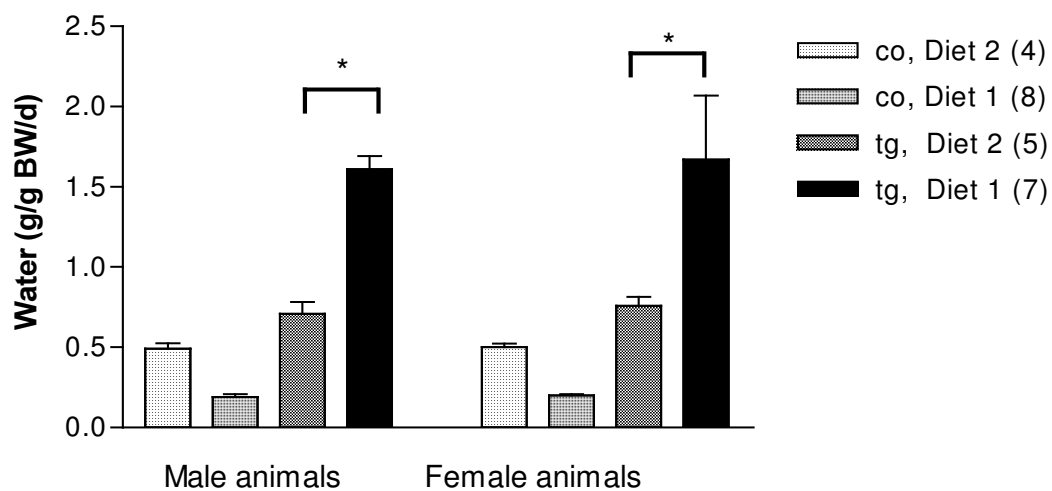
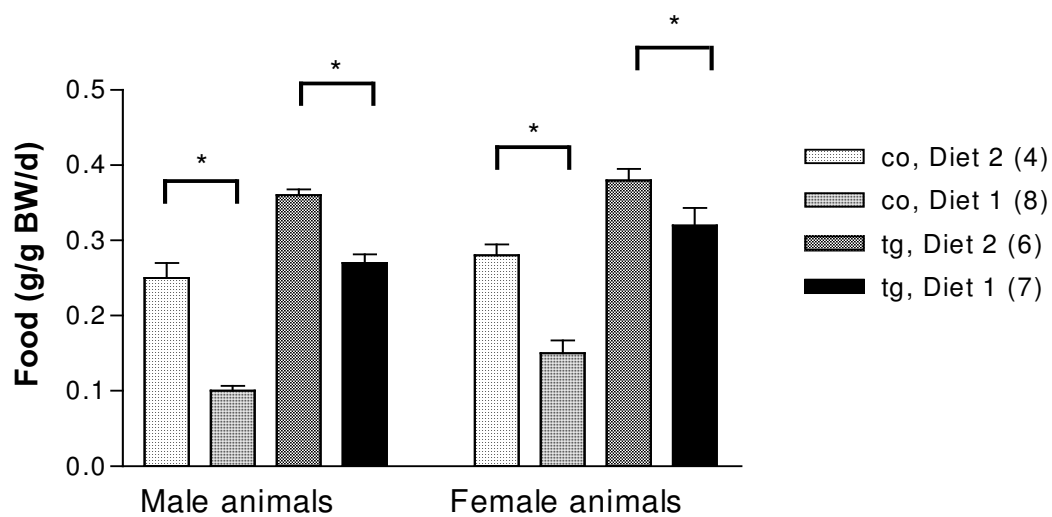
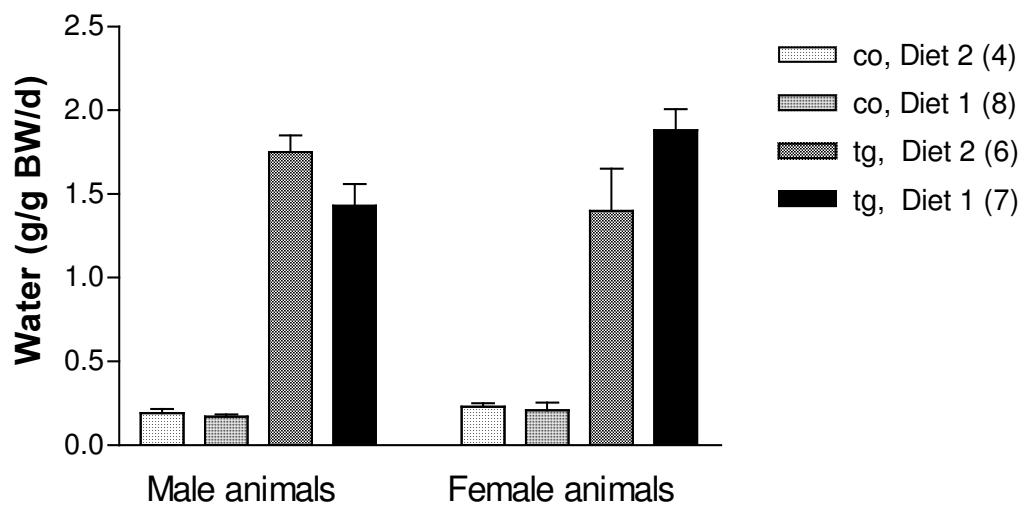


Figure 4.12 (A/B) Comparison of the daily food and water intake of animals receiving Diet 1 and Diet 2 at four months of age; (A) food intake, (B) water intake. (A) The food intake of animals receiving Diet 2 is significantly higher than that of animals receiving Diet 1. (B) Water intake of transgenic (tg) animals receiving Diet 1 is significantly higher than that of transgenic animals receiving Diet 2. Water intake of control (co) animals fed Diet 1 is lower than that of animals receiving Diet 2. Data are expressed as gram (g) per gram body weight (g BW) per day (d). Data are means \pm SEM; (n), number of animals investigated. * $p < 0.05$

(A) Food intake, seven months of age



(B) Water intake, seven months of age



(C) Urine volume, seven months of age

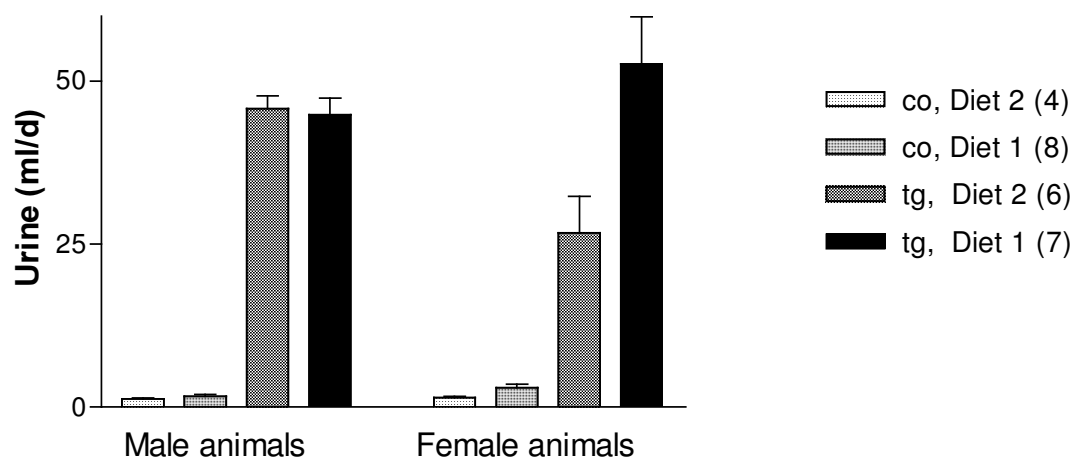


Figure 4.13 (A/B/C) Comparison of the daily food and water intake and urine volume of animals receiving Diet 1 and Diet 2 at seven months of age; (A) food intake, (B) water intake, (C) urine volume. (A) The food intake of animals receiving Diet 2 is higher than that of animals receiving Diet 1. Data are expressed as gram (g) per gram body weight (g BW) per day (d). (B) Water intake of both diet groups is not significantly different. Data are expressed as gram (g) per gram body weight (g BW) per day (d). (C) The 24-hour urine volume of both diet groups is nearly equal. Data are expressed as volume (ml) per day (d).

Data are expressed as means \pm SEM; (co), control; (tg), transgenic; (n), number of animals investigated. * $p < 0.05$.

4.7 Serum parameters

Serum parameters were evaluated in 3-month-old animals receiving standard rodent chow. Sodium and chloride levels were significantly lower in male $GIPR^{dn}$, as compared to control males; in female transgenic mice only chloride levels were significantly reduced as compared to sex-matched wildtype mice. Serum urea and creatinine were both significantly elevated in $GIPR^{dn}$ males and females. Serum triglyceride levels were higher in all transgenic animals than those observed in non-transgenic mice. Values for total protein and albumin were both significantly lower in $GIPR^{dn}$ females vs. wildtype females (Table 4.7).

Group (n)	Sodium (mmol/l)	Chloride (mmol/l)	Crea- tinine (mg/dl)	Urea (mg/dl)	Choles- terol (mg/dl)	Triglyc- eride (mg/dl)	Total protein (g/dl)	Albumin (g/dl)
Co male (4)	162.5 ± 1.0	112.0 ± 0.1	0.30 ± 0.01	63.5 ± 5.4	102.0 ± 8.6	188.5 ± 43.0	5.0 ± 0.1	2.4 ± 0.2
Tg male (4)	146.5* ± 2.1	94.5* ± 2.2	0.55* ± 0.07	113.0* ± 7.6	126.0* ± 4.9	877.5* ± 66.2	4.7 ± 0.3	2.3 ± 0.2
Co female (4)	159.0 ± 1.8	111.5 ± 1.0	0.33 ± 0.03	51.0 ± 6.5	98.5 ± 5.6	126.0 ± 11.5	5.4 ± 0.2	3.0 ± 0.2
Tg female (4)	152.5 ± 3.3	104.0* ± 2.2	0.40* ± 0.01	96.8* ± 1.4	104.5 ± 9.4	519.0* ± 87.4	4.5* ± 0.1	2.3* ± 0.1

Table 4.7 Serum parameters. (co), control; (tg), transgenic. Data are presented as means ± SEM; (n), number of animals investigated. * p<0.05 vs. control.

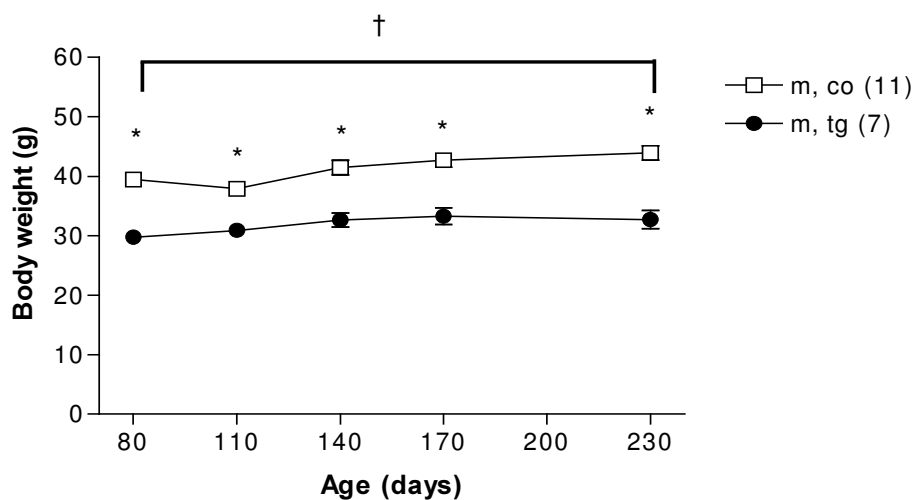
4.8 Body weight

The fasted body weight was determined in monthly intervals between 80 and 230 days of age in the two diet groups.

a) Animals receiving standard rodent chow

After a 12-hour fasting period, body weight of transgenic males receiving standard rodent chow was significantly lower than that of control mice, irrespective of the age at sampling. There was no difference in body weight of female transgenic and control mice (Fig. 4.14 A/B). The body weight increased significantly between 80 and 230 days in male control animals, the body weight of female animals and male transgenic mice remained stable over the period sampled.

(A) Male animals



(B) Female animals

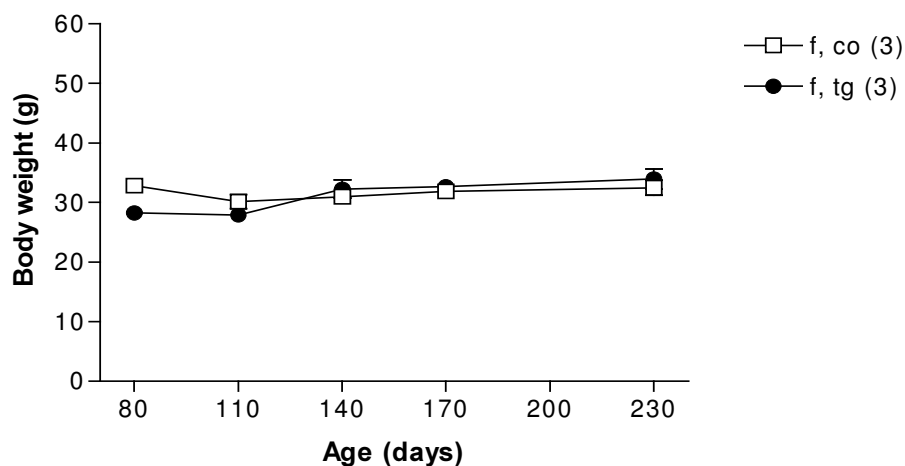


Figure 4.14 (A/B) Body weight between 80 and 230 days of age, animals receiving Diet 1; (A) male animals, (B) female animals. The body weight of transgenic males is significantly higher than that of sex-matched controls. Data are means \pm SEM; (n), number of animals investigated; (co), control; (tg), transgenic; (m), male; (f), female. * $p < 0.05$ vs. control, † $p < 0.05$ vs. previous time point.

In addition, body weight of animals fed ad libitum was determined prior to sacrifice. At 10 days of age, the mean body weight of transgenic animals did not differ from that of control animals. At one and three months of age, animals were weighed before exsanguination and the net body weight was calculated by subtraction of gastric and

intestinal contents. The body weight of transgenic animals was lower than that of control mice; only in three-month-old transgenic females this difference did not reach statistical significance (Table 4.8).

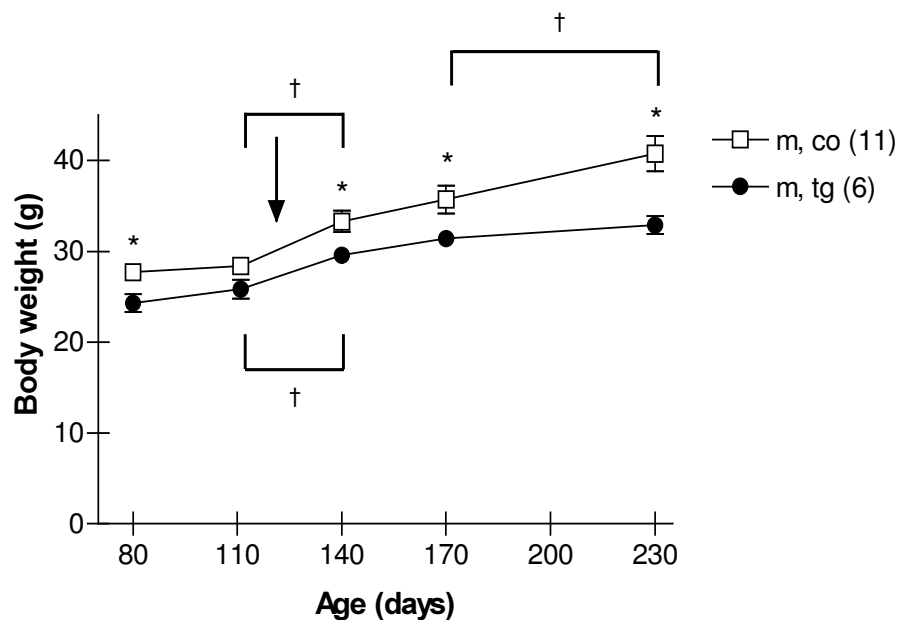
Group (n)	Age (d)		
	10	30	90
Co male (4)	6.0 ± 0.3	28.2 [†] ± 0.3	35.8 [†] ± 0.7
Tg male (4)	5.5 ± 0.2	21.5 ^{*†} ± 0.9	28.0 ^{*†} ± 1.2
Co female (4)	5.7 ± 0.3	21.1 [†] ± 0.1	30.1 [†] ± 1.4
Tg female (4)	5.0 ± 0.5	19.2 ^{*†} ± 0.4	26.9 [†] ± 1.2

Table 4.8 Body weight (g). Body weight increases significantly with age in all groups investigated and is lower in transgenic (tg) animals at 30 and 90 days of age vs. age-matched control (co) mice. Data are means ± SEM; (n), number of animals investigated. * p<0.05 vs. control; † p<0.05 vs. previous time point.

b) Animals receiving the carbohydrate restricted diet

Male and female control mice showed a higher fasted body weight than sex-matched transgenic animals. Statistical significance was reached at 80, 140, 170 and 230 days for male animals and at 80, 110, 140, 170 and 230 days for female animals, respectively. The body weight increased significantly in all animals between 110 and 140 days of age, the time point when the diet was changed from carbohydrate-restricted to standard diet (Fig. 4.15 A/B).

(A) Male animals



(B) Female animals

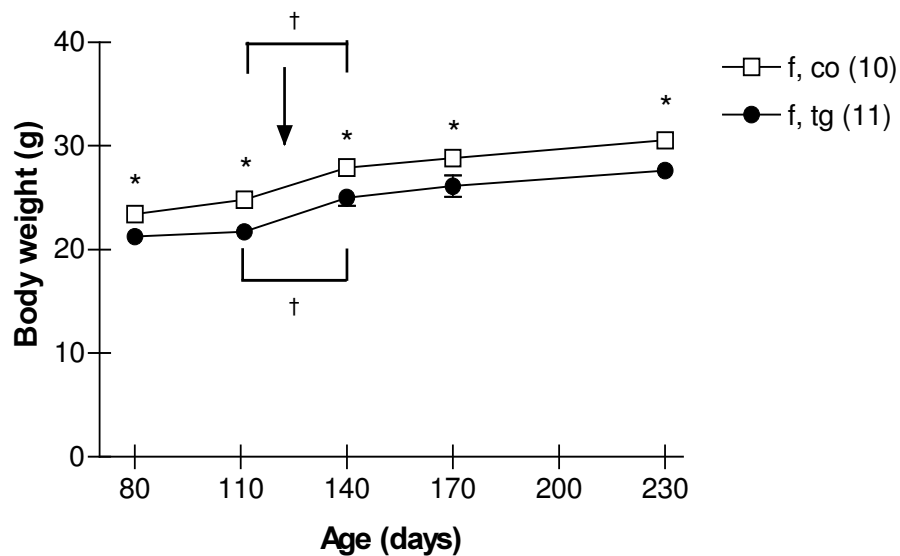
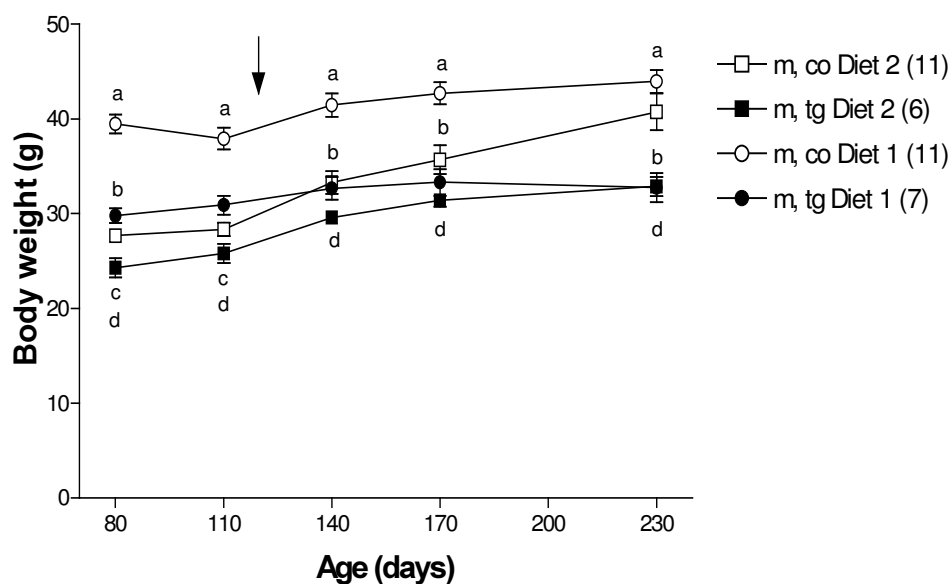


Figure 4.15 (A/B) Body weight between 80 and 230 days of age, animals receiving Diet 2; (A) male animals, (B) female animals. All animals exhibit significant weight gain between 110 and 140 days of age. The time point of diet change is indicated with an arrow. Data are means \pm SEM; (co), control; (tg), transgenic; (m), male; (f), female. * $p < 0.05$ vs. control, † $p < 0.05$ vs. previous time point.

c) Comparison of both diet groups

Data are presented in Figure 4.16 A/B. Transgenic males permanently receiving standard rodent chow showed a significantly higher body weight than transgenic males while they were fed the carbohydrate-restricted diet at 80 and 110 days of age. Control males from group Diet 2 weighed significantly less than control males from group Diet 1, irrespective of the age at weight determination. Transgenic females permanently receiving standard rodent chow weighed significantly more than transgenic females from group Diet 2. The same is true for control females until 140 days of age.

(A) Male animals



(B) Female animals

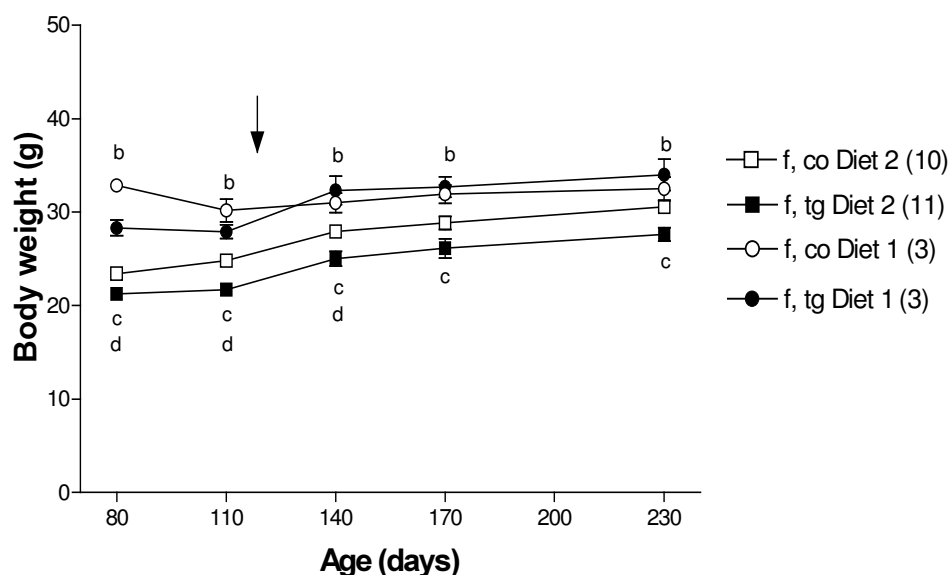


Figure 4.16 (A/B) Body weight between 80 and 230 days of age, comparison of both diet groups; (A) male animals, (B) female animals. At 80 and 110 days of age, transgenic males receiving the carbohydrate-restricted diet (Diet 2) weigh significantly less than transgenic animals receiving the standard diet (Diet 1). After the change of diet (arrow) there is no difference in body weight. Transgenic females receiving Diet 1 weigh significantly more than transgenic females receiving Diet 2. Data are means \pm SEM; (n), number of animals investigated; (co), control; (tg), transgenic; (m), male; (f), female; a-d $p < 0.05$. a: Diet 1 transgenic vs. control, b: Diet 2 transgenic vs. control, c: Diet 1 transgenic vs. Diet 2 transgenic, d: Diet 1 control vs. Diet 2 control.

4.9 Organ weights

Organ weights were determined at 90 days of age (Tables 4.9 and 4.10). The significant reduction of absolute and relative weights of skin, carcass and abdominal fat tissue contributed to the lower body weight of transgenic animals vs. controls. The absolute weight of the heart was significantly lower in male transgenic animals vs. male controls (Table 4.9). Both absolute and relative values for the weights of intestine weight, gastric- and intestinal content, liver and kidney were significantly increased in $GIPR^{dn}$ transgenic vs. control mice (Tables 4.9 and 4.10, Fig. 4.17 A/B). Pancreas weight was determined at 10, 30 and 90 days of age and found to be equal when comparing transgenic and sex-matched control animals (Table 4.11).

Group (n)	Carcass (g)	Skin (g)	Intestine (g)	GIT content (g)	Liver (g)	Kidneys [†] (mg)	Abdomi- nal fat (g)	Heart (mg)
Co male (4)	15.0 ± 0.8	7.0 ± 0.2	1.7 ± 0.1	2.9 ± 0.2	1.8 ± 0.6	583 ± 8	1.85 ± 0.33	174 ± 13
Tg male (4)	10.0* ± 0.5	3.7* ± 0.3	3.3* ± 0.2	5.3* ± 0.5	2.1* ± 0.8	767* ± 20	0.24* ± 0.04	131* ± 6
Co female (4)	12.5 ± 0.6	5.2 ± 0.4	1.5 ± 0.1	2.3 ± 0.5	1.4 ± 0.8	382 ± 29	2.22 ± 1.01	144 ± 7
Tg female (4)	9.8* ± 0.6	3.4* ± 0.1	2.8* ± 0.3	6.7* ± 0.7	1.9* ± 0.1	619* ± 62	0.19* ± 0.01	151 ± 20

Table 4.9 Organ weights. Data are presented as means ± SEM; (n), number of animals investigated; co, control; tg, transgenic; GIT content: gastric and intestinal content; [†] cumulative weight of both kidneys per animal; * p<0.05 vs. control.

Group (n)	Body (g)	Carcass (%)	Skin (%)	Intestine (%)	GIT content (%)	Liver (%)	Kidneys (%)	Abdomi- nal fat (%)	Heart (%)
Co male (4)	35.8 ± 0.7	41.8 ± 0.8	19.7 ± 0.5	4.8 ± 0.1	8.2 ± 0.7	5.1 ± 0.6	1.6 ± 0.4	5.1 ± 0.8	0.48 ± 0.03
Tg male (4)	28.0* ± 1.2	35.5* ± 0.3	13.2* ± 0.7	11.9* ± 0.5	18.7* ± 1.3	7.6* ± 0.9	2.8* ± 0.1	0.8* ± 0.1	0.47 ± 0.02
Co female (4)	30.1 ± 1.4	41.7 ± 1.7	17.2 ± 0.7	5.1 ± 0.3	7.8 ± 2.1	4.8 ± 0.3	1.3 ± 0.9	7.1 ± 1.5	0.48 ± 0.04
Tg female (4)	26.9 ± 1.2	36.2* ± 1.2	12.8* ± 0.5	10.2* ± 0.7	25.2* ± 3.1	7.1* ± 0.2	2.3* ± 0.1	0.7* ± 0.1	0.56 ± 0.05

Table 4.10 Organ-to-body weight ratios. Data are presented as means ± SEM; (n), number of animals investigated; (co), control; (tg), transgenic; GIT content: gastric and intestinal content; * p<0.05 vs. control.

Group (n)	Age (d)		
	10	30	90
Co male (4)	28 ± 1	241* ± 8	401* ± 18
Tg male (4)	25 ± 4	232* ± 11	412* ± 50
Co female (4)	27 ± 1	228* ± 7	342* ± 35
Tg female (4)	19 ± 3	214* ± 4	437* ± 29

Table 4.11 Pancreas weight (mg). Pancreas weight increases significantly with age but is not different comparing transgenic (tg) and age-matched control (co) animals. Data are means ± SEM; (n), number of animals investigated. * p<0.05 vs. previous time point.



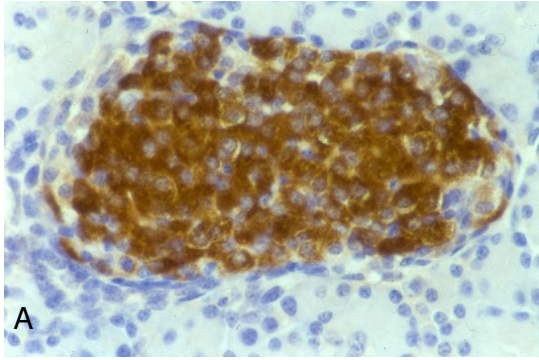
Fig. 4.17 (A) Intestinal tract of an 8-month-old male control (top) and an age-matched male GIPR^{dn} transgenic animal (bottom). The length and the diameter of the stomach and small and large bowel of the transgenic animal are increased as compared to a weight-matched control.



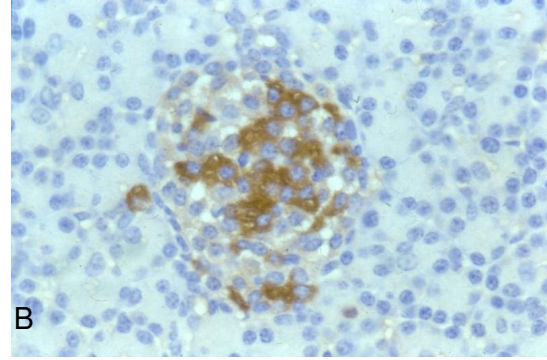
Fig. 4.17 (B) Mesentery of a GIPR^{dn} transgenic (left) and a control male (right) at eight months of age. The mesentery of the transgenic animal contains virtually no fatty tissue.

4.10 Descriptive histologic and immunohistochemical findings of the pancreas

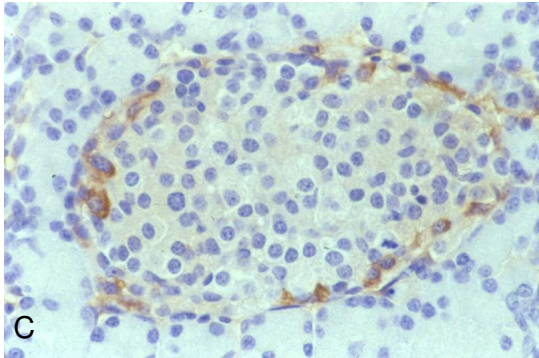
Gross morphology and histologic appearance of the exocrine pancreas was inconspicuous in transgenic mice irrespective of the age investigated. In H&E-stained sections, pancreatic islet profiles of transgenic animals appeared to be much smaller both in size and number as compared to controls. Furthermore, immunohistochemistry for the four principal islet cell hormones revealed an atypical composition and organization of islets in transgenic mice. Very few islet cells stained insulin positive, whereas the proportion of cells expressing glucagon and somatostatin was increased. All cell types were dispersed over the islet profile in GIPR^{dn} transgenic mice, which was markedly different from the typical distribution of endocrine cells in murine pancreatic islets, being characterized by a ring of non-B-cells surrounding a core of B-cells (Fig. 4.18 A-H).



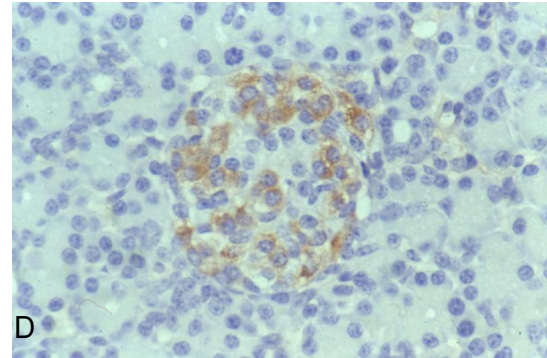
(A) Insulin, co, male 10 days



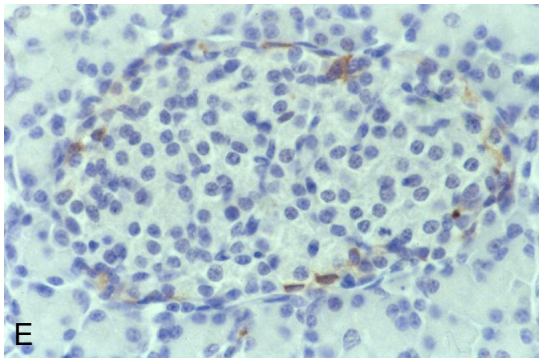
(B) Insulin, tg, male, 10 days



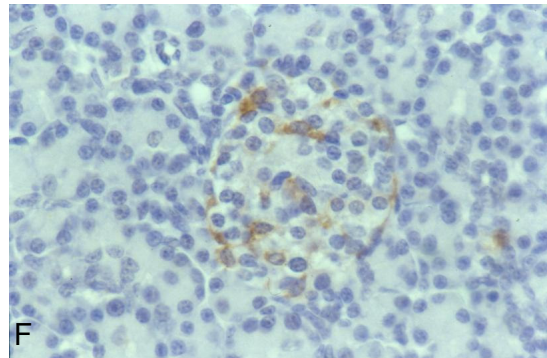
(C) Glucagon, co, male 10 days



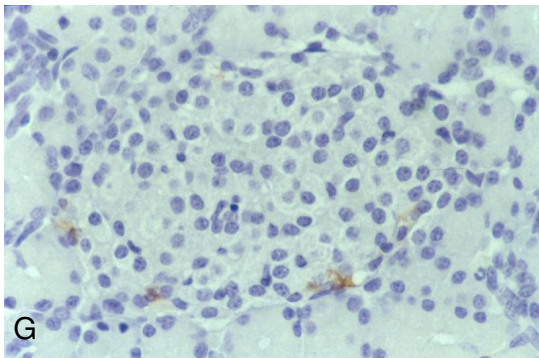
(D) Glucagon, tg, male, 10 days



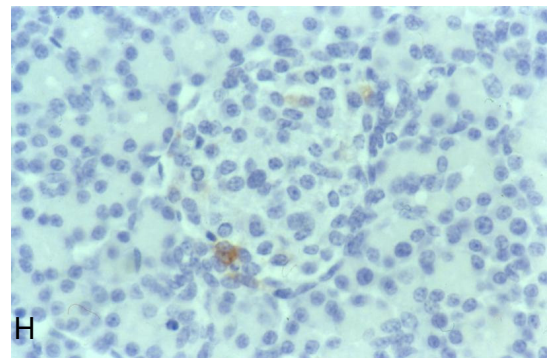
(E) Somatostatin, co, male 10 days



(F) Somatostatin, tg, male, 10 days



(G) PP, co, male 10 days



(H) PP, tg, male, 10 days

Figure 4.18 (A-H): Distribution of endocrine cells in islets in control (A, C, E, G) and GIPR^{dn} transgenic (B, D, F, H) mice at 10 days of age. Immunohistochemistry of serial pancreas sections for the four principle islet cell hormones, insulin (A,B), glucagon (C,D), somatostatin (E,F) and pancreatic polypeptide (PP) (G,H). The distribution of endocrine cells in pancreatic islets from GIPR^{dn} transgenic (tg) mice is severely altered as compared to control (co) mice. The amount of insulin positive cells is clearly reduced, whereas the proportion of islet cells expressing glucagon and somatostatin is increased. Magnification 40x12.5.

4.11 Quantitative-stereological findings of the pancreas

4.11.1 Total islet volume

The total volume of the islets in the pancreas ($V_{(Islet, Pan)}$) was significantly lower (range 54-69%) in transgenic vs. control mice at all time points examined. The $V_{(Islet, Pan)}$ remained stable comparing 10 and 30 day old animals. In all animals at 90 days of age, the $V_{(Islet, Pan)}$ was higher than that of 30-day-old counterparts (Fig. 4.19 A/B).

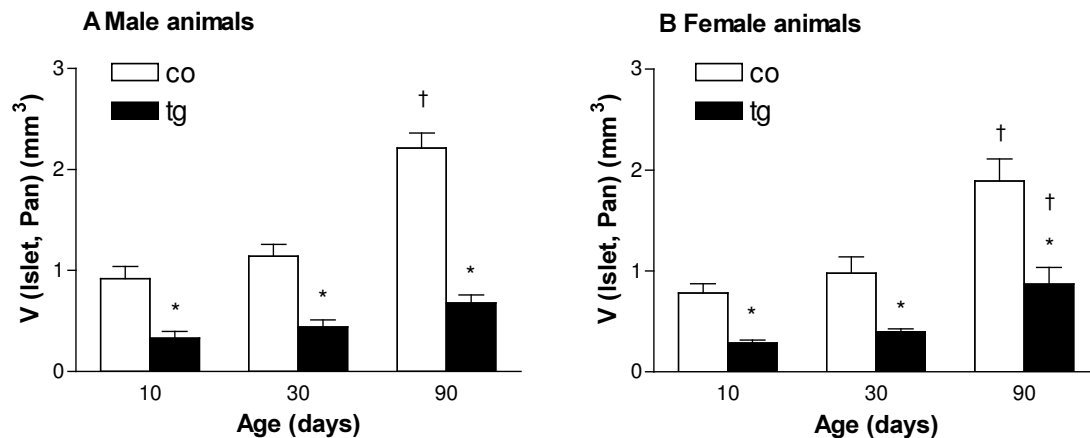


Figure 4.19 Total islet volume ($V_{(Islet, Pan)}$) of GIPR^{dn} transgenic and control mice; (A) male, (B) female animals. The $V_{(Islet, Pan)}$ in transgenic (tg) male and female animals is more than 54% lower as compared to age- and sex-matched littermate controls (co). The $V_{(Islet, Pan)}$ remains stable between 10 and 30 days and increases between 30 and 90 days of age in all animals examined. Data are presented as means \pm SEM; * $p < 0.05$ vs. control; † $p < 0.05$ vs. previous time point.

4.11.2 Volume density of islets in the pancreas

The volume density of islets in the pancreas ($V_{V(\text{Islet/Pan})}$) was reduced by over 52% (range 52-67%) in transgenic mice as compared to sex-matched littermate controls, irrespective of the age at sampling ($p < 0.05$). The $V_{V(\text{Islet/Pan})}$ was significantly decreased in both transgenic and control mice at 30 days of age vs. 10-day-old mice (over 84%). Between 30 and 90 days of age, the $V_{V(\text{Islet/Pan})}$ remained stable in transgenic and control mice (Fig. 4.20 A/B).

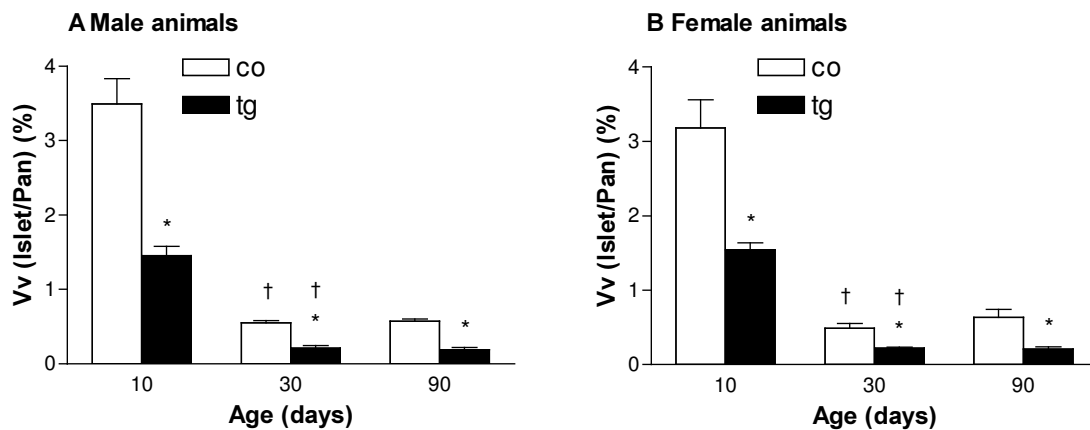


Figure 4.20 Volume density of islets in the pancreas ($V_{V(\text{Islet/Pan})}$) of GIPR^{dn} transgenic and control mice; (A) male, (B) female animals. The $V_{V(\text{Islet/Pan})}$ in transgenic (tg) male and female animals is at least 52% lower compared to age- and sex-matched littermate controls (co). The $V_{V(\text{Islet/Pan})}$ decreases between 10 and 30 days and remains stable between 30 and 90 days of age in all animals examined. Data are presented as means \pm SEM; * $p < 0.05$ vs. control; † $p < 0.05$ vs. previous time point.

4.11.3 Total B-cell volume

In all transgenic animals, the total volume of B-cells in pancreatic islets ($V_{(\text{B-cells,Islet})}$) was severely (by 68-88%; $p < 0.05$) reduced as compared to control mice at all time points investigated. At 90 days of age $V_{(\text{B-cells,Islet})}$ exhibited the most marked reduction of 88% in male and 86% in female transgenic mice, respectively. The $V_{(\text{B-cells,Islet})}$ was not significantly different comparing 10- and 30-day-old mice. In 90-day-old control mice, the $V_{(\text{B-cells,Islet})}$ was almost twice that of 30-day-old control mice. In transgenic animals, the total B-cell volume remained stable over the period sampled (Fig. 4.21 A/B).

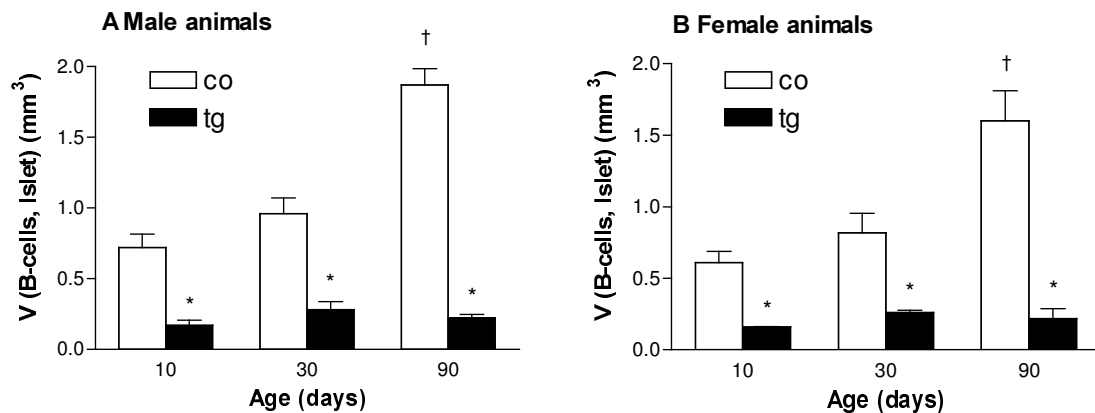


Figure 4.21 Total B-cell volume ($V_{(B-cells, Islet)}$) of $GIPR^{dn}$ transgenic and control mice; (A) male, (B) female animals. The $V_{(B-cells, Islet)}$ in transgenic (tg) male and female animals is more than 68% lower than that of age- and sex-matched littermate controls (co). The $V_{(B-cells, Islet)}$ remains stable between 10 and 30 days in all animals and nearly doubles between 30 and 90 days of age in control mice, whereas the $V_{(B-cells, Islet)}$ remains stable in transgenic animals until 90 days of age. Data are presented as means \pm SEM; * $p < 0.05$ vs. control; † $p < 0.05$ vs. previous time point.

4.11.4 Volume density of B-cells in the islets

The volume density of B-cells in the islets ($Vv_{(B-cells/Islet)}$) was severely reduced in all transgenic animals as compared to age- and sex-matched littermate controls ($p < 0.05$). At 90 days of age, this difference was most distinct and corresponded to a 63% reduction in male and a 71% reduction in female $GIPR^{dn}$ transgenic mice, respectively. The volume density of B-cells in the islet ($Vv_{(B-cells/Islet)}$) was significantly increased in transgenic animals at 30 days of age as compared to 10-day-old transgenic mice. Between 30 and 90 days of age, the $Vv_{(B-cells/Islet)}$ remained stable in control mice, whereas the volume density of B-cells in the islets in $GIPR^{dn}$ transgenic mice was significantly lower at 90 days of age (Fig. 4.22 A/B).

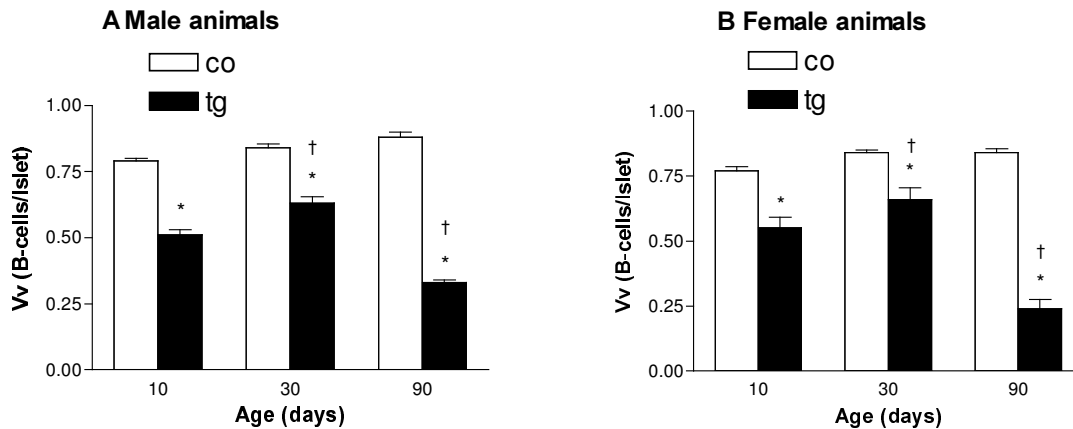


Figure 4.22 Volume density of B-cells in the islets ($Vv_{(B-cells/Islet)}$) of $GIPR^{dn}$ transgenic and control mice; (A) male, (B) female animals. The $Vv_{(B-cells/Islet)}$ in transgenic (tg) male and female animals is largely reduced vs. age- and sex-matched control (co) mice at all time points investigated. The $Vv_{(B-cells/Islet)}$ increases significantly between 10 and 30 days in transgenic animals and remains stable between 30 and 90 days of age in control mice. In transgenic mice, $Vv_{(B-cells/Islet)}$ is significantly decreased at 90 days of age as compared to the previous time point. Data are presented as means \pm SEM; * $p < 0.05$ vs. control; † $p < 0.05$ vs. previous time point.

4.11.5 Total volume of endocrine non-B-cells

At 10 days of age, the total volume of endocrine non-B-cells of islets ($V_{(Non-B-cells,Islet)}$) was similar in transgenic and age-matched control mice. 30-day-old male transgenic mice already exhibited a significantly higher $V_{(Non-B-cells,Islet)}$, mainly due to a significantly higher total volume of A-cells, as compared to male control mice. At 90 days of age, $V_{(Non-B-cells,Islet)}$ was significantly higher in male and female transgenic mice vs. control mice (Fig. 4.23 A/B). This increase of $V_{(Non-B-cells,Islet)}$ was due to a significantly higher total volume of A-cells (male transgenic vs. male control: $0.25 \pm 0.07 \text{ mm}^3$ vs. $0.10 \pm 0.03 \text{ mm}^3$; female transgenic vs. female control: $0.39 \pm 0.01 \text{ mm}^3$ vs. $0.13 \pm 0.01 \text{ mm}^3$) and D-cells (male transgenic vs. male control: $0.09 \pm 0.02 \text{ mm}^3$ vs. $0.04 \pm 0.01 \text{ mm}^3$ and female transgenic vs. female control: $0.16 \pm 0.4 \text{ mm}^3$ vs. $0.04 \pm 0.01 \text{ mm}^3$). In addition, a significantly higher total volume of PP-cells was found in female transgenic mice as compared to female controls ($0.08 \pm 0.04 \text{ mm}^3$ vs. $0.04 \pm 0.01 \text{ mm}^3$). The $V_{(Non-B-cells,Islet)}$ was similar when comparing 10- and 30-day-old animals. At 90 days of age, the $V_{(Non-B-cells,Islet)}$ was significantly increased in all animals, apart from female controls, as compared to the previous time point (Fig. 4.23 A/B).

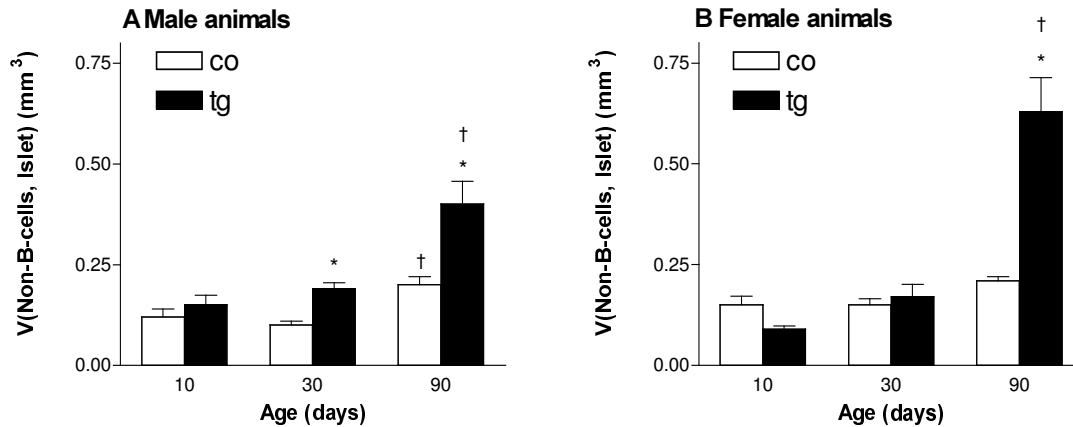


Figure 4.23 Total volume of endocrine non-B-cells ($V_{(\text{Non-B-cells, Islet})}$) of GIPR^{dn} transgenic and control mice; (A) male, (B) female animals. At 30 days of age, $V_{(\text{Non-B-cells, Islet})}$ is significantly higher in transgenic (tg) males vs. male controls (co). The $V_{(\text{Non-B-cells, Islet})}$ is significantly higher in both male and female transgenic animals at 90 days of age vs. age- and sex-matched control mice. The $V_{(\text{Non-B-cells, Islet})}$ increases markedly in transgenic mice between 30 and 90 days of age. Data are presented as means \pm SEM; * $p < 0.05$ vs. control; † $p < 0.05$ vs. previous time point.

4.11.6 Volume density of endocrine non-B-cells in islets

At all time points examined, the volume density of endocrine non-B-cells in islets ($Vv_{(\text{Non-B-cells/Islet})}$) was significantly elevated in transgenic mice, as compared to age- and sex-matched littermate controls (Fig. 4.24 A/B). This elevation was by virtue of a higher A- and D-cell volume fraction in islets at 10, 30 and 90 days of age. The volume density of PP-cells was significantly increased in 10- and 90-day-old male and in 90-day-old female transgenic mice, respectively (Table 4.12). The $Vv_{(\text{Non-B-cells/Islet})}$ remained stable between 10 and 30 days of age in all animals, only in female transgenic mice, there was a significant increase of $Vv_{(\text{Non-B-cells/Islet})}$. There was an age-related significant increase of $Vv_{(\text{Non-B-cells/Islet})}$ from 30 to 90 days of age in GIPR^{dn} transgenic mice (Fig. 4.24 A/B). This increase was due to an elevated volume fraction of the three major non-B-cells (A-, D- and PP-cells; Table 4.12 A-C).

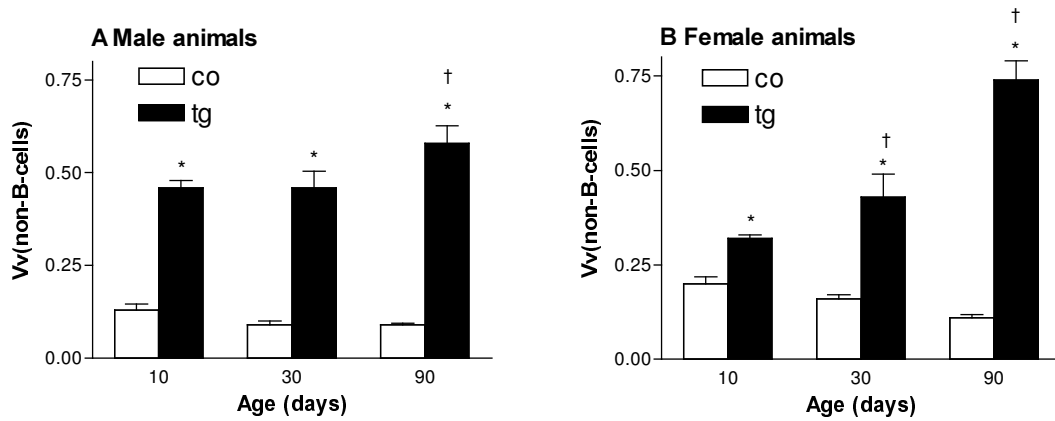


Figure 4.24 Volume density of endocrine non-B-cells in the islets ($Vv_{(\text{Non-B-cells/Islet})}$) of GIPR^{dn} transgenic and control mice; (A) male, (B) female animals. At all time points investigated $Vv_{(\text{Non-B-cells/Islet})}$ is significantly higher in transgenic (tg) male and female animals as compared to age- and sex-matched littermate controls (co). The $Vv_{(\text{Non-B-cells/Islet})}$ increases significantly between 30 and 90 days of age in transgenic mice. Data are presented as means \pm SEM; * $p < 0.05$ vs. control; † $p < 0.05$ vs. previous time point.

(A) Volume density of A-cells in the islets

Group (n)	$Vv_{(\text{A-cells/Islet})}$		
	10	30	90
Co male (4)	0.08 \pm 0.02	0.05 \pm 0.01	0.05 \pm 0.01
Tg male (4)	0.19* \pm 0.03	0.30* \pm 0.05	0.36* \pm 0.03
Co female (4)	0.11 \pm 0.02	0.10 \pm 0.01	0.07 \pm 0.01
Tg female (4)	0.18 \pm 0.01	0.23* \pm 0.05	0.45* \pm 0.04

(B) Volume density of D-cells in the islets

Group (n)	$Vv_{(\text{D-cells/Islet})}$		
	10	30	90
Co male (4)	0.03 \pm 0.02	0.02 \pm 0.01	0.02 \pm 0.01
Tg male (4)	0.12* \pm 0.02	0.10* \pm 0.04	0.14* \pm 0.01
Co female (4)	0.05 \pm 0.01	0.04 \pm 0.01	0.02 \pm 0.01
Tg female (4)	0.07 \pm 0.01	0.14* \pm 0.02	0.19* \pm 0.02

(C) Volume density of PP-cells in the islets

Group (n)	$Vv_{(PP-cells/Islet)}$		
	10	30	90
Co male (4)	0.02 ± 0.01	0.02 ± 0.01	0.03 ± 0.01
Tg male (4)	0.14* ± 0.03	0.06 ± 0.04	0.08* ± 0.01
Co female (4)	0.04 ± 0.01	0.02 ± 0.02	0.02 ± 0.01
Tg female (4)	0.06 ± 0.01	0.05 ± 0.01	0.10* ± 0.02

Table 4.12 (A-C) Volume densities of A-cells (A), D-cells (B), and PP-cells (C) in the islets ($Vv_{(X-cell, Islet)}$) of $GIPR^{dn}$ transgenic and control mice. The $Vv_{(A-cell, Islet)}$ and $Vv_{(D-cell, Islet)}$ is significantly higher in transgenic (tg) male and female animals as compared to age- and sex-matched controls (co). Data are presented as means ± SEM; * $p < 0.05$ vs. control.

4.11.7 Total volume of isolated B-cells

The total volume of isolated B-cells (single interstitial insulin positive cells and small interstitial B-cell clusters, indicating neogenesis of islets) was significantly lower in transgenic mice vs. control mice, irrespective of the age investigated. The total volume of isolated B-cells remained stable in transgenic animals until 90 days of age (Fig. 4.25 A/B).

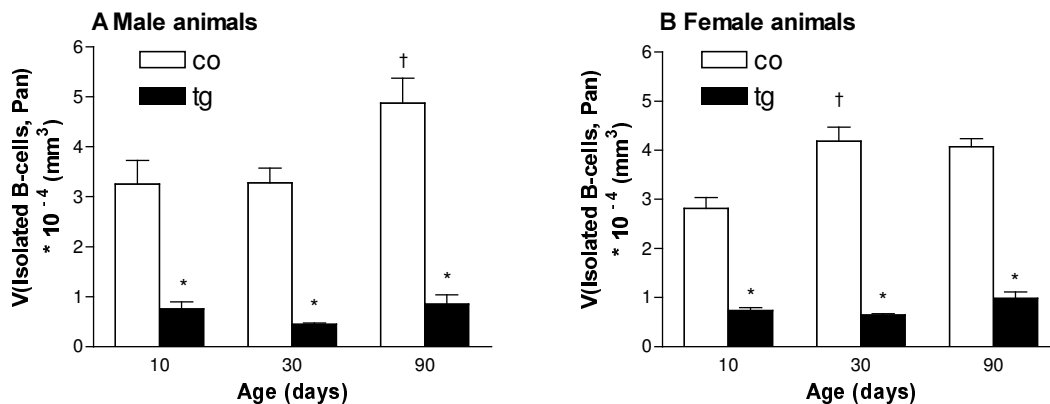


Figure 4.25 Total volume of isolated B-cells in pancreata of $GIPR^{dn}$ transgenic and control mice; (A) male, (B) female animals. In transgenic (tg) male and female animals, the total volume of isolated B-cells is significantly reduced at all time points examined as compared to age- and sex-matched littermate controls (co). Data are presented as means ± SEM; * $p < 0.05$ vs. control; † $p < 0.05$ vs. previous time point.

4.11.8 Volume density of isolated B-cells in the pancreas

The volume density of isolated B-cells in the pancreas was significantly lower in transgenic vs. control mice at all time points investigated. There was an over 80% reduction in the volume density of isolated B-cells in all animals at 30 days of age as compared to the preceding time point ($p < 0.05$). At 90 days of age, the volume density of isolated B-cells was equal in all animals as compared to 30-day-old animals (Fig. 4.26 A/B).

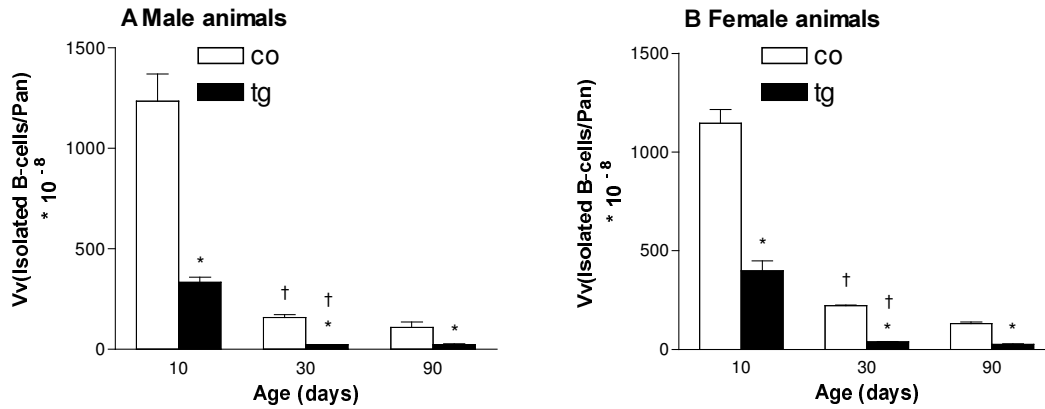


Figure 4.26 Volume density of isolated B-cells in pancreata of GIPR^{dn} transgenic and control mice; (A) male, (B) female animals. In transgenic (tg) male and female animals, the volume density of isolated B-cells is significantly reduced at all time points examined as compared to age- and sex-matched littermate controls (co). In all animals, the volume density of isolated B-cells is more than 80% lower at 30 days as compared to the previous time point. Data are presented as means \pm SEM; * $p < 0.05$ vs. control; † $p < 0.05$ vs. previous time point.

4.12 Urine protein analysis

Urine creatinine concentration of all transgenic animals was significantly lower than of age- and sex-matched controls (Fig. 4.27).

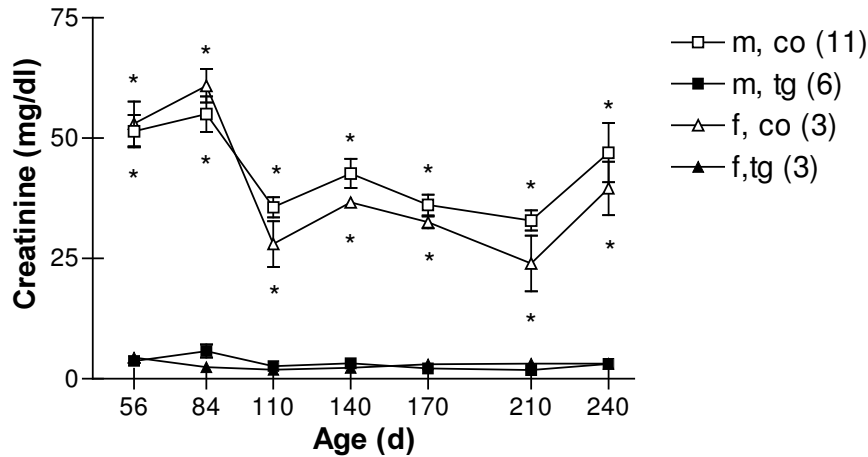
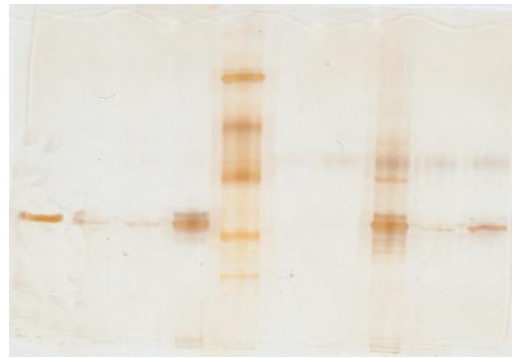
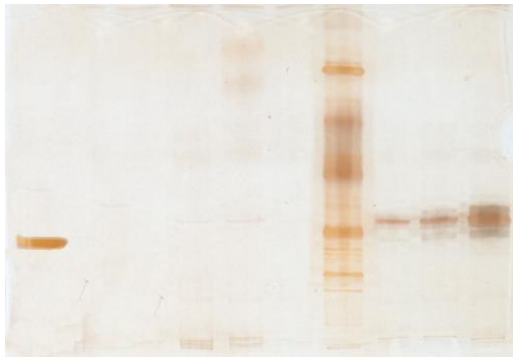


Figure 4.27 Urine creatinine concentration. Transgenic (tg) male (m) and female (f) animals exhibit significantly lower urine creatinine concentrations than non-transgenic controls (co). Data are presented as means \pm SEM; (n), number of animals investigated. * $p < 0.05$ vs. control.

As evidenced by SDS-PAGE, four out of six 56-day-old transgenic males showed a band of approximately 66 kDa, which meets the size of albumin. At 84 days of age, all transgenic males and one transgenic female displayed albuminuria. At 110 days of age, another female transgenic animal was albuminuric; all female transgenic mice showed urine albumin excretion at 240 days of age (Fig. 4.28 A/B). Therefore, all $GIPR^{dn}$ transgenic animals exhibited selective glomerular proteinuria by the end of the survey. Excretion of proteins larger than 37 kDa was not detectable in urine samples of controls. Transgenic animals did not exhibit unselective glomerular or tubular proteinuria at any age sampled. Albuminuria was confirmed in animals at 240 days of age, using Western blot analysis (Fig. 4.29 A/B).

(A) SDS-PAGE gel 1

(B) SDS-PAGE gel 2

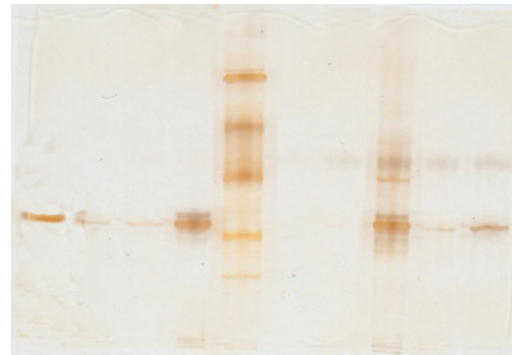
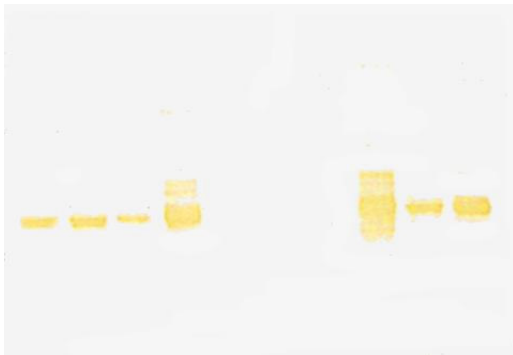


Alb co co co co co M tg tg tg Alb tg tg tg M co co tg tg tg
 ♂ ♂ ♂ ♀

Figure 4.28 (A/B) SDS-PAGE of urine samples of GIPR^{dn} transgenic (tg) and control (co) mice at eight months of age. Alb: Mouse albumin standard, M: Precision Protein Standard (BIORAD, Germany), molecular weight from top to bottom: 150, 100, 75, 50, 37 kDa.

(A) Western blot gel 2

(B) SDS-PAGE gel 2



Alb tg tg tg M co co tg tg tg Alb tg tg tg M co co tg tg tg
 ♂ ♀ ♂ ♀

Figure 4.29 Western blot (A) and corresponding SDS-PAGE (B) of urine samples of GIPR^{dn} transgenic (tg) and control (co) mice at eight months of age. Alb: Mouse albumin standard, M: Precision Protein Standard (BIORAD, Germany), molecular weight from top to bottom: 150, 100, 75, 50, 37 kDa.

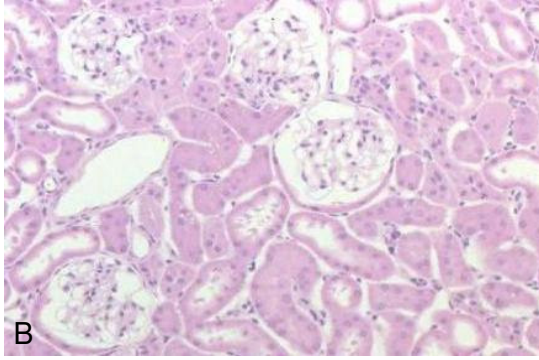
4.13 Macroscopical, histological and immunohistochemical findings of the kidneys

a) Animals receiving standard rodent chow

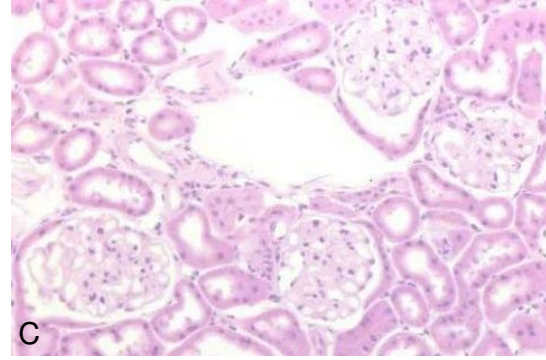
Animals studied were 4- and 8-month-old transgenic and control mice fed standard rodent chow. All transgenic animals exhibited severe renal and glomerular hypertrophy (Fig 4.30 A-C). Glomerular lesions were diffuse segmental to panglomerular, including mesangial expansion, hyalinosis and sclerosis, as well as adhesions between the glomerular tuft and the capsule of Bowman, distension of glomerular capillaries and sometimes cystic appearance of the capsule of Bowman with collapsed capillary tuft (Fig 4.30 E, G-I). Tubulo-interstitial lesions found were tubular atrophy, interstitial fibrosis and proteinuria (Fig 4.30 H/I). Immunohistochemistry for the extracellular matrix proteins collagen type IV (J/K), laminin (L/M) and fibronectin (N/O) revealed a marked deposition of all three extracellular matrix proteins in the glomeruli of transgenic animals as compared to controls. Tubular glycogen storage was demonstrated in a transgenic animal aged eight months (Fig 4.30 P/Q). In the control animal, no Armanni Ebstein lesions were observed. The renal pelvis, ureters and the bladder were largely distended in all transgenic animals fed Diet 1.



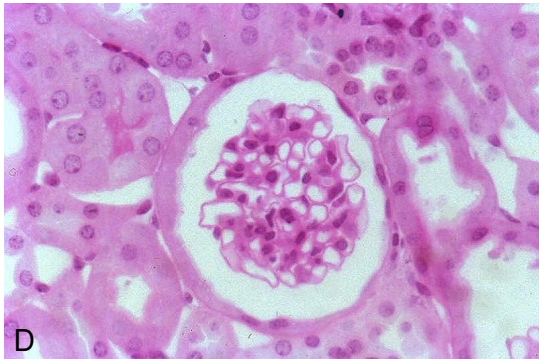
(A) Macroscopic appearance of the right kidney, male control (left), transgenic (right), 8 months



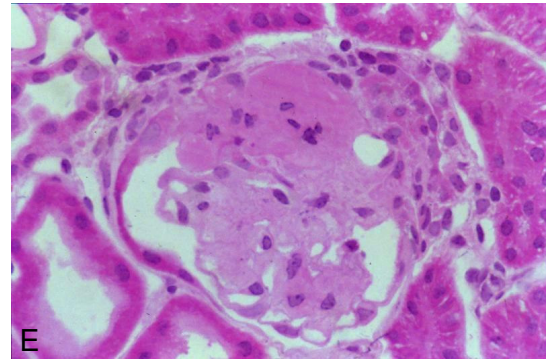
(B) Overview of the renal cortex, co, male, 4 months H&E (6.3 x 25)



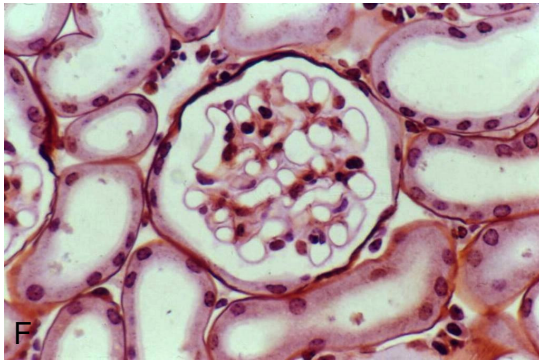
(C) Overview of the renal cortex, tg, male, 4 months H&E (6.3 x 25)



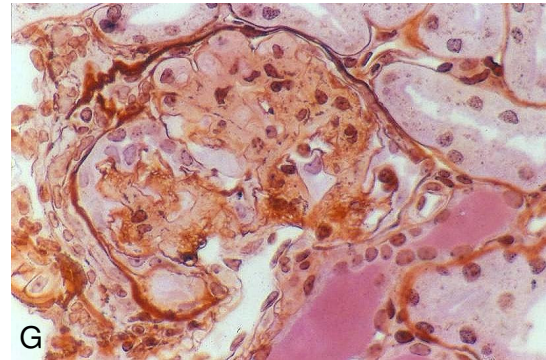
(D) Glomerulus, co, male, 4 months, PAS (12.5 x 40)



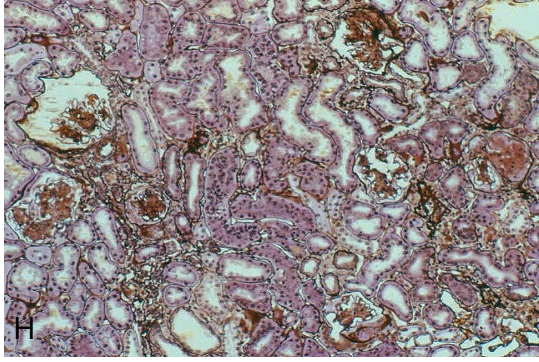
(E) Glomerulus, tg, male, 4 months, PAS (12.5 x 40)



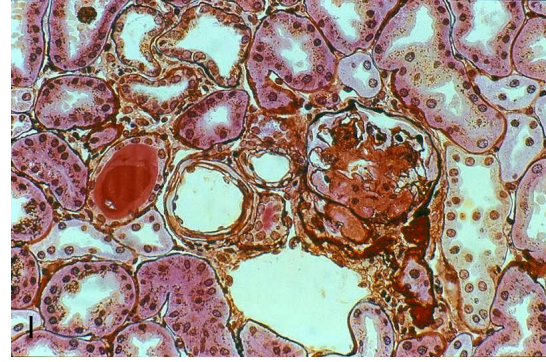
(F) Glomerulus, co, male, 4 months, PASM-PAS (12.5 x 40)



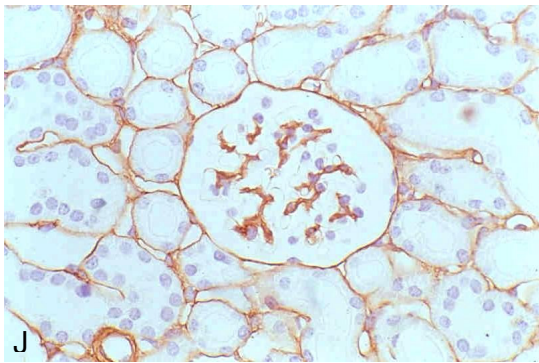
(G) Glomerulus, tg, male, 4 months, PASM-PAS (12.5 x 40)



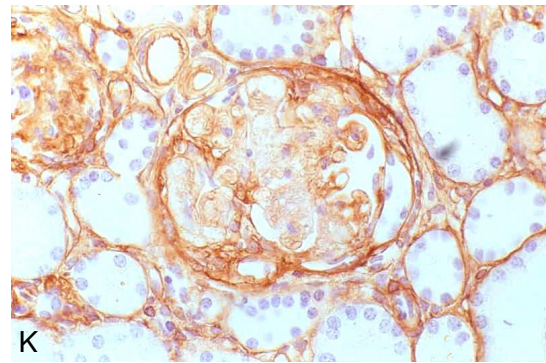
(H) Overview of the renal cortex, tg, male, 4 months, PASM-PAS (6.3 x 10)



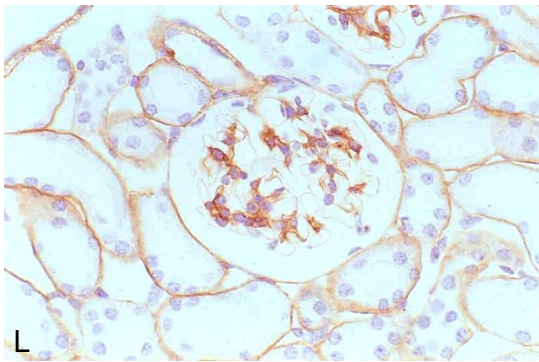
(I) Glomerulus and tubules, tg, male, 4 months, PASM-PAS (6.3 x 40)



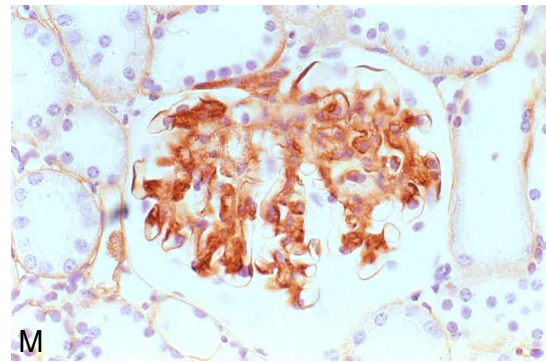
(J) Glomerulus, co, female, 8 months, IHC collagen type IV (10 x 40)



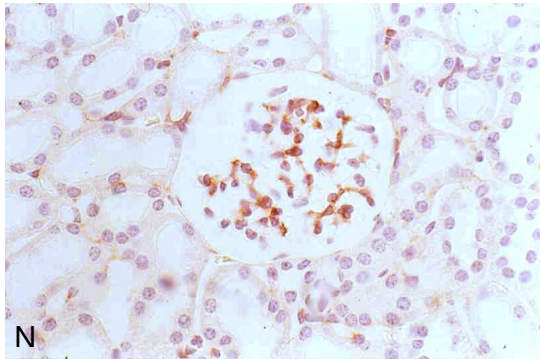
(K) Glomerulus, tg, female, 8 months, IHC collagen type IV (10 x 40)



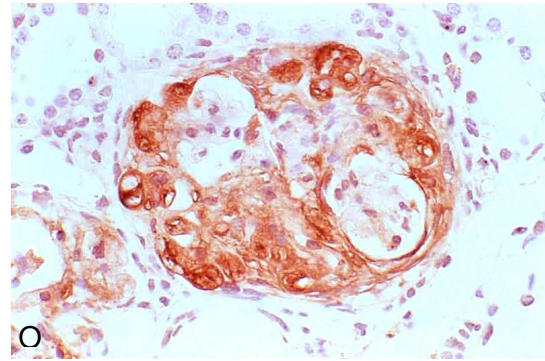
(L) Glomerulus, co, female, 8 months, IHC laminin (10 x 40)



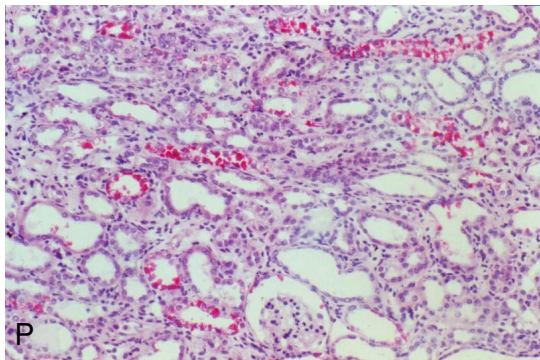
(M) Glomerulus, tg, female, 8 months, IHC laminin (10 x 40)



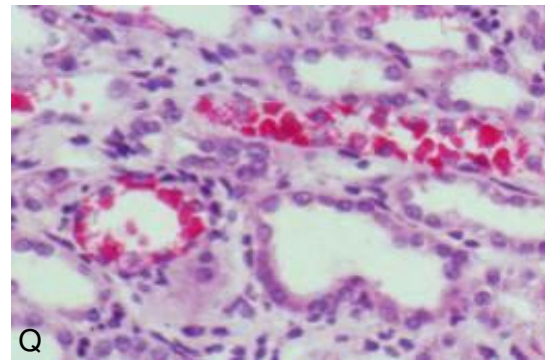
(N) Glomerulus, co, female, 8 months,
IHC fibronectin (10 x 40)



(O) Glomerulus, tg, female, 8 months,
IHC fibronectin (10 x 40)



(P) Overview of the renal cortex and
medulla, tg, male, 8 months,
Best's carmine (6.3 x 25)



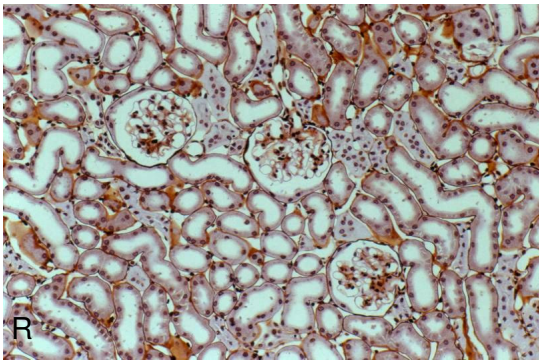
(Q) Glycogen storage in tubular epithelial cells, tg, male, 8 months, Best's carmine (12.5 x 40)

Figures 4.30 (A-Q) Macroscopical and histological appearance of the kidneys of animals fed Diet 1. (A) Kidney male control (left) and a GIPR^{dn} transgenic male (right), age: eight months. Note the renal hypertrophy of the transgenic animal. (B) H&E stained section of the renal cortex of a male control mouse, four months and (C) a male transgenic mouse, four months; note the increased size of glomerular profiles in the transgenic animal as compared to the control. (D) PAS stained glomerular profile of a male control mouse and (E) a male transgenic mouse at four months of age. The transgenic animal shows mesangial expansion, hyalinosis and widespread adhesion between the glomerular tuft and the capsule of Bowman. (F) Silver stained glomerular profile of a 4-month-old control male and (G) an age-matched transgenic animal. Note the glomerular obsolescence due to mesangial expansion, hyalinosis, collapse of capillaries and the circumferential adhesion between the glomerular tuft and the capsule of Bowman. Further, splitting of the basal membrane of Bowman's capsule can be seen, as well as protein casts in the tubular lumen. (H,I) Overviews of the renal cortex of a 4-month old transgenic male; note the glomerulosclerosis, tubular atrophy, protein casts in tubules, interstitial fibrosis and inflammatory cell infiltration. (J-O) Immunohistochemical glomerular staining for type IV collagen (J,K), laminin (L,M) and fibronectin (N,O) in transgenic mice and controls, indirect immunoperoxidase method. (J) collagen type IV detection in the glomerular pro-

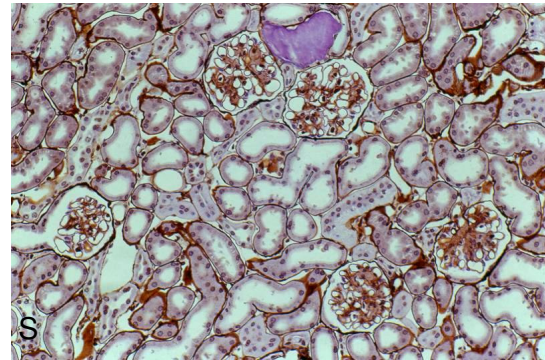
file of a control mouse; (K) glomerular obsolescence due to mesangial expansion with increased deposition of collagen type IV, transgenic animal. (L) Control mouse: staining of a glomerular profile for laminin; (M) glomerulus of a transgenic animal, the expanded glomerular matrix stains positive for laminin. (N) Staining for fibronectin, glomerulus of a control mouse; (O) glomerular obsolescence with abnormal accumulation of fibronectin. (P,Q) Glycogen storage in tubular epithelial cells of a 8-month-old transgenic male (Best's carmine).

b) Animals receiving the carbohydrate-restricted diet

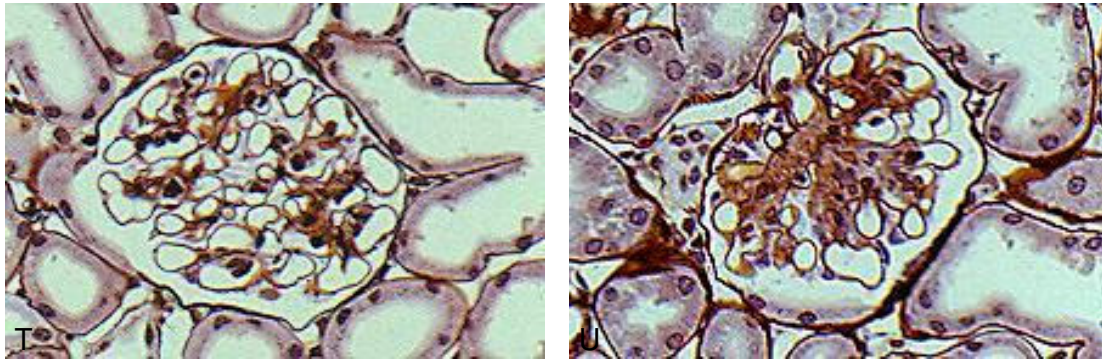
Transgenic animals permanently fed the carbohydrate-restricted diet were studied at the age of 10 and 14 months. In both age groups, transgenic mice did not exhibit marked hyperglycemia, polydipsia, polyuria, or proteinuria. The renal and glomerular changes found in this group were not comparable to those observed in the group fed standard rodent chow. Renal and glomerular hypertrophy was not as pronounced or could not be observed, glomerular changes were rarely observed, only in a focal pattern, including mild mesangial expansion, segmental hyalinosis and sclerosis, and sometimes tubular atrophy (Fig. 4.30 R-U).



(R) Overview of the renal cortex, co, female, 14 months, PASM-PAS (6.3 x 25)



(S) Overview of the renal cortex, tg, female, 14 months PASM-PAS (6.3 x 25)



(T) Glomerulus, tg, female, 14 months,
PASM-PAS (12.5 x 40)

(U) Glomerulus, tg, male, 14 months,
PASM-PAS (12.5 x 40)

Figures 4.30 (R-U) Macroscopical and histological appearance of the kidneys of animals fed Diet 2. (R) Overview of the renal cortex, 14-month-old control female and (S) age-matched female transgenic mouse. Glomerular hypertrophy can be observed in the kidney section of the transgenic mouse; (T) Glomerular profile, 14-month-old transgenic female and (U) age-matched transgenic male. The glomerular profile of the female mouse is inconspicuous; the glomerular profile of the male transgenic animal shows mesangial expansion with an increased amount of silver staining matrix.

4.14 Quantitative-stereological findings of the kidneys

4.14.1 Kidney volume

In the 4-month age group, five male GIPR^{dn} transgenic and four male littermate control mice were studied. The kidney volume was increased by 46% in transgenic vs. control mice (979.4 ± 100.4 vs. 670.2 ± 79.7 mm³, $p < 0.05$). The kidney weight to body weight ratio (relative kidney weight) was increased by 126% ($p < 0.05$) in transgenic vs. control males (Table 4.13).

Group (n)	Body weight (g)	Kidney weight (mg)	Relative kidney weight (%)
Co male (4)	44.2 ± 4.8	703.8 ± 83.7	1.6 ± 0.1
Tg male (5)	$28.7^* \pm 0.7$	$1028.4^* \pm 105.4$	$3.6^* \pm 0.4$

Table 4.13 Body and kidney weight (four months). Transgenic (tg) males show a significantly lower body weight and a significantly higher absolute and relative kidney weight as compared to control (co) males. Data are means \pm SEM; * $p < 0.05$ vs. control.

At the age of eight months, four GIPR^{dn} transgenic and four control males, as well as three GIPR^{dn} transgenic and three control females were examined. In transgenic males, the kidney volume was increased by 47% (1078.8 ± 124.4 vs. 733.1 ± 43.5 mm³, $p < 0.05$) and by 92% (963.5 ± 11.3 vs. 500.6 ± 15.3 mm³, $p < 0.05$) in females, respectively. Male controls showed a significantly higher kidney volume than female control mice. The body weight of male control mice was significantly higher than that of male transgenic and female mice (Table 4.14). The kidney weight-to-body weight ratio was increased by 137% in male and by 105% in female transgenic mice as compared to age- and sex-matched controls (Table 4.14).

Group (n)	Body weight (g)	Kidney weight (mg)	Relative kidney weight (%)
Co male (4)	43.7 \pm 0.7	770 \pm 46	1.8 \pm 0.8
Tg male (4)	27.5* \pm 2.2	1133* \pm 130	4.2* \pm 0.5
Co female (3)	30.4 \pm 0.9	526 \pm 16	1.7 \pm 0.1
Tg female (3)	28.5 \pm 0.5	1012* \pm 12	3.6* \pm 0.1

Table 4.14 Body and kidney weight (eight months). Transgenic (tg) males show a significantly decreased body weight as compared to control (co) males. All transgenic animals studied show a significantly higher absolute and relative kidney weight than sex-matched controls. Data are means \pm SEM; (n), number of animals investigated. * $p < 0.05$ vs. control.

4.14.2 Mean glomerular volume

At four months of age, the mean glomerular volume ($v_{(\text{Glom})}$, corrected for embedding shrinkage) was increased by 122% in male transgenic animals vs. male controls. The $v_{(\text{Glom})}$ -to-kidney weight ratio was increased by 51% and the $v_{(\text{Glom})}$ -to-body weight ratio was increased by 235% in transgenic animals vs. controls ($p < 0.05$). Data are presented in Table 4.15.

Group (n)	$V_{(\text{Glom})}$ ($10^3 \mu\text{m}^3$)	$V_{(\text{Glom})} /$ Kidney weight ($10^3 \mu\text{m}^3/\text{mg}$)	$V_{(\text{Glom})} /$ Body weight ($10^3 \mu\text{m}^3/\text{g}$)
Co male (4)	312.8 ± 35.5	0.5 ± 0.1	7.2 ± 0.8
Tg male (5)	694.3* ± 79.2	0.7* ± 0.1	24.1* ± 2.4

Table 4.15 Morphometric results (four months). The absolute and relative mean glomerular volume ($v_{(\text{Glom})}$) is significantly increased in transgenic (tg) mice as compared to controls (co). Data are means ± SEM; (n), number of animals investigated. * $p < 0.05$ vs. control.

In 8-month-old transgenic males, the $v_{(\text{Glom})}$ was increased by 71% in male and by 80% in female transgenic mice as compared to age- and sex-matched controls.

The $v_{(\text{Glom})}$ -to-kidney weight ratio did not differ between sex-matched control and transgenic mice. Comparing control mice, females had a 41% higher $v_{(\text{Glom})}$ -to-kidney weight ratio. The $v_{(\text{Glom})}$ -to-body weight ratio was 180% increased in male transgenic mice and 91% increased in female transgenic mice vs. sex-matched controls ($p < 0.05$). Data are presented in Table 4.16.

Group (n)	$V_{(\text{Glom})}$ ($10^3 \mu\text{m}^3$)	$V_{(\text{Glom})} /$ Kidney weight ($10^3 \mu\text{m}^3/\text{mg}$)	$V_{(\text{Glom})} /$ Body weight ($10^3 \mu\text{m}^3/\text{g}$)
Co male (4)	347.5 ± 23.7	0.5 ± 0.1	8.0 ± 0.6
Tg male (4)	594.7* ± 38.7	0.6 ± 0.1	22.4* ± 3.3
Co female (3)	341.2 ± 26.4	0.7 ± 0.1	11.3 ± 1.2
Tg female (3)	614.6* ± 74.0	0.6 ± 0.1	21.5* ± 2.4

Table 4.16 Morphometric results (eight months). The mean glomerular volume ($v_{(\text{Glom})}$) and the $v_{(\text{Glom})}$ -to-body weight ratio is significantly increased in transgenic (tg) mice as compared to controls (co). Data are means ± SEM; (n), number of animals investigated. * $p < 0.05$ vs. control.

4.15 Twelve-month survival

a) Animals receiving standard rodent chow

All transgenic male animals (n=9) died/had to be killed until the end of survey. All male animals died from diabetes mellitus, aged 49, 78, 104, 150, 223, 267 and 278 days. One animal was killed at the age of 234 days due to severely disturbed general condition; gross morphology and histology revealed large abscesses in both kidneys. Since the bladder appeared normal a hematogenous pathway was considered as pathogenic mechanism, the etiology was considered a bacterial infection. Finally one animal was euthanized due to a retro-orbital abscess (age 342 days). 16/20 female transgenic animals died from diabetes mellitus or had to be euthanized because of severely disturbed general condition, resulting from the metabolic state at the age of 108, 108, 135, 147, 148, 171, 201, 204, 214, 226, 228, 241, 279, 284, 301, and 321 days. Therefore, all transgenic animals fed Diet 1 died as a result from the metabolic state and all male transgenic animals had died before the age of 12 months (Fig. 4.31 A/B).

1/18 male and 2/7 female control animals had died or had to be euthanized. The male control animal exhibited an untreatable dermatitis and one female animal was killed because of a malignant tumor (lymphoma). The other female control mouse had died at 270 days of age; neither gross morphology nor histology revealed the cause of death. Taken together, both male and female transgenic animals show a significantly reduced life span as compared to sex-matched controls fed standard rodent chow (Table 4.17).

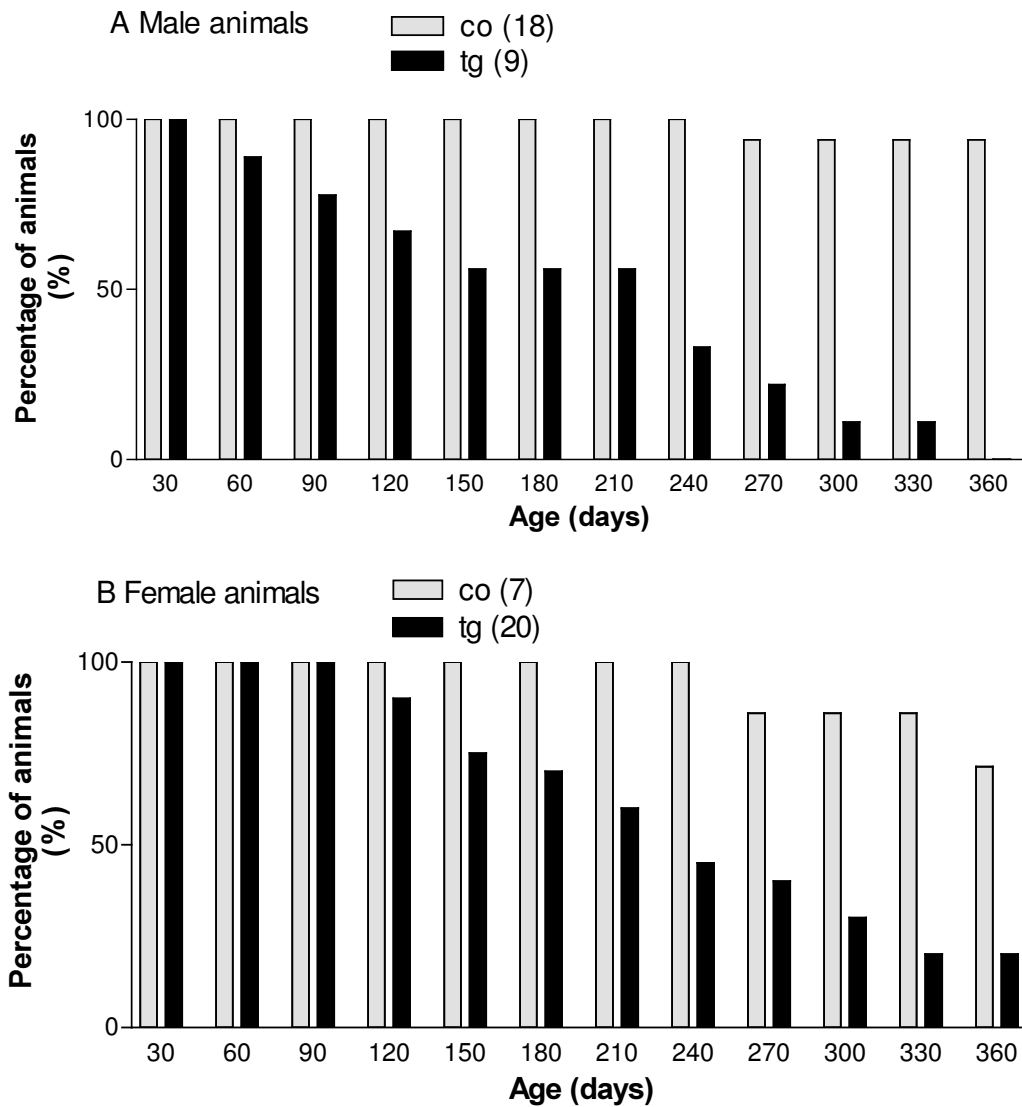


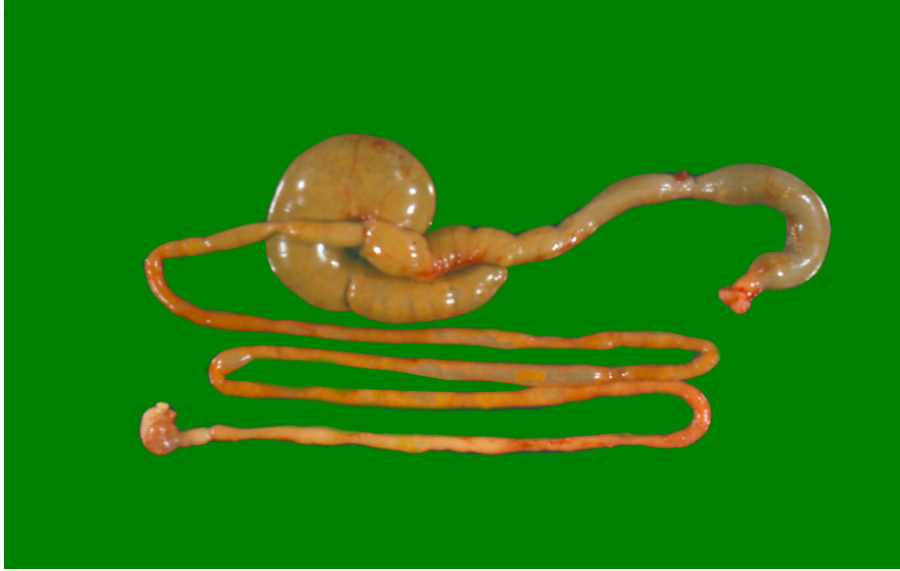
Figure 4.31 Twelve-month survival; (A) male animals, (B) female animals. All male transgenic (tg) animals and 80% of the female transgenic animals died within the period investigated. Data are percentage of living animals out of all animals investigated per group; (n), number of animals examined; co, control.

b) Animals receiving the carbohydrate restricted diet

In the group Diet 2, none of the control males or females had died until the age of twelve months. Four of seven male GIPR^{dn} transgenic animals had died within that period. An 80-day-old animal had died of diabetes mellitus as evidenced by signs of dehydration and of cardiovascular failure (hyperemia of the liver and kidneys, as well as hyperemia, edema and emphysema of the lungs). At the age of 241 days, one GIPR^{dn} transgenic male had to be killed because of a retro-orbital abscess. Another had to be euthanized because of severe, untreatable diabetes-associated opstipation, aged 363 days (Fig. 4.32). One of the GIPR^{dn} transgenic males had to be killed because of a malignant tumor (lymphoma) at the age of 284 days. Until the age of twelve months, 3/12 female transgenic animals from the group Diet 2 had died, two of which died from severe opstipation (aged 114 and 293 days) and one had to be killed due to a retro-orbital abscess at the age of 280 days (Fig. 4.33 A/B). Taken together, both male and female transgenic animals lived significantly shorter than sex-matched controls (Table 4.17).



(A) Corpse of GIPR^{dn} transgenic male with open abdominal cavity



(B) Intestine of the same animal as shown in (A)



(C) Large bowel (opened) from the same animal as shown in (A)

Fig 4.32 (A-C) Pathological findings in a GIPR^{dn} transgenic male that had died from opstipatio coli. A: View of the opened abdominal cavity. Note the marked distension of the caecum. B: Intestine (closed). The caecum and colon are largely distended. The stomach is nearly empty. C: Intestine after removal of the content. The caecum content (not shown) was fluid and the caecum wall appears very thin (left). Note the solid piece of faeces on the top right of the colon, which was thought to be the cause of opstipation.

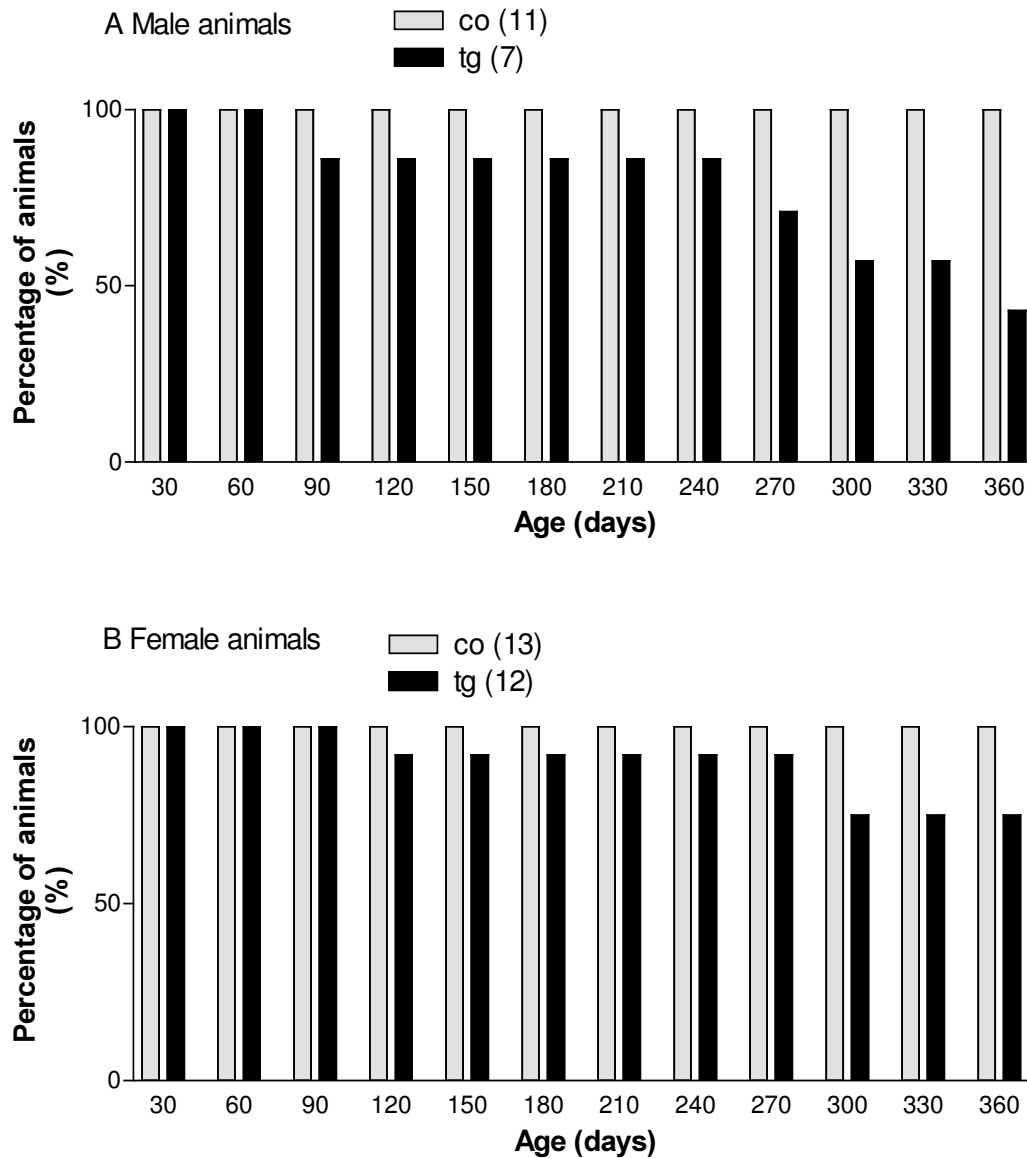


Figure 4.33 Twelve-month survival rate; (A) male animals, (B) female animals. 57% of the male transgenic (tg) animals and 25% of the female transgenic animals died within the period investigated. However, only 29% of the male and 13% of the female transgenic animals died from diabetes mellitus. All control (co) animals survived the twelve-month period. Data are percentage of living animals out of all animals investigated per group.

c) Comparison of both diet groups

Comparing both diet groups, transgenic animals fed the carbohydrate-restricted diet lived significantly longer than those receiving standard rodent chow. The diet had no effect on the 12-month life expectancy of control animals (Table 4.17).

Group (n,n)	12 month Life expectancy	
	Diet 1	Diet 2
Co male (18,11)	359.7 ± 17.3	365.0 ± 22.1
Tg male (9,7)	191.7* ± 24.4	267.0*† ± 25.9
Co female (7,13)	346.1 ± 27.7	365.0 ± 20.3
Tg female (20,12)	238.8* ± 16.4	289.5*† ± 18.9

Table 4.17 12-month life expectancy of animals, comparison of both diet groups. Transgenic (tg) animals lived significantly shorter than sex- and diet-matched controls (co). Transgenic animals fed Diet 2 lived significantly longer than transgenic animals fed Diet 1. (SEM), standard error of least squares means; (n,n), number of animals fed Diet 1/ number of animals fed Diet 2; * p<0.05 transgenic vs. control; † p<0.05 Diet 1 transgenic vs. Diet 2 transgenic.

5. Discussion

Transgenic mice expressing a mutated GIPR under the control of the rat pro-insulin gene promoter were found to develop severe diabetes mellitus (Herbach *et al.* 2001; Volz-Peters *et al.* 2000). The present study was performed in order to characterize clinical and pathological alterations in this new animal model of diabetes in detail.

Based on the results obtained in the present study the onset of diabetes mellitus in GIPR^{dn} transgenic mice was further defined. In all transgenic animals observed, urine glucose excretion was found to occur between 14 and 21 days of age. The development of a diabetic phenotype in suckling GIPR^{dn} transgenic mice could be due to the beginning intake of rodent chow, leading to an increasing importance of the enteroinsular- and especially the GIP-/GIPR-axis in glucose homeostasis. This is supported by the findings in 10-day-old transgenic mice, which did not yet show an altered blood glucose level, despite lower serum insulin concentrations. From 21 days of age onwards, blood glucose levels obviously exceeded the renal threshold. At 30 days of age, significantly elevated serum glucose levels in transgenic animals paralleled urinary glucose excretion.

The diabetic phenotype was further defined by measurement of blood and serum glucose levels, as well as serum insulin values. By the age of 30 days, blood glucose values were largely elevated while insulin levels of transgenic mice were significantly lower in comparison to control mice, demonstrating an absolute insulin deficiency. Both, the high glucose and low insulin levels result from the expression of the dominant negative GIP receptor. However, it is not yet defined whether a defect in GIP receptor signaling is responsible for the phenotype of GIPR^{dn} transgenic mice. The alterations in glucose homeostasis in GIPR^{dn} transgenic mice are much more dramatic than those observed in both GIPR^{-/-} and GLP-1R^{-/-} mice (Miyawaki *et al.* 1999; Scrocchi *et al.* 1996). Pederson *et al.* (1998) could show that the GIP component of the enteroinsular axis, at the level of GIP secretion and action, is upregulated in GLP-1R^{-/-} mice. These findings provide evidence for plasticity in the enteroinsular axis, suggesting that in the mouse, the lack of GLP-1 action is in part compensated by upregulation of the GIP-insulin axis. A similar adaptive mechanism could contribute to the modest changes in GIPR^{-/-} mice (Baggio *et al.* 2000; Lewis *et al.* 2000). A functional endogenous receptor is present in GIPR^{dn} transgenic mice and therefore, the

various possible adaptive or compensatory mechanisms might not be triggered. A functional defect in signal transduction of the GIPR^{dn} was proven *in vitro*, where the GIPR^{dn} was found to bind the ligand GIP with normal affinity but to fail to induce signal transduction (Volz 1997). It was not yet possible to evaluate a disturbance in signal transduction resulting from the expression of the GIPR^{dn} *in vivo*. Since the isolation of intact islets from GIPR^{dn} transgenic animals was found to be impossible so far, signal transduction studies could not be performed. It is possible that signal transduction pathways are disturbed in general, leading to a failure to increase intracellular cAMP levels. That would lead to the loss of both the GIP and GLP-1 mediated insulin secretion and in part explain the unresponsiveness of the B-cells following oral glucose administration observed in GIPR^{dn} transgenic animals. A different line of GIPR^{dn} transgenic animals exhibiting only mild disturbance in glucose homeostasis (Line GIPR^{dn-C}) has been studied concerning the specificity of the phenotype to transgene expression. Administration of 10 µg GIP before oral glucose challenge did not lower the glucose curve of transgenic animals as compared to control animals and to transgenic animals not receiving the peptide prior to glucose challenge. GLP-1 (10 µg) and administration of 100 µg GIP though had the same effect on lowering the glucose curve in transgenic and control mice. Therefore, signaling of the GLP-1 receptor was proven to be unchanged in GIPR^{dn-C} transgenic mice and a competitive mechanism between the mutated and the endogenous GIP receptor was confirmed by excess administration of the ligand (Göke B., Berghöfer P., personal communication). The SCGTT performed in this study could show that GLP-1 but not GIP is capable to reduce the AUC glucose as compared to SCGTT without the peptide. Since neither glucose alone nor the peptides GIP and GLP-1 augmented the serum insulin levels of transgenic mice during SCGTT, the glucose lowering actions of GLP-1 might be due to extrapancreatic actions of GLP-1, such as the increase of liver-glycogen synthesis. However, due to the severe changes of the endocrine pancreas (as further discussed below) in these mice a physiologic glucose-induced insulin secretion cannot be expected. The malformation of the endocrine pancreas might be the leading cause of the unresponsiveness of the islets following oral glucose challenge, rather than the competitive inhibition of GIP receptor signaling (in transgenic mice of the Line GIPR^{dn-C}, islet-cell composition and distribution seemed to be unchanged, B. Göke, personal communication).

GIPR^{dn} transgenic mice show all signs of early onset diabetes. Fasting and post-prandial blood or serum glucose levels and glucose tolerance after oral administration of glucose are severely altered. Abnormally high glucose values are associated with largely reduced fasting insulin levels as well as reduced insulin secretion after oral glucose challenge and nutrient ingestion. The reduction of caloric intake has been shown to improve the diabetic state. Transgenic animals transiently fed a carbohydrate-restricted diet showed lower fasted blood glucose levels than animals fed standard rodent chow. The modulation of blood and serum glucose values using a carbohydrate-restricted diet is therefore considered an important tool for studying the correlation between glucose values and secondary organ lesions. Further, it might be possible to gain insight into the pathogenesis of diabetes mellitus in these rather mildly diabetic animals and to perform signal transduction studies.

The relative physiological roles of GIP and GLP-1 have been studied intensively. The results remain controversial; some investigators found GIP and GLP-1 to be equally potent in their capacity to stimulate insulin release (Suzuki *et al.* 1990), whereas others have suggested GLP-1 to possess greater insulintropic effects (Siegel *et al.* 1992; Wang *et al.* 1995). There is evidence that the importance of GLP-1 has been overestimated (Deacon *et al.* 1995; Gremlich *et al.* 1995; Wheeler *et al.* 1995) and the participation of GLP-1 in the incretin effect (in non-diabetic subjects) has even been questioned (Nauck 1999). Data obtained from studying the human enteroinsular axis suggested GIP to be the more potent incretin hormone (Nauck *et al.* 1993 a). An investigation by Lewis *et al.* (2000) using purified GIP receptor antibody in rats, clearly revealed the importance of GIP as an incretin hormone in the postabsorptive state. Inhibition of GIP-induced insulin release, using the receptor antagonist GIP(7-30)amide reduced circulating insulin concentrations by 72%, when GIP(7-30)amide was administered to rats (Tseng *et al.* 1996 b). The N-terminally modified GIP analogue (Tyr¹-glucitol GIP), which displays profound resistance to degradation in obese mouse plasma, was found to increase both antihyperglycemic and insulin-releasing actions of the peptide in an animal model of type 2 diabetes (O'Harte *et al.* 2000). This finding is in contrast to recent studies, which could only show an improvement of glycemic control by exogenous administration of GLP-1 but not by GIP (Creutzfeldt *et al.* 1996; Elahi *et al.* 1994; Nauck *et al.* 1993 a).

It is well known that the incretin effect is diminished in diabetic patients and rodent models of diabetes (Elahi *et al.* 1994; Nauck *et al.* 1986 a; Suzuki *et al.* 1990). The mechanism of impaired insulin secretion was thought to be associated with a homologous desensitization of the GIP receptor. In the present study, a severe diabetic phenotype was observed in GIPR^{dn} transgenic mice, suggesting that a disturbed GIP/GIPR axis is involved in the pathogenesis of diabetes. The findings of disturbed fasting glucose and insulin levels were somewhat unexpected, considering GIP as incretin hormone, acting predominantly in the postabsorptive state. Neither studies in GIPR knockout mice nor studies using GIPR antibodies in healthy rats revealed a role of GIP in glucose regulation and B-cell function in the fasting state (Baggio *et al.* 2000). The disturbed fasting glucose and insulin levels could be the reflection of the loss of a still undefined non-incretin mediated action of GIP or could result from malformation of the endocrine pancreas (as discussed below). As mentioned above, insulin secretion might be disturbed due to a more complex alteration in signal transduction pathways.

Glycated hemoglobin (HbA_{1c}) was determined in order to underline the long duration of the disturbance in glucose homeostasis. Transgenic animals fed Diet 1 and 2 both showed significantly elevated HbA_{1c} levels, with values obtained from transgenic animals fed the carbohydrate-restricted diet being significantly lower than those obtained from transgenic animals permanently fed standard rodent chow. The latter result is in coincidence with significantly lower blood glucose levels of transgenic animals fed the carbohydrate-restricted diet. The findings in transgenic animals and the fact that HbA_{1c} levels among control mice of the different diet groups, which exhibited similar blood glucose levels, did not differ irrespective of the type of rodent chow, led to the conclusion that HbA_{1c} levels do reflect the metabolic control in mice. HbA_{1c} levels in control mice are lower than those obtained from non-diabetic humans. This could be due to a lower life span of murine erythrocytes. The half-life of glycated hemoglobin A_{1c} is suggested to be 35 days when a human erythrocyte life span is assumed to be 120 days. Since the murine erythrocyte life span was shown to be 40 days, mouse HbA_{1c} levels may only reflect the average past plasma glucose levels for 2 weeks (Dan *et al.* 1997).

The diabetic state in GIPR^{dn} transgenic mice is associated with severe hyperphagia, polydipsia and polyuria, irrespective of the carbohydrate intake. These are well known findings, associated with diabetes mellitus (Böhles & Herwig 1999). All animals fed the carbohydrate-restricted diet showed a significantly higher food intake than animals fed standard rodent chow. This finding can be explained by the low caloric content of the carbohydrate-restricted diet. The water intake of control animals was significantly higher when fed Diet 2, which is probably due to the high fiber content of the carbohydrate-restricted diet. Transgenic animals fed the standard diet showed a significantly higher water intake than animals fed the carbohydrate-restricted diet. The explanation of this difference between both diet groups is the significantly higher blood glucose level, or less precise, the bad metabolic control in animals of the group Diet 1, leading to a higher urine glucose excretion, which in turn results in greater renal loss of water. Due to the high amounts of urine excreted, animals fed standard rodent chow had to be kept on several layers of tissue or even on metal grids while food and water intake was measured. When the diet was changed, blood glucose values were similar in transgenic animals of both diet groups and water intake in turn equalized. As well as that, the 24-hour urine volume was near identical, underlining the explanation above.

With respect to the alterations of serum parameters, GIPR^{dn} transgenic mice exhibited further signs of a diabetic metabolic state. The acute and chronic insulin deficiency has different effects on various organs and metabolic pathways. In adipose tissue, the glucose uptake is reduced; lipogenesis is low and lipolysis increased. Glucose uptake in muscles, too, is insulin dependent and therefore reduced in insulin-deficient diabetes. Further, the amino acid uptake and protein synthesis is disturbed and proteolysis increased. Despite increased supply of free fatty acids, the insulin deficiency results in a catabolism of muscular tissue. The effect of the diabetic metabolism on the liver is an increased glycogenolysis and gluconeogenesis as well as elevated triglyceride synthesis. An increase in hepatic proteolysis results in an increase of urea synthesis (Hepp & Häring 1999; Janka *et al.* 1999).

Serum urea and creatinine were both significantly elevated in GIPR^{dn} mice. This azotemia was not associated with clinical signs of renal failure and is therefore thought to be due to severe diabetes-associated polyuria, resulting in sodium-chloride loss and exsiccosis, leading to the so-called hyponatremic syndrome/chloropenic az-

otemia (Hepp & Häring 1999). Another reason for the occurrence of azotemia in GIPR^{dn} transgenic mice could be decreased glomerular filtration due to advanced kidney changes and therefore compensated retention of urinary excreted substances or a catabolic metabolic state.

The reduced values for total protein and albumin result from protein catabolism and/or renal loss of proteins (Hepp & Häring 1999).

Recently, a significant correlation between serum triglyceride levels, but not between cholesterol levels and severe cardiovascular complications was found (Janka *et al.* 1999). A significant increase in serum triglyceride levels was observed in GIPR^{dn} transgenic mice and thought to result from insulin deficiency and increased hepatic triglyceride synthesis (Rett & Häring 1999).

Male GIPR^{dn} transgenic mice show delayed body weight gain, and the 12-hour fasting body weight is significantly lower, as compared to non-transgenic males. The body weight of transgenic individuals is equal to that of control animals before the onset of diabetes, which was found to occur between two and three weeks of age. The reduced body weight of diabetic GIPR^{dn} transgenic animals was mainly due to the reduction of the weight of skin, carcass and abdominal fatty tissue. The severe reduction of abdominal fat weight is thought to result from absolute insulin deficiency and disturbed lipogenesis (Hepp & Häring 1999).

Taking into account that only the absolute heart weight was decreased, this reduction might be the reflection of the weight loss seen in GIPR^{dn} transgenic mice, resulting in protein catabolism.

The increase in weight of gastric and intestinal content is attributable to diabetes-associated hyperphagia; the same is probably true for the increase of intestine weight. In experimental diabetes of rats, hyperplasia of crypt and villous epithelial cells of the small intestine was found, which was thought to be a consequence of hyperphagia or/and the action of various growth stimulators, e.g. TGF α , EGF, ornithine decarboxylase and polyamines (Zoubi *et al.* 1995).

Hepatomegaly is a well-known finding in both type 1 and 2 diabetic humans (Chatila & West 1996; Marangiello & Giorgetti 1996) and animal models of diabetes (Herrman *et al.* 1999), although the mechanisms involved are still unknown. Recent findings indicate that hepatomegaly could be due to early hyperplasia and later decreased apoptosis of hepatocytes in streptozotocin diabetic rats (Herrman *et al.* 1999).

Herrman *et al.* (1999) suggest glucose stimulated protein kinase C (PKC) and mitogen-activated protein (MAP) kinase activation as a possible explanation for the observed high proliferation rate. The most common hepatic lesion in diabetics is increased glycogen deposition in both cytoplasm and nucleus of the hepatocytes. Steatosis is seen 10 times more often in obese type 2 than in type 1 diabetics. In type 1 diabetics, poor glycemic control and inadequate insulin levels are thought to induce triglyceride accumulation in the liver (Falchuk & Conlin 1993). There is no macroscopical or histological evidence for hepatic steatosis in GIPR^{dn} transgenic mice. Glycogen storage has been looked at qualitatively in alcohol fixed liver tissue, stained with Best's carmine. The amount of glycogen seemed to be equal in transgenic and control mice.

In summary, these clinical results demonstrate that the expression of a dominant negative GIP receptor under the control of the rat insulin gene promoter is associated with severe diabetes mellitus in transgenic mice. Despite the role of GIP as incretin hormone acting predominantly in the postabsorptive state, even fasted glucose and insulin levels are altered in GIPR^{dn} transgenic mice. In addition, several secondary features of the diabetic state, e.g. hyperphagia, polydipsia, polyuria and delayed body weight gain were shown to be overt in this novel animal model of diabetes. Therefore, GIPR^{dn} transgenic mice are a valuable model for answering further questions concerning incretin regulated glucose homeostasis and B-cell function.

The pancreas weight was not altered and both gross morphology and histologic appearance of the exocrine pancreas were inconspicuous in GIPR^{dn} transgenic mice. The endocrine pancreas though, showed striking light microscopic changes: in H&E-stained sections, both number and size of islet profiles appeared to be reduced in GIPR^{dn} transgenic mice as compared to controls. Immunohistochemistry revealed a disturbed islet composition accompanied by a changed distribution of the endocrine cells in islets. Comparable alterations have been observed in GLP-1R knockout mice where the absence of GLP-1R signaling led to a shift of A-cells to the center of the islets. The total volume of A-cells though was only slightly increased (n.s.) and the total B-cell volume was unchanged as compared to wildtype mice (Ling *et al.* 2001).

The morphological changes of the endocrine pancreas in GIPR^{dn} transgenic mice were evaluated quantitatively using unbiased model-independent stereological methods (Gundersen *et al.* 1988; Gundersen & Jensen 1987; Wanke *et al.* 1994).

The expression of a dominant negative GIP receptor was found to be associated with a severe reduction of the total volumes of islets, B-cells and isolated B-cells in GIPR^{dn} transgenic animals as compared to control mice, irrespective of the age at sampling.

The total islet volume and total B-cell volume did not change between 10 and 30 days of age in control mice. These findings are in agreement with the postnatal remodeling of rodent pancreas described in the literature; until weaning, the B-cell mass remains stable due to a wave of apoptosis of B-cells, which occurs during the second week of life, in parallel to a high cell replication rate (Scaglia *et al.* 1997). This remodeling phase is thought to prepare the endocrine pancreas to the changing functional demands (Trudeau *et al.* 2000). Both the total islet and total B-cell volume nearly doubled in control mice between 30 and 90 days of age, which is known to be due to increased islet neogenesis and B-cell replication at a low rate of apoptosis (Scaglia *et al.* 1997; Trudeau *et al.* 2000). In transgenic mice, the total islet volume was also increased at 90 vs. 30 days of age, whereas the total B-cell volume remained unchanged. The islet cell population has therefore been distorted towards non-B-cells. A similar tendency has been observed in PDX-1^{+/-} mice, where the knockout of one allele of the PDX-1 gene was thought to skew the islet cell lineage towards developing into non-B-cells (Dutta *et al.* 1998). It has not yet been evaluated whether disturbed GIPR-signaling affects the expression of transcription factors, such as PDX-1. However, the findings of severely reduced total islet and total B-cell volume and the reduction in islet neogenesis, the latter being evidenced by the dramatically lower total volume of isolated B-cells in GIPR^{dn} transgenic mice, imply an essential effect of GIPR-signaling on B-cell growth and differentiation *in vivo*.

GLP-1 is known to exert its effects on the insulin gene through upregulation of PDX-1 expression and binding of PDX-1 to the insulin gene promoter (Wang *et al.* 1999). Furthermore, in a partial pancreatectomy rat model of diabetes, GLP-1 analogues stimulated regeneration of the endocrine pancreas by both neogenesis and proliferation of B-cells (Xu *et al.* 1999). Stoffers *et al.* (2000) found the administration of GLP-1 to diabetic mice to stimulate PDX-1 expression and to enhance B-cell neogenesis and islet size.

Studies in beta (INS-1)-cells revealed GIP as a mitogenic factor for B-cells via pleiotropic signaling pathways (Trümper *et al.* 2001 b). As evidenced by BrdU (5-bromo-deoxyuridine) incorporation, the proliferation of beta (INS-1)-cells was stimulated dose-dependently by glucose, and GIP addition further instigated the INS-1 cell proliferation at glucose concentrations between 2.5 and 15 mM. The GIP-induced rise in proliferation was found to be dose dependent at 15 mM glucose. The PKA/CREB signaling module activation was measured and GIP was found to instigate a dose-dependent increase in CREB phosphorylation. Further, MAPK pathway signaling module activation and PI3K/PKB stimulation was determined in beta (INS-1)-cells following GIP administration. The findings in GIPR^{dn} transgenic mice provide evidence for the role of GIP in islet and B-cell development *in vivo*. The alterations of the endocrine pancreas in GIPR^{dn} transgenic mice were already observed before onset of diabetes and therefore could not be secondary to the diabetic state. The results obtained in the present study rather suggest GIP to stimulate islet neogenesis involving an intact GIP receptor mediated signal cascade. However, it is also possible that a general loss of function of signal transduction pathways is attributable to the changes of the endocrine compartment of the pancreas observed in GIPR^{dn} transgenic mice. The further deterioration of the islet and B-cell volume between 30 and 90 days of age could contribute in part to chronic hyperglycemia (Jonas *et al.* 1999). The severely reduced total B-cell volume and the disturbed distribution of endocrine cells in the islets, as well as the increased A-cell volume provide further explanation for the severely altered glucose homeostasis in GIPR^{dn} transgenic mice (Pipeleers *et al.* 1982).

Since GIPR^{dn} transgenic animals exhibit such a severe diabetic phenotype it was interesting to know whether transgenic mice develop secondary kidney lesions. Renal hypertrophy is a characteristic change in early stages of human diabetes (Schwieger & Fine 1990) and various rodent models of diabetes (Velasquez *et al.* 1990). Both male and female GIPR^{dn} transgenic animals show an at least 75% increase in kidney weight; these pathological findings were in coincidence with severe polyuria, reflecting renal hyperfunction. Renal damage was identified clinically and histologically. Clinically, all transgenic animals examined developed albuminuria until the age of 8 months, indicating overt diabetic kidney disease (Parving *et al.* 1996). The urinary loss of albumin was in concurrence with significantly lower serum albu-

min levels in transgenic animals, however, it is not clear whether the reduced serum albumin levels result from urinary loss of albumin or the catabolic state due to severe weight loss. Another clinically relevant parameter concerning kidney damage is azotemia. Both urea and creatinine levels were increased in transgenic animals, however, no signs of renal failure, such as anemia, oliguria, gastric ulcers, were observed in 4- or 8-month-old animals and therefore dehydration might account for the observed azotemia (Hepp & Häring 1999). Histological examination of the kidneys showed the development of glomerulosclerosis, including mesangial expansion with hyalinosis, increased deposition of the extracellular matrix proteins collagen type IV, laminin and fibronectin, collapse of glomerular capillaries and adhesions between the glomerular tuft and the capsule of Bowman. Further capillary distension and sometimes cystic appearance of Bowman's capsule was observed. Tubulo-interstitial lesions included tubular atrophy, tubular glycogen storage and PAS positive, eosinophilic hyalin casts in the tubular lumen indicating proteinuria. Interstitial inflammatory cell infiltration and mild to severe interstitial fibrosis could be seen in transgenic mice. The findings appear more marked than in other rodent models of diabetic kidney disease (Janssen *et al.* 1999; Steffes & Mauer 1984), however, the lesions typically been found in the human diabetic kidney, such as the so-called nodular glomerulosclerosis and arteriolar hyalin changes (Heptinstall 1991; Olsen 1969) were not observed in the age groups studied. Further examinations on older animals are currently being performed in order to study advanced kidney lesions. Quantitative-stereological data from the current investigation show a large increase in glomerular size, which is in coincidence with the clinically observed renal hyperfunction. Preliminary data from animals studied receiving a carbohydrate-restricted diet provide good evidence for the correlation between kidney damage and glucose control. In contrast to preexisting rodent models of diabetic kidney disease, the renal changes in GIPR^{dn} transgenic animals have many features in common with the changes in human diabetic kidney disease. Large animals models of diabetic nephropathy do show kidney damage closely related to the changes observed in humans but as discussed earlier, large animals are more difficult to handle, lesions take a long time to develop and are more expensive to obtain and maintain (Steffes & Mauer 1984). This novel animal model of diabetes mellitus characterized in the present study is considered a valuable model for studying the pathomechanisms of diabetes-associated kidney changes.

The twelve-month life expectancy demonstrated that all GIPR^{dn} transgenic animals, receiving standard rodent chow died until the age of twelve months. One of the main causes of death was cardiovascular failure. Interestingly cases of opstipation were observed, which can be found frequently in human patients with diabetes mellitus (Vogt *et al.* 1999). Another frequent disease of GIPR^{dn} transgenic animals was the development of retroorbital abscesses, which are thought to result from diabetes-associated increased susceptibility to infections (Haupt 1999). Whereas about 80% of all transgenic animals in this diet group died from diabetes mellitus, less than half of the animals on the carbohydrate-restricted diet died from disturbance in the metabolic state. Preliminary data on diabetes development in mice receiving the diet, which is low in carbohydrate content, showed that all animals exhibited lower fasting blood glucose and insulin levels. Some animals even lost the diabetic phenotype despite changing the diet from carbohydrate restricted to standard rodent chow. Taken together, these results indicate that metabolic control can increase life expectancy in GIPR^{dn} transgenic mice. However, if diabetes-associated organ changes are to be examined, feeding a carbohydrate-restricted diet is not advisable, since kidney lesions observed in 14-month-old transgenic mice, fed this diet from weaning were only mild.

In summary, the clinical and pathological findings show that GIPR^{dn} transgenic mice are valuable for further studies concerning the role of the enteroinsular axis in the pathogenesis of diabetes mellitus. The quantitative-stereological findings of the endocrine pancreas imply the importance of the GIP/GIP receptor axis in pancreas development. Further, the present study provides evidence that GIPR^{dn} transgenic mice are a promising model for studying diabetes-associated organ lesions.

6. Perspective

The mechanisms of disturbance in pancreas development should be studied in detail, including quantitative evaluation of mitotic and apoptotic indices and the expression of several B-cell specific transcription factors involved in the development of the endocrine pancreas on protein and RNA level.

Prenatal and early postnatal examinations, regarding pancreas development would be helpful for getting insight into the mechanisms involved in disturbed pancreas development in GIPR^{dn} transgenic mice. *In vitro* studies, using cells stably transfected with the mutated GIP receptor would answer questions about the changes in signal transduction and factors altered, acting downstream of the ligand-receptor level.

The changes involved in the increase of liver and intestine weight should be looked at, since those changes are frequently observed in human diabetes. Many diabetic animals from the life expectancy experiment observed in the present study had died from opstipation and therefore, clinical observations would include the motility and absorption capacity of the small intestine of GIPR^{dn} transgenic animals. Measurement of intestine length and morphometric evaluations of different compartments of the intestine should additionally be carried out.

7. Summary

Clinical and pathological characterization of a novel transgenic animal model of diabetes mellitus expressing a dominant negative glucose-dependent insulinotropic polypeptide receptor (GIPR^{dn})

Gastrointestinal hormones like glucose-dependent insulinotropic polypeptide have recently been shown to be involved in the pathogenesis of diabetes mellitus in humans and animals models of diabetes mellitus. The aim of this study was to characterize a novel transgenic mouse model expressing a dominant negative glucose-dependent insulinotropic polypeptide receptor (GIPR^{dn}) under the control of the rat insulin gene promoter and their non-transgenic counterparts. Detailed analysis of clinical parameters was performed, including urine glucose, blood or serum glucose and serum insulin values. In addition, oral and subcutaneous glucose tolerance tests were performed, and HbA_{1c} levels and various serum parameters were determined. The detection of the daily food and water intake and the daily urine volume was performed in two age groups. Further, body and organ weights were determined. Qualitative and quantitative morphological changes of the pancreas and the kidneys were investigated in several age groups. Some of the parameters were studied in different diet groups, one of them received standard rodent chow, and the other received a carbohydrate-restricted diet until four months of age. All transgenic mice studied exhibited severe glucosuria from 21 days of age onwards. From 30 days of age onwards, GIPR^{dn} transgenic males and females showed severe hyperglycemia and hypoinsulinemia ($p < 0.05$). In male transgenic animals, the fasted body weight was found to be lower than in age-matched male control mice. The daily food and water intake and the 24-hour urine volume were significantly higher in all transgenic animals investigated. Histological and immunohistochemical survey of the pancreas revealed a striking change of the islet cell composition and distribution. Further, quantitative-stereological analysis of the pancreas revealed a significant reduction of the total volumes of pancreatic islets, B-cells in the islets and isolated B-cells in the exocrine pancreas indicating neogenesis of islets. Kidney changes included renal and glomerular hypertrophy, glomerulosclerosis and tubulo-interstitial changes. In conclusion, transgenic mice expressing a dominant negative GIP receptor under the control of the rat insulin gene promoter develop a severe diabetic phenotype and striking

histological changes of the endocrine pancreas. Further, advanced diabetes-associated organ lesions, particularly of the kidney were observed and therefore, GIPR^{dn} transgenic mice are considered a valuable model for studying long-term complications of diabetes mellitus.

Zusammenfassung

Klinische und pathomorphologische Befunde bei einem neuartigen transgenen diabetischen Tiermodell, das einen dominant negativen glucose-dependent insulinotropic polypeptide Rezeptor (GIPR^{dn}) exprimiert.

In den letzten Jahren wurde beim Studium der Pathogenese des Diabetes mellitus die Aufmerksamkeit zunehmend auf die Beteiligung gastrointestinaler Hormone wie zum Beispiel glucose-dependent insulinotropic polypeptide gerichtet. Ziel dieser Studie war es, bei einem neuartigen transgenen Tiermodell, klinische und pathomorphologische Veränderungen eingehend zu charakterisieren. Bei den untersuchten Tieren handelte es sich um transgene Mäuse, die einen dominant negativen glucose-dependent insulinotropic polypeptide Rezeptor (GIPR^{dn}) unter der Kontrolle des Ratteninsulingenpromotors exprimieren und um nicht-transgene Geschwistertiere. Es erfolgte eine detaillierte Untersuchung Diabetes-relevanter klinischer Parameter, unter der Berücksichtigung von Harnglukoseausscheidung, Blut- bzw. Serumglukose- und Seruminsulinwerten. Zusätzlich wurden orale und subkutane Glukosetoleranztests durchgeführt und HbA_{1c}-Werte sowie verschiedene Serumparameter bestimmt. Die tägliche Futter- und Wasseraufnahme und das tägliche Harnvolumen wurden bei zwei Altersgruppen gemessen. Körper- und Organgewichte wurden ebenfalls erfasst. Die Erfassung morphologischer und histopathologischer Veränderungen des Pankreas und der Nieren erfolgte sowohl qualitativ als auch quantitativ-stereologisch an mehreren Altersgruppen. Einige der untersuchten Parameter wurden an Tieren, die mit Haltungsfutter gefüttert wurden und an Vergleichstieren erhoben, die bis zum Alter von 4 Monaten mit einer kohlenhydratarmen Diät ernährt wurden. Alle untersuchten transgenen Tiere zeigten ab einem Alter von 21 Tagen eine schwere Glukosurie. Im Alter von 30 Tagen zeigten GIPR^{dn} transgene männliche und weibliche Mäuse eine hochgradige Hyperglykämie und eine hochgradige Hypoinsulinämie. Bei männlich-transgenen Tieren war das Körpergewicht im Vergleich zu gleichgeschlechtlichen

Kontrolltieren reduziert ($p < 0.05$). Die tägliche Futter- und Wasseraufnahme und das tägliche Harnvolumen war bei allen untersuchten transgenen Tieren signifikant höher als bei Kontrolltieren. Histologische und immunhistochemische Untersuchungen am Pankreas zeigten schwere Veränderungen der Zusammensetzung und Verteilung der Inselzellen auf. Diese qualitativen Befunde konnten durch quantitativ-stereologische Untersuchungen eingehend charakterisiert werden. Das Gesamtvolumen der Pankreasinseln und der B-Zellen in den Inseln war bei GIPR^{dn} transgenen Mäusen signifikant niedriger als bei Kontrolltieren. Gleiches gilt für das Gesamtvolumen isolierter B-Zellen im exokrinen Pankreas, die als Indikator für Inselneogenese angesehen werden. Die festgestellten Nierenveränderungen umfassen renale und glomeruläre Hypertrophie, Glomerulosklerose und tubulointerstitielle Veränderungen. Die quantitativ-stereologische Auswertung konnte die subjektiven Befunde bestätigen, sowohl das Nierenvolumen als auch das mittlere Glomerulumvolumen waren bei transgenen Mäusen signifikant erhöht. Aus den erhobenen Befunden ergibt sich die Schlussfolgerung, dass transgene Mäuse, die einen dominant-negativen GIP Rezeptor unter der Kontrolle des Ratteninsulingenpromoters exprimieren eine hochgradigen diabetischen Phänotyp und prägnante histologische Veränderungen am endokrinen Pankreas entwickeln. Weiterhin konnten Diabetes-assoziierte Alterationen diverser Organe, insbesondere der Niere festgestellt werden, woraufhin GIPR^{dn} transgene Mäuse als ein wertvolles Tiermodell für die Untersuchung diabetischer Spätkomplikationen angesehen werden.

8. References

- The Diabetes Control and Complications Trial Research Group: The effect of intensive treatment of diabetes on the development and progression of long-term complications in insulin-dependent diabetes mellitus. *N Engl J Med* 329: 977-986, 1993.
- The expert committee on the diagnosis and classification of diabetes mellitus: Report of the Expert Committee on the Diagnosis and Classification of Diabetes Mellitus. *Diabetes Care* 20: 1183-1197, 1997.
- Ahlgren U, Jonsson J, Edlund H: The morphogenesis of the pancreatic mesenchyme is uncoupled from that of the pancreatic epithelium in IPF1/PDX1-deficient mice. *Development* 122:1409-1416, 1996.
- Ahlgren U, Jonsson J, Jonsson L, Simu K, Edlund H: beta-cell-specific inactivation of the mouse *Ip1/Pdx1* gene results in loss of the beta-cell phenotype and maturity onset diabetes. *Genes Dev* 12:1763-1768, 1998.
- Ahlgren U, Pfaff SL, Jessell TM, Edlund T, Edlund H: Independent requirement for ISL1 in formation of pancreatic mesenchyme and islet cells. *Nature* 385:257-260, 1997.
- Alberti KG, Zimmet PZ: Definition, diagnosis and classification of diabetes mellitus and its complications. Part 1: diagnosis and classification of diabetes mellitus provisional report of a WHO consultation. *Diabet Med* 15:539-553, 1998.
- Apelqvist A, Li H, Sommer L, Beatus P, Anderson DJ, Honjo T, Hrabe de Angelis M, Lendahl U, Edlund H: Notch signalling controls pancreatic cell differentiation. *Nature* 400:877-881, 1999.
- Baggio L, Kieffer TJ, Drucker DJ: Glucagon-like peptide-1, but not glucose-dependent insulinotropic peptide, regulates fasting glycemia and nonenteral glucose clearance in mice. *Endocrinology* 141:3703-3709, 2000.
- Bergstein JM: A practical approach to proteinuria. *Pediatr Nephrol* 13:697-700, 1999.
- Bloodworth JM, Jr., Engerman RL, Powers KL: Experimental diabetic microangiopathy. I. Basement membrane statistics in the dog. *Diabetes* 18:455-458, 1969.
- Böhles H, Herwig J: Klinik, Diagnose und Therapie des Typ -1-Diabetes im Kindes- und Jugendalter. In *Diabetologie in Klinik und Praxis*. H. Mehnert, E. Standl and K.-H. Usadel, Eds. p. 240-260, 1999.
- Bonner-Weir S: Islet growth and development in the adult. *J Mol Endocrinol* 24:297-302, 2000 a.

- Bonner-Weir S: Life and death of the pancreatic beta cells. *Trends Endocrinol Metab* 11:375-378, 2000 b.
- Bonner-Weir S: Perspective: Postnatal pancreatic beta cell growth. *Endocrinology* 141:1926-1929, 2000 c.
- Bonner-Weir S, Baxter LA, Schuppin GT, Smith FE: A second pathway for regeneration of adult exocrine and endocrine pancreas. A possible recapitulation of embryonic development. *Diabetes* 42:1715-1720, 1993.
- Bonner-Weir S, Deery D, Leahy JL, Weir GC: Compensatory growth of pancreatic beta-cells in adult rats after short-term glucose infusion. *Diabetes* 38:49-53, 1989.
- Bonner-Weir S, Withers DJ, Weir GC, Jonas JC: Impaired survival of differentiating B-cells but no insulin secretory defects result from ablation of IRS-2. *Diabetes* 48 Suppl1:A3, 1999.
- Bouwens L: Transdifferentiation versus stem cell hypothesis for the regeneration of islet beta-cells in the pancreas. *Microsc Res Tech* 43:332-336, 1998.
- Bouwens L, Kloppel G: Islet cell neogenesis in the pancreas. *Virchows Arch* 427:553-560, 1996.
- Bouwens L, Pipeleers DG: Extra-insular beta cells associated with ductules are frequent in adult human pancreas. *Diabetologia* 41:629-633, 1998.
- Bouwens L, Wang RN, De Blay E, Pipeleers DG, Kloppel G: Cytokeratins as markers of ductal cell differentiation and islet neogenesis in the neonatal rat pancreas. *Diabetes* 43:1279-1283, 1994.
- Brown JC, Dryburgh JR, Ross SA, Dupre J: Identification and actions of gastric inhibitory polypeptide. *Recent Prog Horm Res* 31:487-532, 1975.
- Brown JC, Pederson RA, Jorpes JE, Mutt V: Preparation of a highly active enterogasttrone. *Can J Physiol Pharmacol* 47:113-114, 1969.
- Buchan A, Polak J, Capella C, Solcia E, Pearse A: Electronimmunocytochemical evidence of the K cell localization of gastric inhibitory polypeptide (GIP) in man. *Histochemistry* 56:37-44, 1978.
- Buschard K: Diabetic animal models. *Apmis* 104:609-614, 1996.
- Buteau J, Roduit R, Susini S, Prentki M: Glucagon-like peptide-1 promotes DNA synthesis, activates phosphatidylinositol 3-kinase and increases transcription factor pancreatic and duodenal homeobox gene 1 (PDX-1) DNA binding activity in beta (INS-1)-cells. *Diabetologia* 42:856-864, 1999.

- Chatila R, West AB: Hepatomegaly and abnormal liver tests due to glycogenosis in adults with diabetes. *Medicine (Baltimore)* 75:327-333, 1996.
- Cobb MH, Goldsmith EJ: How MAP kinases are regulated. *J Biol Chem* 270:14843-14846, 1995.
- Craighead JE: Viral diabetes mellitus in man and experimental animals. *Am J Med* 70:127-134, 1981.
- Creutzfeldt W: Design of the entero-insular axis. In *The insulinotropic gut hormone glucagon-like peptide-1*. H. C. Fehmann and B. Göke, Eds. Basel, p. 1-14, 1997.
- Creutzfeldt W, Nauck M: Gut hormones and diabetes mellitus. *Diabetes Metab Rev* 8:149-177, 1992.
- Creutzfeldt WO, Kleine N, Willms B, Ørskov C, Holst JJ, Nauck MA: Glucagonostatic actions and reduction of fasting hyperglycemia by exogenous glucagon-like peptide I(7-36) amide in type I diabetic patients. *Diabetes Care* 19:580-586, 1996.
- Dahl U, Sjodin A, Semb H: Cadherins regulate aggregation of pancreatic beta-cells in vivo. *Development* 122:2895-2902, 1996.
- Dan K, Fujita H, Seto Y, Kato R: Relation between stable glycated hemoglobin A1C and plasma glucose levels in diabetes-model mice. *Exp Anim* 46:135-140, 1997.
- Deacon CF, Nauck MA, Toft-Nielsen M, Pridal L, Willms B, Holst JJ: Both subcutaneously and intravenously administered glucagon-like peptide I are rapidly degraded from the NH₂-terminus in type II diabetic patients and in healthy subjects. *Diabetes* 44:1126-1131, 1995.
- Dutta S, Bonner-Weir S, Montminy M, Wright C: Regulatory factor linked to late-onset diabetes? *Nature* 392:560, 1998.
- Edlund H: Transcribing pancreas. *Diabetes* 47:1817-1823, 1998.
- Edlund H: Pancreas: how to get there from the gut? *Curr Opin Cell Biol* 11:663-668, 1999.
- Edvell A, Lindstrom P: Initiation of increased pancreatic islet growth in young normoglycemic mice (Umea +/-). *Endocrinology* 140:778-783, 1999.
- Eisenbarth GS: Type I diabetes mellitus. A chronic autoimmune disease. *N Engl J Med* 314:1360-1368, 1986.
- Elahi D, Andersen DK, Brown JC, Debas HT, Hershcopf RJ, Raizes GS, Tobin JD, Andres R: Pancreatic alpha- and beta-cell responses to GIP infusion in normal man. *Am J Physiol* 237:E185-191, 1979.

Elahi D, McAloon-Dyke M, Fukagawa NK, Meneilly GS, Sclater AL, Minaker KL, Habener JF, Andersen DK: The insulinotropic actions of glucose-dependent insulinotropic polypeptide (GIP) and glucagon-like peptide-1 (7-37) in normal and diabetic subjects. *Regul Pept* 51:63-74, 1994.

Elrick H, Stimmler L, Hlad JCJ, Arai Y: Plasma insulin response to oral and intravenous glucose administration. *J Clin Endocrinol* 24:1076-1082, 1964.

Falchuk KR, Conlin D: The intestinal and liver complications of diabetes mellitus. *Adv Intern Med* 38:269-286, 1993.

Faure M, Voyno-Yasenetskaya TA, Bourne HR: cAMP and beta gamma subunits of heterotrimeric G proteins stimulate the mitogen-activated protein kinase pathway in COS-7 cells. *J Biol Chem* 269:7851-7854, 1994.

Fehmann HC, Göke R, Göke B: Cell and molecular biology of the incretin hormones glucagon-like peptide-I and glucose-dependent insulin releasing polypeptide. *Endocr Rev* 16:390-410, 1995.

Fehmann HC, Göke R, Göke B, Bachle R, Wagner B, Arnold R: Priming effect of glucagon-like peptide-1 (7-36) amide, glucose-dependent insulinotropic polypeptide and cholecystokinin-8 at the isolated perfused rat pancreas. *Biochim Biophys Acta* 1091:356-363, 1991.

Finegood DT, Scaglia L, Bonner-Weir S: Dynamics of beta-cell mass in the growing rat pancreas. Estimation with a simple mathematical model. *Diabetes* 44:249-256, 1995.

Frodin M, Sekine N, Roche E, Filloux C, Prentki M, Wollheim CB, Van Obberghen E: Glucose, other secretagogues, and nerve growth factor stimulate mitogen-activated protein kinase in the insulin-secreting beta-cell line, INS-1. *J Biol Chem* 270:7882-7889, 1995.

Gallwitz B, Witt M, Morys-Wortmann C, Folsch UR, Schmidt WE: GLP-1/GIP chimeric peptides define the structural requirements for specific ligand-receptor interaction of GLP-1. *Regul Pept* 63:17-22, 1996.

Gefel D, Barg Y, Zimlichman R: Glucagon-like peptide-1 structure, function and potential use for NIDDM. *Isr J Med Sci* 33:690-695, 1997.

Gelling RW, Wheeler MB, Xue J, Gyomory S, Nian C, Pederson RA, McIntosh CH: Localization of the domains involved in ligand binding and activation of the glucose-dependent insulinotropic polypeptide receptor. *Endocrinology* 138:2640-2643, 1997.

- Gepts W, Toussaint D: Spontaneous diabetes in dogs and cats. A pathological study. *Diabetologia* 3:249-265, 1967.
- Göke R, Fehm H, Göke B: Glucagon-like peptide 1 (7-36) amide is a new incretin/enterogastrone candidate. *Eu J Clin Invest* 21:135-144, 1991.
- Göke R, Göke B, Richter G, Arnold R: The entero-insular axis: the new incretin candidate glucagon-like peptide-1(7-36)amide (GLP-1(7-36))amide. *Z Gastroenterol* 26:715-719, 1988.
- Gomori G: A new histochemical test for glycogen and mucin. *Am J Clin Pathol* 16:177-179, 1946.
- Gremlich S, Porret A, Hani EH, Cherif D, Vionnet N, Froguel P, Thorens B: Cloning, functional expression, and chromosomal localization of the human pancreatic islet glucose-dependent insulinotropic polypeptide receptor. *Diabetes* 44:1202-1208, 1995.
- Gundersen HJ, Bendtsen TF, Korbo L, Marcussen N, Møller A, Nielsen K, Nyengaard JR, Pakkenberg B, Sørensen FB, Vesterby A, West MJ: Some new, simple and efficient stereological methods and their use in pathological research and diagnosis. *Apmis* 96:379-394, 1988.
- Gundersen HJ, Jensen EB: The efficiency of systematic sampling in stereology and its prediction. *J Microsc* 147:229-263, 1987.
- Guz Y, Montminy MR, Stein R, Leonard J, Gamer LW, Wright CV, Teitelman G: Expression of murine STF-1, a putative insulin gene transcription factor, in beta cells of pancreas, duodenal epithelium and pancreatic exocrine and endocrine progenitors during ontogeny. *Development* 121:11-18, 1995.
- Hanahan D: Heritable formation of pancreatic beta-cell tumours in transgenic mice expressing recombinant insulin/simian virus 40 oncogenes. *Nature* 315:115-122, 1985.
- Harrison KA, Thaler J, Pfaff SL, Gu H, Kehrl JH: Pancreas dorsal lobe agenesis and abnormal islets of Langerhans in Hlxb9-deficient mice. *Nat Genet* 23:71-75, 1999.
- Haupt E: Diabetes mellitus und Infektionskrankheiten. In *Diabetologie in Klinik und Praxis*. H. Mehnert, E. Standl and K.-H. Usadel, Eds. p. 541-544, 1999.
- Hepp K, Häring H: Einführung in die Biochemie und Pathophysiologie des Stoffwechsels. In *Diabetologie in Klinik und Praxis*. H. Mehnert, E. Standl and K. Usadel, Eds. Stuttgart, p. 1-31, 1999.

- Heptinstall R: Diabetes mellitus and gout. In *Pathology of the kidney*. R. Heptinstall, Eds. Boston/Toronto, p. 1397-1453, 1991.
- Herbach N, Göke B, Hermanns W, Wolf E, Wanke R: Klinische Charakterisierung eines neuartigen diabetischen Tiermodells. *Tagungsbericht des 24. Kongresses der Deutschen Veterinärmedizinischen Gesellschaft* 418-426, 2001.
- Hermanns W, Liebig K, Schulz LC: Postembedding immunohistochemical demonstration of antigen in experimental polyarthritis using plastic embedded whole joints. *Histochemistry* 73:439-446, 1981.
- Herrera PL, Huarte J, Sanvito F, Meda P, Orci L, Vassalli JD: Embryogenesis of the murine endocrine pancreas; early expression of pancreatic polypeptide gene. *Development* 113:1257-1265, 1991.
- Herrman CE, Sanders RA, Klaunig JE, Schwarz LR, Watkins JB, 3rd: Decreased apoptosis as a mechanism for hepatomegaly in streptozotocin-induced diabetic rats. *Toxicol Sci* 50:146-151, 1999.
- Hill DJ, Strutt B, Arany E, Zaina S, Coukell S, Graham CF: Increased persistent circulating insulin-like growth factor II in neonatal transgenic mice suppresses developmental apoptosis in the pancreatic islets. *Endocrinology* 141:1151-1157, 2000.
- Hoeflich A, Wu M, Mohan S, Foll J, Wanke R, Froehlich T, Arnold GJ, Lahm H, Kolb HJ, Wolf E: Overexpression of insulin-like growth factor-binding protein-2 in transgenic mice reduces postnatal body weight gain. *Endocrinology* 140:5488-5496, 1999.
- Holst JJ: Glucagonlike peptide 1: a newly discovered gastrointestinal hormone. *Gastroenterology* 107:1848-1855, 1994.
- Holst JJ, Gromada J, Nauck MA: The pathogenesis of NIDDM involves a defective expression of the GIP receptor. *Diabetologia* 40:984-986, 1997.
- Janka H, Standl E, Standl R: Allgemeiner Überblick über die Angiopathien. In *Diabetologie in Klinik und Praxis*. H. Mehnert, E. Standl and K. Usadel, Eds. p. 334-372, 1999.
- Janle-Swain E: Animal models of diabetic nephropathy. In *CRC handbook of animal models of renal failure*. S. R. Ash and J. A. Thornhill, Eds. Boca Raton, Florida, p. 183-214, 1985.
- Janssen U, Phillips AO, Floege J: Rodent models of nephropathy associated with type II diabetes. *J Nephrol* 12:159-172, 1999.
- Jensen J, Heller RS, Funder-Nielsen T, Pedersen EE, Lindsell C, Weinmaster G, Madsen OD, Serup P: Independent development of pancreatic alpha- and beta-cells

from neurogenin3-expressing precursors: a role for the notch pathway in repression of premature differentiation. *Diabetes* 49:163-176, 2000 a.

Jensen J, Pedersen EE, Galante P, Hald J, Heller RS, Ishibashi M, Kageyama R, Guillemot F, Serup P, Madsen OD: Control of endodermal endocrine development by Hes-1. *Nat Genet* 24:36-44, 2000 b.

Jensen J, Serup P, Karlsen C, Nielsen TF, Madsen OD: mRNA profiling of rat islet tumors reveals nkx 6.1 as a beta-cell- specific homeodomain transcription factor. *J Biol Chem* 271:18749-18758, 1996.

Jonas JC, Sharma A, Hasenkamp W, Ilkova H, Patane G, Laybutt R, Bonner-Weir S, Weir GC: Chronic hyperglycemia triggers loss of pancreatic beta cell differentiation in an animal model of diabetes. *J Biol Chem* 274:14112-14121, 1999.

Jonsson J, Carlsson L, Edlund T, Edlund H: Insulin-promoter-factor 1 is required for pancreas development in mice. *Nature* 371:606-609, 1994.

Kato I, Suzuki Y, Akabane A, Yonekura H, Tanaka O, Kondo H, Takasawa S, Yoshimoto T, Okamoto H: Transgenic mice overexpressing human vasoactive intestinal peptide (VIP) gene in pancreatic beta cells. Evidence for improved glucose tolerance and enhanced insulin secretion by VIP and PHM-27 in vivo. *J Biol Chem* 269:21223-21228, 1994.

Kilpatrick ES, Maylor PW, Keevil BG: Biological variation of glycated hemoglobin. Implications for diabetes screening and monitoring. *Diabetes Care* 21:261-264, 1998.

Kimmelstiel P, Wilson C: Intercapillary lesions in the glomeruli of the kidney. *Am J Pathol* 12:83-96, 1936.

Klahr S: Mechanisms of progression of chronic renal damage. *J Nephrol* 12 Suppl 2:S53-62, 1999.

Kondo K, Nozawa K, Tomida T, Ezaki K: Inbred strains resulting from Japanese mice. *Bull Exp Animals* 6:107-112, 1957.

LaBarre J, Still E: Studies on the physiology of secretin. III. Further studies on the effects of secretin on the blood sugar. *Am J Physiol* 91:649-653, 1930.

Larsson LI: On the development of the islets of Langerhans. *Microsc Res Tech* 43:284-291, 1998.

Laybutt DR, Hasenkamp W, Grey S, Groff A, Jonas JC, Kaneto H, Ferran C, Sharma A, Bonner-Weir S, Weir GC: Activation of protective and destructive stress genes accompanies beta cell hypertrophy in hyperglycemic rats. *Diabetes* 49 Suppl1:A417, 2000.

- Leahy JL, Bonner-Weir S, Weir GC: Beta-cell dysfunction induced by chronic hyperglycemia. Current ideas on mechanism of impaired glucose-induced insulin secretion. *Diabetes Care* 15:442-455, 1992.
- Lehmann R, Spinas GA: Screening, diagnosis and management of diabetes mellitus and diabetic complications. *Ther Umsch* 57:12-21, 2000.
- Lewis JT, Dayanandan B, Habener JF, Kieffer TJ: Glucose-dependent insulintropic polypeptide confers early phase insulin release to oral glucose in rats: demonstration by a receptor antagonist. *Endocrinology* 141:3710-3716, 2000.
- Li H, Arber S, Jessell TM, Edlund H: Selective agenesis of the dorsal pancreas in mice lacking homeobox gene Hlxb9. *Nat Genet* 23:67-70, 1999.
- Ling Z, Wu D, Zambre Y, Flamez D, Drucker DJ, Pipeleers DG, Schuit FC: Glucagon-like peptide 1 receptor signaling influences topography of islet cells in mice. *Virchows Arch* 438:382-387, 2001.
- Linn T, Schneider K, Göke B, Federlin K: Glucagon-like-peptide-1 (7-36) amide improves glucose sensitivity in beta-cells of NOD mice. *Acta Diabetol* 33:19-24, 1996.
- Lu M, Wheeler MB, Leng XH, Boyd AE, 3rd: The role of the free cytosolic calcium level in beta-cell signal transduction by gastric inhibitory polypeptide and glucagon-like peptide I(7-37). *Endocrinology* 132:94-100, 1993 a.
- Lu M, Wheeler MB, Leng XH, Boyd AE, 3rd: Stimulation of insulin secretion and insulin gene expression by gastric inhibitory polypeptide. *Trans Assoc Am Physicians* 106:42-53, 1993 b.
- Lynn FC, Pamir N, Ng EH, McIntosh CH, Kieffer TJ, Pederson RA: Defective glucose-dependent insulintropic polypeptide receptor expression in diabetic fatty Zucker rats. *Diabetes* 50:1004-1011, 2001.
- Madsen OD, Jensen J, Petersen HV, Pedersen EE, Oster A, Andersen FG, Jorgensen MC, Jensen PB, Larsson LI, Serup P: Transcription factors contributing to the pancreatic beta-cell phenotype. *Horm Metab Res* 29:265-270, 1997.
- Mannucci E, Bardini G, Ognibene A, Rotella CM: Comparison of ADA and WHO screening methods for diabetes mellitus in obese patients. American Diabetes Association. *Diabet Med* 16:579-585, 1999.
- Marangiello R, Giorgetti R: A case of glycogenosis in a patient with insulin dependent diabetes. *Minerva Pediatr* 48:279-281, 1996.
- Marshall T, Williams KM: Clinical analysis of human urinary proteins using high resolution electrophoretic methods. *Electrophoresis* 19:1752-1770, 1998.

- Mayfield J: Diagnosis and classification of diabetes mellitus: new criteria. *Am Fam Physician* 58:1355-1362, 1369-1370, 1998.
- McIntyre N, Holdsworth CD, Turner DS: New interpretation of oral glucose tolerance. *Lancet* 2:20-21, 1964.
- Miralles F, Czernichow P, Scharfmann R: Follistatin regulates the relative proportions of endocrine versus exocrine tissue during pancreatic development. *Development* 125:1017-1024, 1998.
- Miyawaki K, Yamada Y, Yano H, Niwa H, Ban N, Ihara Y, Kubota A, Fujimoto S, Kajikawa M, Kuroe A, Tsuda K, Hashimoto H, Yamashita T, Jomori T, Tashiro F, Miyazaki J, Seino Y: Glucose intolerance caused by a defect in the entero-insular axis: a study in gastric inhibitory polypeptide receptor knockout mice. *Proc Natl Acad Sci U S A* 96:14843-14847, 1999.
- Montrose-Rafizadeh C, Avdonin P, Garant MJ, Rodgers BD, Kole S, Yang H, Levine MA, Schwindinger W, Bernier M: Pancreatic glucagon-like peptide-1 receptor couples to multiple G proteins and activates mitogen-activated protein kinase pathways in Chinese hamster ovary cells. *Endocrinology* 140:1132-1140, 1999.
- Morgan LM: The metabolic role of GIP: physiology and pathology. *Biochem Soc Trans* 24:585-591, 1996.
- Nakamura M, Yamada K: Studies on a diabetic (KK) strain of the mouse. *Diabetologia* 3:212-221, 1967.
- Nakane PK, Pierce GB, Jr.: Enzyme-labeled antibodies for the light and electron microscopic localization of tissue antigens. *J Cell Biol* 33:307-318, 1967.
- Nauck M, Schmidt WE, Ebert R, Strietzel J, Cantor P, Hoffmann G, Creutzfeldt W: Insulinotropic properties of synthetic human gastric inhibitory polypeptide in man: interactions with glucose, phenylalanine, and cholecystokinin-8. *J Clin Endocrinol Metab* 69:654-662, 1989.
- Nauck M, Stöckmann F, Ebert R, Creutzfeldt W: Reduced incretin effect in type 2 (non-insulin-dependent) diabetes. *Diabetologia* 29:46-52, 1986 a.
- Nauck MA: Is glucagon-like peptide 1 an incretin hormone? *Diabetologia* 42:373-379, 1999.
- Nauck MA, Bartels E, Ørskov C, Ebert R, Creutzfeldt W: Additive insulinotropic effects of exogenous synthetic human gastric inhibitory polypeptide and glucagon-like peptide-1-(7-36) amide infused at near-physiological insulinotropic hormone and glucose concentrations. *J Clin Endocrinol Metab* 76:912-917, 1993 a.

- Nauck MA, Heimesaat MM, Orskov C, Holst JJ, Ebert R, Creutzfeldt W: Preserved incretin activity of glucagon-like peptide 1 [7-36 amide] but not of synthetic human gastric inhibitory polypeptide in patients with type-2 diabetes mellitus. *J Clin Invest* 91:301-307, 1993 c.
- Nauck MA, Homberger E, Siegel EG, Allen RC, Eaton RP, Ebert R, Creutzfeldt W: Incretin effects of increasing glucose loads in man calculated from venous insulin and C-peptide responses. *J Clin Endocrinol Metab* 63:492-498, 1986 b.
- Nauck MA, Kleine N, Orskov C, Holst JJ, Willms B, Creutzfeldt W: Normalization of fasting hyperglycaemia by exogenous glucagon-like peptide 1 (7-36 amide) in type 2 (non-insulin-dependent) diabetic patients. *Diabetologia* 36:741-744, 1993 b.
- Naya FJ, Huang HP, Qiu Y, Mutoh H, DeMayo FJ, Leiter AB, Tsai MJ: Diabetes, defective pancreatic morphogenesis, and abnormal enteroendocrine differentiation in BETA2/neuroD-deficient mice. *Genes Dev* 11:2323-2334, 1997.
- Odoni G, Ritz E: Diabetic nephropathy--what have we learned in the last three decades? *J Nephrol* 12 Suppl 2:S120-124, 1999.
- Offield MF, Jetton TL, Labosky PA, Ray M, Stein RW, Magnuson MA, Hogan BL, Wright CV: PDX-1 is required for pancreatic outgrowth and differentiation of the rostral duodenum. *Development* 122:983-995, 1996.
- O'Harte FP, Mooney MH, Kelly CM, Flatt PR: Improved glycaemic control in obese diabetic ob/ob mice using N-terminally modified gastric inhibitory polypeptide. *J Endocrinol* 165:639-648, 2000.
- Ohlsson H, Karlsson K, Edlund T: IPF1, a homeodomain-containing transactivator of the insulin gene. *Embo J* 12:4251-4259, 1993.
- Olsen TS: Diabetic glomerulosclerosis: a comparison between human and experimental lesions. *Int Rev Exp Pathol* 7:271-304, 1969.
- Oser BM, Boesken WH: Rational diagnosis in kidney diseases. *Z Arztl Fortbild (Jena)* 87:211-215, 1993.
- Pang K, Mukonoweshuro C, Wong GG: Beta cells arise from glucose transporter type 2 (Glut2)-expressing epithelial cells of the developing rat pancreas. *Proc Natl Acad Sci U S A* 91:9559-9563, 1994.
- Parving H, Østerby R, Anderson P, Hsueh W: Diabetic nephropathy. In *The kidney*. B. Brenner, Eds. Philadelphia, p. 1864-1977, 1996.
- Pederson RA, Satkunarajah M, McIntosh CH, Scrocchi LA, Flamez D, Schuit F, Drucker DJ, Wheeler MB: Enhanced glucose-dependent insulinotropic polypeptide

secretion and insulinotropic action in glucagon-like peptide 1 receptor $-/-$ mice. *Diabetes* 47:1046-1052, 1998.

Perley MJ, Kipnis DM: Plasma insulin responses to oral and intravenous glucose: studies in normal and diabetic subjects. *J Clin Invest* 46:1954-1962, 1967.

Petrik J, Arany E, McDonald TJ, Hill DJ: Apoptosis in the pancreatic islet cells of the neonatal rat is associated with a reduced expression of insulin-like growth factor II that may act as a survival factor. *Endocrinology* 139:2994-3004, 1998.

Petrik J, Pell JM, Arany E, McDonald TJ, Dean WL, Reik W, Hill DJ: Overexpression of insulin-like growth factor-II in transgenic mice is associated with pancreatic islet cell hyperplasia. *Endocrinology* 140:2353-2363, 1999 a.

Petrik J, Reusens B, Arany E, Remacle C, Coelho C, Hoet JJ, Hill DJ: A low protein diet alters the balance of islet cell replication and apoptosis in the fetal and neonatal rat and is associated with a reduced pancreatic expression of insulin-like growth factor-II. *Endocrinology* 140:4861-4873, 1999 b.

Pictet RL, Clark WR, Williams RH, Rutter WJ: An ultrastructural analysis of the developing embryonic pancreas. *Dev Biol* 29:436-467, 1972.

Pipeleers D, In'T Veld PI, Maes E, Van De Winkel M: Glucose-induced insulin release depends on functional cooperation between islet cells. *Proc Natl Acad Sci U S A* 79:7322-7325, 1982.

Rahier JRD, Ibrahim M, Channaoui K: Islet cell populations in obese subjects and type 2 (non-insulin-dependent) diabetic patients. *Diabetologia* 32:532A, 1989.

Rett K, Häring H: Andere Stoffwechselkrankheiten. In *Diabetologie in Klinik und Praxis*. H. Mehnert, E. Standl and K. Usadel, Eds. p. 545-566, 1999.

Ritz E, Usadel K-H: Nierenkrankheiten. In *Diabetologie in Klinik und Praxis*. H. Mehnert, E. Standl and K.-H. Usadel, Eds. p. 416-432, 1999.

Romen W: Diabetic glomerulosclerosis: current status of its morphology and pathogenesis. *Klin Wochenschr* 58:1013-1022, 1980.

Sander M, Neubuser A, Kalamaras J, Ee HC, Martin GR, German MS: Genetic analysis reveals that PAX6 is required for normal transcription of pancreatic hormone genes and islet development. *Genes Dev* 11:1662-1673, 1997.

Scaglia L, Cahill CJ, Finegood DT, Bonner-Weir S: Apoptosis participates in the remodeling of the endocrine pancreas in the neonatal rat. *Endocrinology* 138:1736-1741, 1997.

- Scaglia L, Smith FE, Bonner-Weir S: Apoptosis contributes to the involution of beta cell mass in the post partum rat pancreas. *Endocrinology* 136:5461-5468, 1995.
- Schwieger J, Fine LG: Renal hypertrophy, growth factors, and nephropathy in diabetes mellitus. *Semin Nephrol* 10:242-253, 1990.
- Scrocchi LA, Brown TJ, MacLusky N, Brubaker PL, Auerbach AB, Joyner AL, Drucker DJ: Glucose intolerance but normal satiety in mice with a null mutation in the glucagon-like peptide 1 receptor gene. *Nat Med* 2:1254-1258, 1996.
- Sharma A, Zangen DH, Reitz P, Taneja M, Lissauer ME, Miller CP, Weir GC, Habener JF, Bonner-Weir S: The homeodomain protein IDX-1 increases after an early burst of proliferation during pancreatic regeneration. *Diabetes* 48:507-513, 1999.
- Siegel EG, Schulze A, Schmidt WE, Creutzfeldt W: Comparison of the effect of GIP and GLP-1 (7-36amide) on insulin release from rat pancreatic islets. *Eur J Clin Invest* 22:154-157, 1992.
- Simon D, Senan C, Balkau B, Saint-Paul M, Thibault N, Eschwege E: Reproducibility of HbA1c in a healthy adult population: the Telecom Study. *Diabetes Care* 22:1361-1363, 1999.
- Slack JM: Developmental biology of the pancreas. *Development* 121:1569-1580, 1995.
- Sosa-Pineda B, Chowdhury K, Torres M, Oliver G, Gruss P: The Pax4 gene is essential for differentiation of insulin-producing beta cells in the mammalian pancreas. *Nature* 386:399-402, 1997.
- Steffes MW, Mauer SM: Diabetic glomerulopathy in man and experimental animal models. *Int Rev Exp Pathol* 26:147-175, 1984.
- Stierle HE, Oser B, Boesken WH: Improved classification of proteinuria by semiautomated ultrathin SDS polyacrylamide gel electrophoresis. *Clin Nephrol* 33:168-173, 1990.
- Stoffers DA, Kieffer TJ, Hussain MA, Drucker DJ, Bonner-Weir S, Habener JF, Egan JM: Insulinotropic glucagon-like peptide 1 agonists stimulate expression of homeodomain protein IDX-1 and increase islet size in mouse pancreas. *Diabetes* 49:741-748, 2000.
- St-Onge L, Sosa-Pineda B, Chowdhury K, Mansouri A, Gruss P: Pax6 is required for differentiation of glucagon-producing alpha-cells in mouse pancreas. *Nature* 387:406-409, 1997.

St-Onge L, Wehr R, Gruss P: Pancreas development and diabetes. *Curr Opin Genet Dev* 9:295-300, 1999.

Sussel L, Kalamaras J, Hartigan-O'Connor DJ, Meneses JJ, Pedersen RA, Rubenstein JL, German MS: Mice lacking the homeodomain transcription factor Nkx2.2 have diabetes due to arrested differentiation of pancreatic beta cells. *Development* 125:2213-2221, 1998.

Suzuki S, Kawai K, Ohashi S, Mukai H, Murayama Y, Yamashita K: Reduced insulinotropic effects of glucagonlike peptide I-(7-36)-amide and gastric inhibitory polypeptide in isolated perfused diabetic rat pancreas. *Diabetes* 39:1320-1325, 1990.

Thomas S, Viberti GC: Proteinuria in diabetes. *J R Coll Physicians Lond* 34:336-339, 2000.

Thorens B: Glucagon-like peptide-1 and control of insulin secretion. *Diabete Metab* 21:311-318, 1995.

Tominaga M, Eguchi H, Manaka H, Igarashi K, Kato T, Sekikawa A: Impaired glucose tolerance is a risk factor for cardiovascular disease, but not impaired fasting glucose. The Funagata Diabetes Study. *Diabetes Care* 22:920-924, 1999.

Tronier B, Deigard A, Andersen T, Madsbad S: Absence of incretin effect in obese type 2 and diminished effect in lean type 2 and obese subjects. *Diabetes Res Clin Pract* Suppl1:S568, 1985.

Trudeau JD, Dutz JP, Arany E, Hill DJ, Fieldus WE, Finegood DT: Neonatal beta-cell apoptosis: a trigger for autoimmune diabetes? *Diabetes* 49:1-7, 2000.

Trümper A, Trümper K, Trusheim H, Arnold R, Göke B, Hörsch D: Glucose-dependent insulinotropic peptide is a growth and anti-apoptotic factor for beta (INS-1) cells by pleiotropic signaling. *Diabetes und Stoffwechsel* 10 Suppl1:35, 2001 a.

Trümper A, Trümper K, Trusheim H, Arnold R, Göke B, Hörsch D: Glucose-dependent insulinotropic polypeptide is a growth factor for β (INS-1) cells by pleiotropic signaling. *Mol Endocrinol* 15:1559-1570, 2001 b.

Trümper A, Trümper K, Trusheim H, Arnold R, Hörsch D: Protein kinase B activation by glucose-dependent insulinotropic polypeptide and growth hormone in β (INS-1)-cells (Abstract). *Diabetologia* 43 (Suppl.1):A136, 2000 b.

Trümper K, Trümper A, Trusheim H, Arnold R, Göke B, Hörsch D: Integrative mitogenic role of protein kinase B/Akt in beta-cells. *Ann N Y Acad Sci* 921:242-250, 2000 a.

- Trümper K, Trümper A, Trusheim H, Arnold R, Göke B, Hörsch D: Mitogenic and anti-apoptotic action of glucagon-like peptide-1 in beta (INS-1) cells is mediated by pleiotropic stimulation of phosphatidylinositol 3-kinase and protein kinase B isoforms. *Diabetes und Stoffwechsel* 10 Suppl1:35, 2001 c.
- Tseng CC, Boylan MO, Jarboe LA, Usdin TB, Wolfe MM: Chronic desensitization of the glucose-dependent insulintropic polypeptide receptor in diabetic rats. *Am J Physiol* 270:E661-666, 1996 a.
- Tseng CC, Jarboe LA, Landau SB, Williams EK, Wolfe MM: Glucose-dependent insulintropic peptide: structure of the precursor and tissue-specific expression in rat. *Proc Natl Acad Sci U S A* 90:1992-1996, 1993.
- Tseng CC, Kieffer TJ, Jarboe LA, Usdin TB, Wolfe MM: Postprandial stimulation of insulin release by glucose-dependent insulintropic polypeptide (GIP). Effect of a specific glucose-dependent insulintropic polypeptide receptor antagonist in the rat. *J Clin Invest* 98:2440-2445, 1996 b.
- Tseng CC, Zhang XY: Role of regulator of G protein signaling in desensitization of the glucose-dependent insulintropic peptide receptor. *Endocrinology* 139:4470-4475, 1998.
- Unger RH, Eisentraut AM: Entero-insular axis. *Arch Intern Med* 123:261-266, 1969.
- Usdin TB, Mezey E, Button DC, Brownstein MJ, Bonner TI: Gastric inhibitory polypeptide receptor, a member of the secretin- vasoactive intestinal peptide receptor family, is widely distributed in peripheral organs and the brain. *Endocrinology* 133:2861-2870, 1993.
- Velasquez MT, Kimmel PL, Michaelis OEt: Animal models of spontaneous diabetic kidney disease. *Faseb J* 4:2850-2859, 1990.
- Vogt M, Adamek HE, Arnold JC, Schilling D, Schleiffer T, Riemann JF: Gastrointestinal complications of diabetes mellitus. *Med Klin* 94:329-337, 1999.
- Volz A: Klonierung und funktionelle Charakterisierung des humanen GIP-Rezeptors. *Dissertation zur Erlangung des Doktorgrades der Naturwissenschaften*, University of Marburg, 1-159, 1997.
- Volz A, Göke R, Lankat-Buttgereit B, Fehmann HC, Bode HP, Göke B: Molecular cloning, functional expression, and signal transduction of the GIP-receptor cloned from a human insulinoma. *FEBS Lett* 373:23-29, 1995.

- Volz-Peters A, Peters H, Berghöfer P, Jiang J, Göke R, Balling R, Wanke R, Wolf E, Göke B: Expression of a dominant-negative GIP receptor induces diabetes mellitus in transgenic mice (Abstract). *Exp Clin Endocrinol Diabetes* 108:S40, 2000.
- Wang S, LaPage J, Hirschberg R: Proteinuria and progression of chronic renal disease. *Kidney Blood Press Res* 23:167-169, 2000.
- Wang X, Cahill CM, Piñeyro MA, Zhou J, Doyle ME, Egan JM: Glucagon-like peptide-1 regulates the beta cell transcription factor, PDX-1, in insulinoma cells. *Endocrinology* 140:4904-4907, 1999.
- Wang Z, Wang RM, Owji AA, Smith DM, Ghatei MA, Bloom SR: Glucagon-like peptide-1 is a physiological incretin in rat. *J Clin Invest* 95:417-421, 1995.
- Wanke R: Zur Morpho- und Pathogenese der progressiven Glomerulosklerose. *Habilitationsschrift*, Ludwig-Maximilians-Universität München, 1-257, 1996.
- Wanke R, Weis S, Kluge D, Kahnt E, Schenck E, Brem G, Hermanns W: Morphometric evaluation of the pancreas of growth hormone-transgenic mice. *Acta Stereol* 13:3-8, 1994.
- Wehner H, Petri M: Glomerular alterations in experimental diabetes of the rat. *Pathol Res Pract* 176:145-157, 1983.
- Weibel E, Gomez D: A principle for counting tissue structures on random sections. *J Appl Physiol* 17:343-348, 1962.
- Weibel ER: Stereological methods: I. Practical methods for biological morphometry. *Academic Press*, London, p. 1-415, 1979.
- Weil R, 3rd, Nozawa M, Koss M, Weber C, Reemtsma K, McIntosh R: The kidney in streptozotocin diabetic rats. Morphologic, ultrastructural, and function studies. *Arch Pathol Lab Med* 100:37-49, 1976.
- Wheeler MB, Gelling RW, McIntosh CH, Georgiou J, Brown JC, Pederson RA: Functional expression of the rat pancreatic islet glucose-dependent insulinotropic polypeptide receptor: ligand binding and intracellular signaling properties. *Endocrinology* 136:4629-4639, 1995.
- Withers DJ, Burks DJ, Towery HH, Altamuro SL, Flint CL, White MF: Irs-2 coordinates Igf-1 receptor-mediated beta-cell development and peripheral insulin signalling. *Nat Genet* 23:32-40, 1999.
- Withers DJ, Gutierrez JS, Towery H, Burks DJ, Ren JM, Previs S, Zhang Y, Bernal D, Pons S, Shulman GI, Bonner-Weir S, White MF: Disruption of IRS-2 causes type 2 diabetes in mice. *Nature* 391:900-904, 1998.

- Withers DJ, White M: Perspective: The insulin signaling system--a common link in the pathogenesis of type 2 diabetes. *Endocrinology* 141:1917-1921, 2000.
- Xu G, Stoffers DA, Habener JF, Bonner-Weir S: Exendin-4 stimulates both beta-cell replication and neogenesis, resulting in increased beta-cell mass and improved glucose tolerance in diabetic rats. *Diabetes* 48:2270-2276, 1999.
- Yamauchi J, Nagao M, Kaziro Y, Itoh H: Activation of p38 mitogen-activated protein kinase by signaling through G protein-coupled receptors. Involvement of Gbeta-gamma and Galphaq/11 subunits. *J Biol Chem* 272:27771-27777, 1997.
- Yasuda K, Inagaki N, Yamada Y, Kubota A, Seino S, Seino Y: Hamster gastric inhibitory polypeptide receptor expressed in pancreatic islets and clonal insulin-secreting cells: its structure and functional properties. *Biochem Biophys Res Commun* 205:1556-1562, 1994.
- Yip RG, Boylan MO, Kieffer TJ, Wolfe MM: Functional GIP receptors are present on adipocytes. *Endocrinology* 139:4004-4007, 1998.
- Yip RG, Wolfe MM: GIP biology and fat metabolism. *Life Sci* 66:91-103, 2000.
- Young AA, Gedulin BR, Bhavsar S, Bodkin N, Jodka C, Hansen B, Denaro M: Glucose-lowering and insulin-sensitizing actions of exendin-4: studies in obese diabetic (ob/ob, db/db) mice, diabetic fatty Zucker rats, and diabetic rhesus monkeys (*Macaca mulatta*). *Diabetes* 48:1026-1034, 1999.
- Zangen DH, Bonner-Weir S, Lee CH, Latimer JB, Miller CP, Habener JF, Weir GC: Reduced insulin, GLUT2, and IDX-1 in beta-cells after partial pancreatectomy. *Diabetes* 46:258-264, 1997.
- Zhou J, Wang X, Pineyro MA, Egan JM: Glucagon-like peptide 1 and exendin-4 convert pancreatic AR42J cells into glucagon- and insulin-producing cells. *Diabetes* 48:2358-2366, 1999.
- Ziegler A, Scherbaum W: Epidemiologie, Ätiologie und Pathogenese des Typ-1-Diabetes. In *Diabetologie in Klinik und Praxis*. H. Mehnert, E. Standl and K.-H. Usadel, Eds. p. 40-52, 1998.
- Zoubi SA, Mayhew TM, Sparrow RA: The small intestine in experimental diabetes: cellular adaptation in crypts and villi at different longitudinal sites. *Virchows Arch* 426:501-507, 1995.

9. Attachment

9.1 Silver stain for SDS-PAGE gels

1. Fixation solution	60 minutes
99.6% Ethanol	500 ml
Glacial acetic acid (Applichem, Germany)	120 ml
37% Formaldehyde (Applichem, Germany)	0.5 ml
Ad 1000 ml distilled water	
2. Washing in 50% ethanol	3 times 20 min
3. Pre-treatment	1 minute
Sodium thiosulphate (Applichem, Germany)	0.05 g
in 50 ml distilled water	
4. Washing in distilled water	3 times 20 seconds
5. Impregnation	20 minutes
Silver nitrate (Applichem, Germany)	0.05 g
37% Formaldehyde	35 μ l
ad 50ml distilled water	
6. Washing in distilled water	2 times 20 seconds
7. Develop	until bands become visible
Sodium carbonate (Merck, Germany)	3 g
Sodium thiosulphate	0.2 mg
37% Formaldehyde	50 μ l
ad 100 ml distilled water	
8. Wash in distilled water	20 seconds
9. Stop solution	
0.1 M EDTA (Sigma, Germany)	

9.2 Drying of SDS-PAGE gels

The DryEase™ Mini-Gel Drying System, Novex, Germany was used for drying poly-acrylamid gels.

Material

DryEase Mini-Gel Dryer Frame

DryEase Mini-Gel Drying Base

DryEase Mini Cellophane

Gel-Dry Drying Solution

Method

Stained gels are washed in distilled water 3 times for 2 minutes

Equilibration of gels in Gel-dry Solution for 15-20 minutes (rotary shaker)

Cutting of rough edges with a razor blade

Pre-wet 2 pieces of cellophane in Gel-Drying Solution for 15-20 seconds

DryEase gel drying frame, placed on the gel dryer base is covered with one cellophane piece

Gel is being placed in the center of the cellophane sheet; no air should be trapped between gel and cellophane

Cover gel with second layer of cellophane; no air should be trapped; wrinkles are removed with a gloved hand

Remaining frame is aligned so that its corner pins fit into the holes on the bottom frame. Plastic clamps are pushed onto the four edges of the frame

The assembly is to stand upright on a benchtop; drafts should be avoided.

Drying of gels for 12-36 hours

The gel/cellophane sandwich is removed and excess cellophane is trimmed off.

Dried gels are pressed between pages of a book for approximately 2 days

9.3 Staining procedures for plastic embedded sections

9.3.1 H&E

- | | |
|--|------------|
| 1. Mayer's hemalaun (Applichem, Germany) | 30 minutes |
| 2. Rinse in tap water | 10 minutes |
| 3. 1% HCl-Alcohol | 1 second |
| 4. Rinse in tap water | 10 minutes |
| 6. Dry | |
| 7. Eosine Y (Merck, Germany) | 5 minutes |

8. Distilled water 3 times 3 seconds
9. Dry
10. Mount with glass cover slips using Histofluid® (Superior, Germany)

9.3.2 Periodic acid-Schiff stain (PAS)

1. 1% periodic acid (Applichem, Germany) 15 minutes
2. Distilled water 3 times 3 seconds
3. Schiff's reagent (Merck, Germany) 30-60 minutes
4. Rinse in tap water 30 minutes
- Dry
- Mayer's hemalaun (Applichem, Germany) 35 minutes
- Rinse in tap water 10 minutes
- 1% HCl alcohol 1 second
- Rinse in tap water 10 minutes
- Dry
- Mount under glass cover slips using Histofluid® (Superior, Germany)

9.3.3 Periodic acid silver methenamine PAS stain (Gomori 1946), modified

1. 1% periodic acid (Applichem, Germany) 15 minutes
2. Distilled water 3 times 3 seconds
- Dry
- Silver-methenamine solution containing:

3% Methenamine solution	50 ml
5% Silver nitrate (Applichem, Germany)	2.5 ml
2% Sodium tetraborate decahydrate (Borax)	6 ml
Distilled water	45 ml
Pre-heat to 60° in a water bath	5 minutes
- Staining (shake in a closed water bath at 60°C) 15-50 minutes, staining intensity has to be controlled repeatedly
- Distilled water 3 times 3 seconds
- 1.5% Sodium thiosulphate solution 2 minutes

Rinse in tap water	5 minutes
Dry	
Schiff's reagent (Merck, Germany)	60 minutes
Rinse in tap water	30 minutes
Dry	
Mayer's hemalaun (Applichem, Germany)	25 minutes
Rinse in tap water	10 minutes
1% HCl alcohol	1 second
Rinse in tap water	10 minutes
Dry	
Mount under glass cover slips using Histofluid® (Superior, Germany)	

9.4 Staining procedures for paraffin embedded sections

9.4.1 H&E

1. Xylene	10 minutes
2. Descending series of alcohols	
3. Mayer's hemalaun solution	5 minutes
4. Rinse in tap water	5 minutes
5. 0.5% HCl-alcohol	until slides have cleared
6. Rinse in tap water	5 minutes
7. Eosine	dip 2-7 times
8. Rinse in distilled water	
9. Ascending series of alcohols	
10. Carbolxylene	
11. Xylene	
Mount under glass cover slips using Histofluid (Superior, Germany)	

9.4.2 PAS

1. Xylene	10 minutes
2. Descending series of alcohols	
3. 1% periodic acid (Applichem, Germany)	10 minutes

- | | |
|--|------------|
| 4. Rinse in tap water | 10 minutes |
| 5. Rinse in distilled water | |
| 6. Schiff's reagent (Merck, Germany) | 30 minutes |
| 7. Rinse in tap water | 5 minutes |
| 8. Mayer's hemalaun (Applichem, Germany) | 2 minutes |
| 9. Rinse in tap water | 5 minutes |
| 10. 1% HCl alcohol | |
| 11. Rinse in tap water | 5 minutes |
| 12. Ascending series of alcohols | |
| 13. Xylene | |
- Mount under glass cover slips using Histofluid

9.4.3 Gomori's silver stain (modified)

- | | |
|--|-------------|
| 1. Xylene | 10 minutes |
| 2. Descending series of alcohols | |
| 3. Potassium permanganate 0.5% (Merck, Germany) | 1-2 minutes |
| 4. Rinse in tap water | 5 minutes |
| 5. Potassium disulphite 2% (Merck, Germany) | 1 minute |
| 6. Rinse in tap water | 5 minutes |
| 7. Ammonium iron (III) sulphate 2%
(Merck, Germany) | 1 minute |
| 8. Rinse in tap water | 5 minutes |
| 9. Distilled water | 2 minutes |
| 10. Distilled water | 2 minutes |
| 11. Silver nitrate in ammonia (see below) | 1 minute |
| 12. Formaldehyde 4% | 5 minutes |
| 13. Rinse in tap water | 5 minutes |
| 14. Gold chloride 0.1% (Applichem, Germany) | 30 seconds |
- Rinse in distilled water
- | | |
|--|-----------|
| Potassium disulphite 2% (Merck, Germany) | 1 minute |
| Rinse in tap water | 5 minutes |
| Sodium thiosulphate 1% (Merck, Germany) | 1 minute |
| Rinse in tap water | |

Ascending series of alcohols

Xylene

Mount under glass cover slips using Histofluid

Silver nitrate in ammonia:

Silver nitrate (Applichem, Germany) 10%	25 ml
Potassium hydroxide (Merck, Germany) 10%	5 ml
Ammonia solution 25% (Applichem, Germany)	approximately 4 ml, add slowly
until brown precipitate dissolves	
Silver nitrate (Applichem, Germany) 10%	approximately 1 ml, until
solution turns brownish	
Distilled water	30 ml
Use within 2 days, store at 4°C in a dark bottle	

9.4.4 Best's Carmine

Cut sections for glycogen determination have to be transferred into 85% Ethanol for mounting on glass slides.

a) Impregnation of sections:

1. Xylene	10 minutes
2. Ethanol 100%	
3. Ether-Ethanol (50:50)	1-2 minutes
4. Collodion solution 1%	2-3 minutes
5. Ethanol 80%	2 minutes

b) Staining procedure

1. Mayer's hemalaun (Applichem, Germany)	10 minutes
2. Rinse in tap water	10-15 minutes
3. Carmine solution (see below)	10-30 minutes
4. Differentiate (see below)	1 minute
5. Differentiate (see below)	1 minute
6. Ethanol 80%	
7. Ether-Ethanol (50:50)	3-5 minutes
8. Ethanol 99.6%	

9. Xylene

10. Mount under glass cover slips using Histofluid

Carmine stock solution:

Carmine (Merck, Germany)	2g
Potassium carbonate (Applichem, Germany)	1g
Potassium chloride (Merck, Germany)	5g
Distilled water	60 ml
Boil for 2-3 minutes	
Ammonia solution (Applichem, Germany)	20 ml
Store at 4°C in a dark bottle, use within 2 months	

Carmine solution, ready to use:

Stock solution	20 ml
Ammonia solution (Applichem, Germany)	30 ml
Methanol (Applichem, Germany)	30 ml

Differentiation solution:

Methanol (Applichem, Germany)	40 ml
Ethanol 99.6%	80 ml
Distilled water	100 ml

9.5 Fat Red stain

1. Transfer cut sections into distilled water
2. Ethanol 50% 0.5 minutes
3. Fat red solution (see below) 5 minutes
4. Ethanol 50% 2 seconds
5. Rinse in distilled water
6. Mayer's hemalaun (Applichem, Germany) 2 seconds
7. Rinse in distilled water
8. Rinse in tap water
9. Mount on glass slides
10. Dry

11. Mount under glass cover slips using Kaiser's glycerol gelatin (Merck, Germany)

Fat red solution:

Ethanol 96% 140 ml

Distilled water 52 ml

Boil shortly

Fat red 7B (Serva, Germany) 0.5g

Boil shortly and stir for 30 minutes

Filtrate before using

Acknowledgement

I would like to thank Prof. Dr. R. Wanke for giving me the opportunity to do this dissertation, for the time he spent discussing all the different features of this doctorate, especially the study design, morphometric evaluations and the possible pathogenetic mechanisms. I am very grateful for his great support.

I wish to thank Prof. Dr. E. Wolf for his kind support and giving me the opportunity to work in his laboratories. Thanks to all the co-workers at the Institute of Molecular Animal Breeding/Gene Center, especially Dr. A. Höflich and PD Dr. H. Lahm as well as Petra Renner, Norman Rieger and Petra Demleitner.

I show my gratitude to Prof. Dr. B. Göke for the time he spent discussing the study design and possible pathogenetic features, and for all the background information he shared with me.

Further, I am very grateful for having the opportunity to do the HbA_{1c} determination at Recipe Chemicals and Instruments, and I would like to thank Mr. H. Nader and Mr. A. Bauer for their generous support.

Another acknowledgement goes to the staff of the Institute of Clinical Chemistry and the Hormone Laboratory, Hospital Harlaching, Munich for handling the serum samples, especially I would like to thank Prof. Dr. Kolb, Dr. Fuchs, Mrs. Dryer and Mrs. Wolniak.

I wish to thank the laboratory for clinical chemistry of the Department of Internal Medicine I of the Ludwig-Maximilian-University, Munich for analyzing urine samples.

Prof. Dr. Gabius gave me the opportunity to work in his laboratories and learn to do the SDS-PAGE, I am very grateful for his friendly support. Thanks as well to PD Dr. Kaltner and Andrea Hellwig for their kind help.

Further, I thank Prof. Dr. Osterkorn and Dr. Stanglmeier for their kind support with statistical analysis.

I wish to thank all employees at the Institute of Veterinary Pathology for their help, especially Heike Boos, Adrian Ciolovan, Elisabeth Kemper, Bettina Spindler, Kathrin Sterr and Sabine Zwirz.

Curriculum vitae

Nadja Herbach
 Luisenstraße 62
 D-80798 München
 Tel.:089/21802530
 E-Mail: Herbach@patho.vetmed.uni-muenchen.de

Nationality : German
 Date of birth : 12.08.1970
 Place of birth : Berlin-Schmargendorf

1976 – 1980	Grundschule Lautergrund
1980 – 1989	Meranier-Gymnasium Lichtenfels
24.06.1989	Allgemeine Hochschulreife
1989 – 1991	Apprenticeship for medical technician of veterinary medicine (VMTA) at the “Landesuntersuchungsamt für das Gesundheitswesen” (LUA), South-Bavaria
31.08.1991	Final exams: “staatliche Prüfung für veterinärmedizinisch-technische Assistenten”
1991 – 1992	Employment as VMTA at the LUA, South-Bavaria (bacteriological examination of milk)
1993 – 1999	Student of veterinary medicine at the Ludwig-Maximilian-University, Munich
01.02.1999	Final exams
22.02.1999	Begin of the dissertation at the Institute of Veterinary Pathology at the Ludwig-Maximilian-University, Munich
09.03. 1999	Approbation
01.04.2001	Employment at the Institute of Veterinary Pathology, Ludwig-Maximilian-University, Munich